PREPARATION AND CHARACTERIZATION OF COMPLETELY BIODEGRADABLE POLYMER-TITANIA NANOCOMPOSITES

by

JULIA PUSELETSO MOFOKENG (M.Sc)

Submitted in accordance with the requirements for the degree

DOCTOR OF PHILOSOPHY (Ph.D.) In Polymer Science

Department of Chemistry

Faculty of Natural and Agricultural Sciences

at the

UNIVERSITY OF THE FREE STATE (QWAQWA CAMPUS)

SUPERVISOR: PROF AS LUYT

January 2015

Declaration

I hereby declare that the thesis submitted by me for the degree Philosophiae Doctor at the University of the Free State is my own independent work, and has not previously been submitted by me at any other university/faculty. I furthermore cede copyright of the thesis in favour of the University of the Free State.

Ms. J.P. Mofokeng

Dedication

I would like to dedicate this thesis to my mother Mmakeletso Mofokeng, the woman of strength who made it her mission to see that I become the best in life. If it was not because of your unconditional love, encouragements and directions, Mother, I would not have achieved this great milestone, I crown you my Dr.

I would also like to dedicated this thesis to my beloved late grandmother Mmamokgae Mokoena moradi wa Tibisa, Lekgwakgwa laha Sidimo Nthole, may your soul continue to rest in eternal peace, you will always be in my heart.

Abstract

PLA/PHBV, PLA/PCL and PHBV/PCL blends were prepared through melt-mixing in the absence and presence of small amounts of titania (TiO_2) nanoparticles. The effect of blending and the presence of nanoparticles on the morphology, thermal degradation behaviour and kinetics, and the dynamic mechanical properties of the different blends and nanocomposites was investigated. The dispersion and distribution of the TiO_2 nanoparticles in the blends was studied using scanning electron microscopy (SEM) and transmission electron microscopy (TEM), and contact angle measurements were used to assist in the explanation of the nanoparticle dispersion in the different blends. The thermal stabilities and degradation kinetics of the different samples were investigated using thermogravimetric analysis (TGA), and the Flynn-Wall-Ozawa method was used to estimate the activation energies of degradation. Fourier transform infrared (FTIR) spectroscopy connected to the TGA was used to evaluate the nature of volatile degradation products and the time taken for these products to be released from the sample. The storage and loss moduli, as well as the mechanical damping, of the blends and nanocomposites were investigated using dynamic mechanical analysis (DMA), and these results were related to the effect of blending and the presence of nanoparticles on the glass transition temperature, miscibility, and compatibility of the polymers in the different samples.

All three polymer pairs were immiscible and showed a co-continuous structure for the 50/50 w/w blend compositions. In the PLA/PHBV system the nanoparticles were well dispersed in the PLA phase and on the interface between the two polymers, with a few large agglomerates in the PHBV phase. The nanoparticles were found to be equally dispersed in both polymer phases of PLA/PCL and PHBV/PCL, but some agglomerates were also observed. These observations were explained through differences in the surface energies, interfacial tensions, molecular weights, viscosities, and crystallinities.

For the PLA/PHBV blends the thermal stability of PHBV was improved through blending with PLA, while that of PLA was reduced due to the low thermally stable PHBV. The presence of TiO_2 nanoparticles improved the thermal stability of both polymers in the blends. The degradation kinetics results showed changes in the activation energy of degradation that could have been brought about by the nanoparticles catalysing the degradation process and/or retarding the volatilization of the degradation products, depending on their localization and their interaction

with the polymer in question. Blending of PLA and PCL reduced the thermal stabilities of both polymers, which was attributed to the incompatibility of the polymers. The presence of TiO_2 nanoparticles in these blends improved the polymers' thermal stabilities. This was also explained in terms of the catalysis and immobilization effects of the nanoparticles. The thermal stability of PHBV was improved when blended with the more thermally stable PCL, but the thermal stability of PCL decreased. The introduction of only 1 wt% of TiO_2 nanoparticles observably improved the thermal stabilities of both polymers in the blend, but it is quite possible that the nanoparticles only retarded the evolution of the degradation products through their interaction with these products.

The storage modulus of the PLA/PHBV blends was higher than those of both PLA and PHBV in the temperature region below the glass transition of PHBV, but the PLA/PCL and PHBV/PCL bends did not show a similar feature. The E' values between the glass transitions of PLA and PHBV depended on the blend compositions and morphologies. The presence of titania nanoparticles had little effect on the E' values of all the investigated blends. The cold crystallization transition of PLA shifted to lower temperatures in the PLA/PHBV blends, and shifts in the T_gs of the two polymers indicated partial miscibility at the polymer-polymer interfaces. This partial miscibility reduced the chain mobilities of these polymers, which could be seen in a reduction in the damping during their respective glass transitions. Blending and nanoparticle addition had little influence on the glass transition temperatures of PLA and PCL, but the glass transitions of PHBV and PCL in the PHBV/PCL blends were respectively at higher and lower temperatures than those of the neat polymers, which is a somewhat abnormal observation. The PCL glass transition peaks became broader as a result of blending, and this was attributed to incompatibility between the polymers, because blending had no influence on the PCL crystallinity.

Conference presentations

1. J.P. Mofokeng, A.S. Luyt. Preparation and characterisation of biodegradable PLA/PHBV, PLA/PCL and PHBV/PCL polymer blends and their nanocomposites with TiO_2 as filler. 12th Annual UNESCO/IUPAC Workshop and Conference on Macromolecules & Materials, 25-28 March 2013, Stellenbosch, South Africa (oral presentation).
2. J.P. Mofokeng, A.S. Luyt. Preparation and characterisation of biodegradable PLA/PHBV, PLA/PCL and PHBV/PCL polymer blends and their nanocomposites with TiO_2 as filler. BiPoCo 2014, 2nd International Conference on Bio-based Polymers and Composites, 24-28 August 2014, Visegrád, Hungary (oral presentation).

Table of contents

List of tables

List of figures

List of symbols and abbreviations

AAC	aliphatic-aromatic copolymer
D	dispersity index
DC	degree of crystallinity
ΔH_m	melting enthalpy
ΔH^o_m	melting enthalpy of 100% crystalline polymer
DMA	dynamic mechanical analysis
E_a	activation energy
E'	storage modulus
E″	loss modulus
γ	surface energy
γ^d	dispersive component of surface energy
γ^p	polar component of surface energy
MFI	melt flow index
M_n	number average molar mass
M_w	weight average molar mass
MWCNTs	multi walled carbon nanotubes
M_z	viscosity average molar mass
ω_α	wetting coefficient
PBSA	poly(butylene succinate adipate)
PCL	poly(ε-caprolactone)
PGA	polyglycolide
PHA	poly(hyroxy alkanoate)
PHB	poly(hydroxy butyrate)
PHBV	poly(3-hydroxybutyrate-co-3-hydroxyvalerate)
PHV	poly(hydroxy valerate)
PLA	poly(lactic acid)
PVOH	polyvinyl alcohol
PW_{HH}	peak width at half height
SEC	size exclusion chromatography

SEM	scanning electron microscopy
tan δ	loss tangent
TEM	transmission electron microscopy
TEM-EDS	TEM-energy dispersive specroscopy
T_g	glass transition temperature
TGA	thermogravimetric analysis
TGA-FTIR	TGA-Fourier-transform infrared
X_c	degree of crystallinity

Chapter1

General introduction

The recent advances in the field of light-weight materials, and related methods, entail the development of new and promising materials in order to replace the heavy conventional materials such as metals and ceramics. This is done by modifying the current technologies and optimizing the processing conditions to achieve low-cost, high-speed and high quality mass production. There are also research efforts aimed at finding suitable preparation methods, study the compatibility of the constituents making up the final product, determining whether the final product will meet industrial application requirements and whether it will be strong enough to last for the required period, and determining whether the product can be made cost-effectively.

In the past decades many synthetic polymers made from non-renewable fossil fuel have been, and are still, widely used. However, the production of these polymers not only leads to the exhaustion of the petroleum resources, but also to the serious environmental pollution. Those used for disposable products and short term packaging especially, cause a lot of harm because they are resistant to chemicals and microbial attack [1]. The first drawback associated with the disposal of plastic waste is the fact that landfill facilities occupy space that could be utilised for more productive means such as agriculture [2]. These non-degradable polymers also pose a danger to our wildlife as the plastic waste accumulate and end up spreading in the environment during windy conditions, and end up at the places where animals reside. The animals mistake these plastics for food, but since they are indigestible, these plastics are a health hazard to animals, and with time we will end up having reduced or no wildlife. The other concern is the environmental pollution in the marine world, where these plastics are carried by rivers and municipal drainage systems and end up in the sea, where they endanger the marine life [3-5]. Although work has been done to blend these synthetic polymers with natural biodegradable materials to produce plastics that meet the functional requirements with the possibility of biodegradation, the worldwide consumer plastic production volumes still continue to accumulate due to the slow degradation or non-degradability of the final products. For people and animals to lead a comfortable life, and free from environmental pollution issues, new and useful materials

need to be developed. The search for new materials began a long time ago, and a lot of progress has already been made. There are a number of biodegradable polymers, and their blends and nanocomposites provide opportunities for developing materials with tailor-made properties.

Biopolymers are polymers generated from renewable natural resources such as corn, rice, potato, animal fat and others, and they are often biodegradable. They can be produced by biological means or chemically synthesised from biological materials. These polymers are materials that are not harmful to the environment, and they degrade naturally. Biodegradable polymers normally degrade in different ways in the environment; some are bio-erodable, while others are hydrobiodegradable or photobiodegradable. Their biodegradability depends on the chemical structure of the polymer and on the constitution of the final product (blends, nanocomposites, blends nanocomposites and others), and not just on the initially produced raw polymer [6]. The polyester family play a major role as biodegrdable polymers due to their potentially hydrolysable ester bonds. Polyesters are made up of two major groups, aliphatic (linear) polyesters, and aromatic (ring) polyesters. There are a number of biodegrdable polyesters that have been developed and are already commercially available. These include polyvinyl alcohol (PVOH), polylactic acid (PLA), polybutylene succinate adipate (PBSA), aliphatic-aromatic copolymers (AAC), poly(ε-caprolactone) (PCL), polyhyroxy alkanoates (PHAs), which include polyhydroxybutyrate (PHB), polyhydroxyvalerate (PHV), and the co-polymer poly(3-hydroxybutyrate-co-3hydroxyvalerate) (PHBV). These biodegradable thermoplastic polyesters are melt processable biometerials that present a number of promising properties in a number of applications in the packaging, automotive and biomedical sectors. Specifically, thermoplastic biodegrdable polymers such as PLA, PCL and PHBV, that exhibit a combination of good properties [1,7,8], have been widely investigated and are already used for a number of applications.

PLA is a biodegradable polymer resourced from corn starch, and the existance of hydroxyl and carboxyl groups in the lactic acid monomer enables it to be converted directly into a polyester *via* a condensation reaction during its polymerisation, or it can be polymerized through the ring opening of lactide. The latter method is prefarred since the polymerization can be controlled in terms of molecular weight [6]. PLA is mainly used in the medical industry for controlled release devices, surgical implants, or sutures, enterior parts in the automotive industry, disposable cups and napies, and many other applications in the packaging industry. PLA has been

produced with different structural forms, which include amorphous, semi-crystalline, or highly crystalline. Its melting temperature ranges from 140 to 180 °C, and its glass transition temperature from 50 to 70 °C [9,10], but it has a low crystallinity and generally undergoes cold crystallization when heated. PLA properties similar to those of conventional thermoplastics like PP and LDPE, but it has poor processing properties and thermal stability, and is unacceptably brittle.

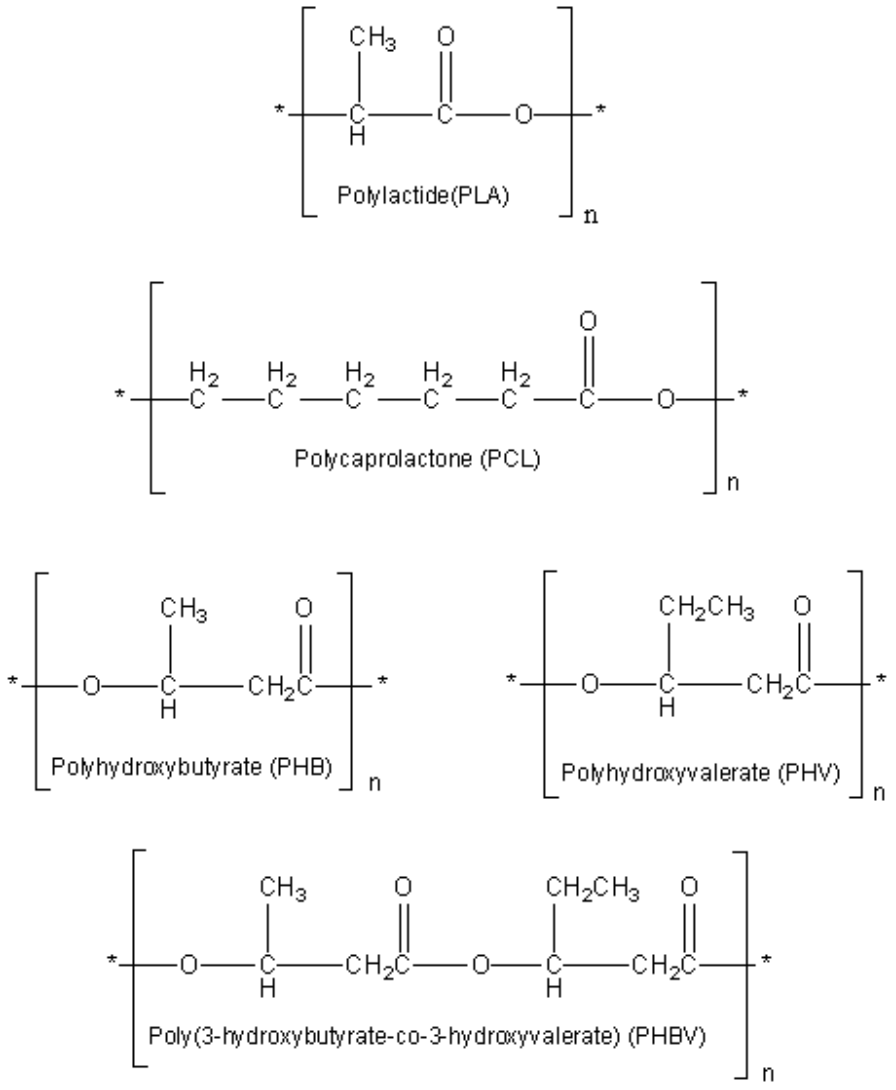

Figure 1.1 Chemical structures of PLA, PCL, PHB, PHV and PHBV

PCL is a linear semicrystalline polyester with a moderate degree of crystallinty, and characterised by a low glass transition temperature (-60 °C). It is produced by ring opening polymerization of ε-caprolactone. It is a biocompatible and biodegrdable polymer, and its chains undergo degradation through hydrolytic or enzymatic reactions. PCL is used in medical applications as controlled drug release carriers, and lately it has also been examined as potencial biodegradable material for packaging applications. Due to its excellent toughness, high thermal stability and rubbery properties, it has also been used as a blend component to improve the toughness in brittle biodegrdable polymers like PLA and PHB. The main disadvantages of PCL are the low melting temperature (60 °C), modulus, abrasion, slow degradation, and its relatively high cost, which resticts its individual usage [11,12].

PHBV, the co-polymer from PHB and PHV, has mainly been used in medical applications due to its enviromental friendliness, biocompatibility, biodegrdability and its thermoplastic properties similar to other conventional synthetic petroleum-based polymers, although it is still has a high degree of crystallinity, brittleness and low thermal stability [13,14]. Figure 1 illustrates the chemical structures of PLA, PCL, PHB, PHV, and PHBV.

Blending is the most convenient way to generate new materals that combine the properties of the components, and improve the not-so-good thermal, mechanical, and dynamic mechanical properties of the individual polymers. The usual objective for preparing a blend of two or more polymers is not to significantly change the properties of the components, but to capitalize on the good properties of each component in the blend [15-17]. Therefore blending biodegradable polymers has been explored as an alternative way of aquiring novel materials with desired properties in a cheaper way. Most polymer blends are thermodynamically immiscible, and consequently the phase morphology is ussually observed as multi-phase. It is well known that the size of the dispersed phase can significantly influence the physical and mechanical properties of the final immiscible polymer blends. During blending, there are several factors that are important in determining the final particle size of the dispersed phases of the blend components, such as surface energy, interfacial tension, polar character, blend composition, viscosity ratio, differences between the degree of crystallinity of the components in the blend, as well as time, shear stress, and temperature of mixing [16].

The use of inorganic nanofillers to stabilize the interface between immiscible polymers in a blend has been lately studied. One would ask, why nanofillers over conventional micro-particles?

The nanoscopic dimension and inherent extreme aspect ratios of nanofillers result in the following interrelated characteristics which distinguish them from microparticles: (i) Large number density of particles per particle volume; (ii) Extensive interfacial area per volume of particles; (iii) Short distance between the particles; (iv) Comparable size scales among the rigid nanoparticles inclusion, distance between the particles, and the relaxation volume of the polymer chains [18]. Sometimes the inorganic nanofiller/nanoparticles can be selectivelly localized in one of the polymeric components, where the affinity between the nanoparticles and the polymer is high. The affinity between the inorganic nanoparticles and the polymer is controlled mainly by thermodynamic and kinetic effects. When the surface energies and polar characters of the nanoparticles and the polymer are similar, it is likely that the nanoparticles will easily disperse in the polymer, but if there is a big difference, the nanoparticles will migrate to the interface between the components of the blend or they will form agglomerates that indicate that the nanoparticles have a higher affinity for each other than for the polymer. An important requirement in obtaining blend nanocomposites with improved properties, is that the nanofiller must interact with the polymeric components, or be well dispersed in one or both of the componets and/or on the inetrface between these components in the blend.

Some of the nanomaterals reported in the literature are good in compatibilising the polymers in a blend. Examples are carbon black, calcium carbonate ($CaCO_3$), zinc odide (ZnO), graphite, silica, silver, clays, carbon nanotubes, and titanium dioxide (TiO_2) [16,18,19]. TiO_2 received a lot of attention as nanofiller in polymers because of its good thermal stability, accessibility, and catalytic properties. It is generally used for various applications such as photo electrochemical activity, solar energy conversion, photocatalysis, UV detection, ultrasonic sensing, and as a promising material in applications such as water or wastewater treatment. Its environmental compatibility, non-toxicity and low price are some practical advantages of TiO_2 [20-24].

The most important properties that need to be improved in biodegrdable polymer blends are thermal stability, since most of them suffer from low thermal stability compared to conventional synthetic polymers, and the dynamic mechanical properties. The thermal stability of materials is important in determining the limit of their working temperature and the envoronmental conditions for use, that are related to their thermal decomposition temperature and decomposition rate [25]. The study of dynamic mechanical properties is important because it gives information

on properties such as glass transition temperatures, stress relaxation behaviour, dynamic fragility parameters, miscibility of polymer blends, interfacial compatibility of individual composite components, and filler effectiveness [26-28]. A number of previous studies showed that inorganic nanoparticles improved the thermal stabilities and dynamic mechanical properties of polymers and blends [29-32]

The blends of PLA with polymers such as PCL and PHBV have been widely researched, and most of these blends were reported to have an immiscible/phase separated morphology. PLA/PHBV blends and their blend nanocomposites have been moderately studied and they are reported to be immiscible but compatible. The compatibility was reported to further improve in the presence of inorganic nanoparticles, and some of these studies reported on the thermal degradation and dynamic mechanical properties [33-35]. The immiscible, biodegradable PLA/PCL blends have been fairly intensively studied and some papers mentioned that PLA and PCL are compatible immiscible polymers, while others indicated that PLA and PCL are incompatible, and therefore inorganic micro or nanomaterials were utilised as reinforcements to stabilise the interface between the polymers. The reports on thermal stability and degradation mostly involved standard TGA analyses, with almost no in-depth studies of the thermal degradation behaviour and kinetics of similar blends and nanocomposites. Most of these studies investigated the dynamic mechanical properties using dynamic mechanical analysis (DMA), but different types of nanoparticles were used, giving rise to different, non-comparable results [36-42]. Although the PHBV/PCL blends show potential in the medical and packaging industries, these blends and their nanocomposites have been the least studied, probably due to their high cost [43-45].

1.1 Objectives of the study

In this work TiO_2 nanoparticles were used to stabilize the interface between the immiscible polymers, and to improve the thermal stability and thermo-mechanical properties of the blends. The PLA/PHBV, PLA/PCL and PHBV/PCL biodegradable polymer blends and their nanocomposites with small amounts of titania were preapared through melt-mixing. The effect of blending and nanoparticle filling on the morphology of the blends and nanocomposites was investigated by scanning electron microscopy (SEM), transmission electron microscopy (TEM),

and surface energy measurements. Their thermal degradation behaviour and kinetics were studied using thermogravimetric analysis (TGA), and TGA-Fourier-transform infrared (FTIR) spectroscopy was used to determine the nature of volatile degradation products and to study the rate at which they were released. The dynamic mechanical properties of the different systems were also studied and compared.

1.2 Structure of the thesis

The thesis is comprised of six chapters. The thesis does not have the experimental chapter because the materials and methods details are included in Chapters 2 to 5 that are in a scientific journal paper format. The organization of these chapters is as follows:

Chapter 1: General introduction

Chapter 2: Morphology and thermal degradation studies of melt-mixed PLA/PHBV biodegradable polymer blend nanocomposites with TiO_2 as filler

Chapter 3: Morphology and thermal degradation studies of melt-mixed PLA/PCL biodegradable polymer blend nanocomposites with TiO_2 as filler

Chapter 4: Morphology and thermal degradation studies of melt-mixed PHBV/PCL biodegradable polymer blend nanocomposites with TiO_2 as filler

Chapter 5: Dynamic mechanical properties of PLA/PHBV, PLA/PCL, PHBV/PCL blends and their nanocomposites with TiO_2 as nanofiller

Chapter 6: Conclusions

1.3 References

1. M.D. Sanchez-Garcia, E. Gimenez, J.M. Lagaron. Morphology and barrier properties of nanobiocomposites of poly(3-hydroxybutyrate) and layered silicates. Journal of Applied Polymer Science 2008; 108:2787-2801.
DOI: 10.1002/app.27622

2. J. Zhang, X. Wang, J. Gong, Z. Gu. A study on the biodegradability of polyethylene terephthalate fiber and diethylene glycol terephthalate. Journal of Applied Polymer Science 2004; 93:1089-1096.
DOI: 10.1002/app.20556
3. M.R. Gregory. Environmental implications of plastic debris in marine settings – entanglement, ingestion, smothering, hangers-on, hitch-hiking and alien invasions. Philosophical Transaction of the Royal Society B 2009; 364:2013-2025.
DOI: 10.1098/rstb.2008.0265
4. J.G.B. Derraik. The pollution of the marine environment by plastic debris: A review. Marine Pollution Bulletin 2002; 44:842-852.
PII: S0025-326X(02)00220-5
5. H.K. Webb, J. Arnott, R.J. Crawford, E.P. Ivanova. Plastic degradation and its environmental implications with special reference to poly(ethylene terephthalate). Polymers 2013; 5:1-18.
DOI: 10.3390/polym5010001
6. K.M. Nampoothiri, N.R. Nair, R.P. John. An overview of the recent developments in polylactide (PLA) research. Bioresource Technology 2010; 101:8493-8501.
DOI: 10.1016/j.biortech.2010.01.092
7. M.D. Sanchez-Garcia, A. Lopez-Rubio, J.M. Lagaron. Natural micro and nanobiocomposites with enhanced barrier properties and novel functionalities for food biopackaging applications. Trends in Food Science & Technology 2010; 21:528-536.
DOI: 10.1016/j.tifs.2010.07.008
8. J. Li, Y. He, Y. Inoue. Thermal and mechanical properties of biodegradable blends of poly(L-lactic acid) and lignin. Polymer International 2003; 52:949-955.
DOI: 10.1002/pi.1137
9. X. Pang, X. Zhuang, Z. Tang, X. Chen. Polylactic acid (PLA): Research, development and industrialization. Biotechnology Journal 2010; 5:1125-1136.
DOI: 10.1002/biot.201000135
10. R.M. Rasal, A.V. Janorkar, D.E. Hirt. Poly(lactic acid) modifications. Progress in Polymer Science 2010; 35:338-356.
DOI: 10.1016/j.progpolymsci.2009.12.003

11. J. Peña, T. Corrales, I, Izquierdo-Barba, A.L. Doadrio, M. Vallet-Regí. Long term degradation of poly(ε-caprolactone) films in biologically related fluids. Polymer Degradation and Stability 2006; 91:1424-1432.
DOI: 10.1016/j.polymdegradstab.2005.10.016
12. Y. Xu, C. Wang, N.M. Stark, Z. Cai, F. Chu. Miscibility and thermal behavior of poly(ε-caprolactone)/long-chain ester of cellulose blends. Carbohydrate Polymers 2012; 88:422-427.
DOI: 10.1016/j.carbpol.2011.11.079
13. H.X. Xiang, S.H. Chen, Y.H. Cheng, Z. Zhou, M.F. Zhu. Structural characteristics and enhanced mechanical and thermal properties of full biodegrdable tea polyphenol/poly(3-hydroxybutyrate-co-3-hydroxyvalerate) composite films. eXPRESS Polymer Letters 2013; 7:778-786.
DOI: 10.3144/expresspolymlett.2013.75
14. I. Zembouai, M. Kaci, S. Bruzaud, A. Benhamida, Y.-M. Corre, Y. Grohens. A study of morphological, thermal, rheological and barrier properties of poly(3-hydroxybutyrate-co-3-hydroxyvalerate)/polylactide blends prepared by melt mixing. Polymer Testing 2013; 32:842-851.
DOI: 10.1016/j.polymertesting.2013.04.004
15. M.J. Jenkins, Y. Cao, L. Howell, G.A. Leeke. Miscibility in blends of poly(3-hydroxybutyrate-co-3-hydroxyvalerate) and poly(ε-caprolactone) induced by melt blending in the presence of supercritical CO_2. Polymer 2007; 48:6304-6310.
DOI: 10.1016/j.polymer.2007.08.033
16. T. Hanemann, D.V. Szabó. Polymer-nanoparticle composites: From synthesis to modern applications. Materials 2010; 3:3468-3517.
DOI: 10.3390/ma3063468
17. G. Kfoury, J.-M. Raquez, F. Hassouna, J. Odent, V. Toniazzo, D. Ruch, P. Dubois. Recent advances in high performance poly(lactide): From "green" plasticization to super tough materials via (reactive) compounding. Frontiers in Chemistry 2013; 1:1-46.
DOI: 10.3389/fchem.2013.00032

18. A.P. Kumar, D. Depan, N.S. Tomer, R.P. Singh. Nanoscale particles for polymer degradation and stabilization-trends and future perspectives. Progress in Polymer Science 2009; 34:479-515.
DOI: 10.1016/j.progpolymsci.2009.01.002
19. F. Fenouillot, P. Cassagnau, J.C. Majeste. Uneven distribution of nanoparticles in immiscible fluids: Morphology development in polymer blends. Polymer 2009; 50:1333-1350.
DOI: 10.1016/j.polymer.2008.12.029
20. Y. Shi , X. Feng , H. Wang, X. Lu. The effect of surface modification on the friction and wear behavior of carbon nanofiber-filled PTFE composites. Wear 2008; 264:934-939. DOI: 10.1016/j.wear.2007.06.014
21. A. Maurya, P. Chauhan. Synthesis and characterization of sol-gel derived PVA-titanium dioxide (TiO_2) nanocomposites. Polymer Bulletin 2012; 68:961-972.
DOI: 10.1007/s00289-011-0589-6
22. F. Shi, Y. Ma, J. Ma, P. Wang, W. Sun. Preparation and characterization of PVDF/TiO_2 hybrid membranes with different dosage of nano-TiO_2. Journal of Membrane Science 2012; 389:522-531.
DOI: 10.1016/j.memsci.2011.11.022
23. N. Nakayama, T. Hayashi. Preparation and characterization of poly(L-lactic acid)/TiO_2 nanoparticle nanocomposite films with high transparency and efficient photodegradability. Polymer Degradation and Stability 2007; 92:1255-1264.
DOI: 10.1016/j.polymdegradstab.2007.03.026
24. P.M. Chou, M. Mariatti, A. Zulkifli, S. Sreekantan. Evaluation of the flexural properties and bioactivity of bioresorbable PLLA/PBSL/CNT and PLLA/PBSL/TiO_2 nanocomposites. Composites Part B 2012; 43:1374-1381.
DOI: 10.1016/j.compositesb.2011.11.023
25. H. Shi, R. Magaye, V. Castranova, J. Zhao. Titanium dioxide nanoparticles: A review of current toxicological data. Particle and Fibre Toxicology 2013; 10:1-33.
DOI: 10.1186/1743-8977-10-15

26. A. Gregorova, M. Machovsky, R. Wimmer. Viscoelastic properties of mineral-filled poly(lactic acid) composites. International Journal of Polymer Science 2012; 252981. DOI: 10.1155/2012/252981
27. R.P. Chartoff, J.D. Menczel, S. H. Dillman. Dynamic mechanical analysis (DMA). In: J.D. Menczel, R.B. Prime. Thermal Analysis of Polymers – Fundamentals and Applications. John Wily & Sons: New Jersey (2009).
28. A.N. Frone, S. Berlioz, J.-F. Chailan, D.M. Panaitescu, D. Donescu. Cellulose fibre-reinforced polylactic acid. Polymer Composites 2011; 32:976-985.
DOI: 10.1002/pc.21116
29. D. Bikiaris. Can nanoparticles really enhance thermal stability of polymers? Part II: An overview on thermal decomposition of polycondensation polymers. Thermochimica Acta 2011; 523:25-45.
DOI: 10.1016/j.tca.2011.06.012
30. E.G. Bajsić, V.O. Bulatović, M. Slouf, A. Šitum. Characterization of biodegradable polycaprolactone containing titanium dioxide micro and nanoparticles. International Journal of Chemical, Nuclear, Metallurgical and Materials Engineering 2014; 8:572-576.
31. M. Naffakh, A.M. Díez-Pascua. Thermoplastic polymer nanocomposites based on inorganic fullerene-like nanoparticles and inorganic nanotubes. Inorganics 2014; 2:291-312.
DOI: 10.3390/inorganics2020291
32. A.K.F. Dyab, H.A. Al-Lohedan, H.A. Essawy, A.I.A.A. El-Mageed, F. Taha. Fabrication of core/shell hybrid organic–inorganic polymer microspheres via Pickering emulsion polymerization using laponite nanoparticles. Journal of Saudi Chemical Society 2014; 18:610-617.
DOI: 10.1016/j.jscs.2011.12.008
33. A.K. Bledzki, A. Jaszkiewicz. Mechanical performance of biocomposites based on PLA and PHBV reinforced with natural fibres – A comparative study to PP. Composites Science and Technology 2010; 70:1687-1696.
DOI: 10.1016/j.compscitech.2010.06.005

34. S. Modi, K. Koelling, Y. Vodovotz. Miscibility of poly(3-hydroxybutyrate-co-3-hydroxyvalerate) with high molecular weight poly(lactic acid) blends determined by thermal analysis. Journal of Applied Polymer Science 2012; 124:3074-3081.
DOI: 10.1002/app.35343

35. B.M.P. Ferreira, C.A.C. Zavaglia, E.A.R. Duek. Films of PLLA/PHBV: The thermal, morphological and mechanical characterization. Journal of Applied Polymer Science 2002; 86:2898-2906.
DOI: 10.1002/app.11334

36. E. Laredo, M. Grimau, A. Bello, D.F. Wu, Y.S. Zhang, D.P. Lin. AC conductivity of selectively located carbon nanotubes in poly(ε-caprolactone)/polylactide blend nanocomposites. Biomacromolecules 2010; 11:1339-1347.
DOI: 10.1021/bm100135n

37. L. Cabedo, J.L. Feijoo, M.P. Villanueva, J.M. Lagarón, E. Giménez. Optimization of biodegradable nanocomposites based on aPLA/PCL blends for food packaging applications. Macromolecular Symposia 2006; 233:191-197.
DOI: 10.1002/masy.200650124

38. S. Jain, M.M. Reddy, A.K. Mohanty, M. Misra, A.K. Ghosh. A new biodegradable flexible composite sheet from poly(lactic acid)/poly(ε-caprolactone) blends and micro-talc. Macromolecular Materials and Engineering 2010; 295:750-762.
DOI: 10.1002/mame.201000063

39. M. Amirian, A.N. Chakoli, W. Cai, J.H. Sui. In vitro degradation of poly(L-lactide)/poly(ε-caprolactone) blend reinforced with MWCNTs. Iranian Polymer Journal 2012; 21:165-174.
DOI: 10.1007/s13726-012-0014-5

40. D. Wu, Y. Zhang, M. Zhang, W. Yu. Selective localization of multiwalled carbon nanotubes in poly(ε-caprolactone)/polylactide blend. Biomacromolecules 2009; 10:417-424.
DOI: 10.1021/bm801183f

41. D. Wu, D. Lin, J. Zhang, W. Zhou, M. Zhang, Y. Zhang, D. Wang, B. Lin. Selective localization of nanofillers: Effect on morphology and crystallization of PLA/PCL blends. Macromolecular Chemistry and Physics 2011; 212:613-6256.
DOI: 10.1002/mapc.201000579

42. Z. Yu, J. Yin, S. Yan, Y. Xie, J. Ma, X. Chen. Biodegradable poly(L-lactide)/poly(ε-caprolactone)-modified montmorillonite nanocomposites: Preparation and characterization. Polymer 2007; 48:6439-6447.
DOI: 10.1016/j.polymer.2007.07.024
43. D. Ju, L. Han, F. Li, S. Chen, L. Dong. Poly(ε-caprolactone) composites reinforced by biodegradable poly(3-hydroxybutyrate-co-3-hydroxyvalerate) fiber. International Journal of Biological Macromolecules 2014; 67:343-350.
DOI: 10.1016/j.ijbiomac.2014.03.048
44. K. Wessler, M.H. Nishida, J. da Silva Jr, A.P.T. Pezzin, S.H. Pezzin. Thermal properties and morphology of poly(3-hydroxybutyrate-co-3-hydroxyvalerate) with poly(caprolactone triol) mixtures. Macromolecular Symposia 2006; 245-246:161-165.
DOI: 10.1002/masy.200651322
45. V. Chiono, G. Ciardelli, G. Vozzi, M. G. Sotgiu, B. Vinci, C. Domenici, P. Giusti. Poly(3-hydroxybutyrate-co-3-hydroxyvalerate)/poly(ε-caprolactone) blends for tissue engineering applications in the form of hollow fibers. Journal of Biomedical Materials Research Part A 2008; 85A:938-953.
DOI: 10.1002/jbm.a.31513

Chapter 2

Morphology and thermal degradation studies of melt-mixed PLA/PHBV biodegradable polymer blend nanocomposites with TiO_2 as filler

This chapter has been published as:
J.P. Mofokeng, A.S. Luyt. Morphology and thermal degradation studies of melt-mixed PLA/PHBV biodegradable polymer blend nanocomposites with TiO_2 as filler. Journal of Applied Polymer Science 2015; 132:42138
DOI: 10.1002/app.42138

Abstract

The morphology and thermal stability of melt-mixed PLA/PHBV blends and nanocomposites with small amounts of TiO_2 nanoparticles were investigated. PLA/PHBV at 50/50 w/w formed a co-continuous structure, and most of the TiO_2 nanoparticles were well dispersed in the PLA phase and on the interface between PLA and PHBV, with a small number of large agglomerates in the PHBV phase. Thermogravimetric analysis (TGA) and TGA-Fourier-transform infrared (FTIR) spectroscopy was used to study the thermal stability and degradation behaviour of the two polymers, their blends and nanocomposites. The thermal stability of PHBV was improved through blending with PLA, while that of PLA was reduced through blending with PHBV, and the presence of TiO_2 nanoparticles seemingly improved the thermal stability of both polymers in the blend. However, the degradation kinetics results revealed that the nanoparticles could catalyse the degradation process and/or retard the volatilization of the degradation products, depending on their localization and their interaction with the polymer in question.

Keywords: poly(lactic acid); poly(hydroxybutyrate-co-valerate); titania; blends; nanocomposites; thermal degradation

2.1. Introduction

In recent years, environmental pollution has become a great concern due to the high impact of plastic waste in daily use and the out of control emission of carbon dioxide into the atmosphere. Studies of biobased and biodegradable polymers, more so from renewable resources, have attracted increased attention due to the great demand to reduce dependence on petroleum-based polymers which is the main source of plastic waste. Biodegradable polymers are believed to be an environmentally friendly replacement of the current petrochemical based polymers. Recent interests in these biodegradable polymers are encouraged by the increasing cost of petroleum oil, as well as concerns for the environment and a shift towards sustainable manufacturing [1-5]. The applications of biodegradable polymers currently include mainly agriculture, biomedical, and food packaging applications. However, there is a large potential for many other applications such as automotive, aerospace, medical equipment, and various sanitary products [6].

One of the most commonly used bio-based and biodegradable polymers, poly(lactic acid) (PLA), is produced by the ring opening polymerization of lactide or the condensation polymerization of lactic acid monomers produced from renewable resources *via* a fermentation process [7,8]. Due to its commercial availability at a low cost, it has been broadly studied and used mainly for packaging and biomedical applications. PLA has good mechanical properties and biocompatibility, as well as thermo-plasticity comparable to that of petro-chemically derived polymers. It is known to degrade well when disposed along with municipal waste, so it is less of a burden to the environment [2,3]. Even though PLA is a very attractive biodegradable polymer, it cannot fully satisfy the requirements of industry. Disadvantages like poor melt properties, brittleness and low thermal resistance limits its use in different applications. To overcome these problems, several methods were implemented and used to improve the lacking properties in PLA. These include blending with other biodegradable polymers, plasticization, and copolymerization. Among these methods, blending was reported to be the easiest and most cost effective [9]. Polymer blends had been extensively studied because it presents the possibility of enhancing the overall properties of the final material through a synergistic combination of the desirable properties of each component in one system [10-12].

A range of renewable biodegradable polymers are currently available on the market, amongst others the polyhydroxyalkanoates (PHAs). The PHAs are a family of polyesters

produced by microorganisms. The most common PHA is poly(hydroxybutyrate) (PHB). Poly(hydroxybutyrate-co-valerate) (PHBV) is another PHA and is a co-polymer of PHB with randomly arranged 3-hydroxybutyrate and 3-hydroxyvalerate groups. This co-polymer was developed to improve PHB flexibility and thermal stability, and to lower its melting temperature and reduce its high crystallinity. PHBV has good flexibility and processing capabilities [13].

Most polymer pairs are thermodynamically immiscible as a result of their unfavourable interaction. The macrophase separation and poor interfacial adhesion restrict property combination of the two components in the blend. In recent years a new concept of compatibilisation by using inorganic nanoparticles has been introduced. Unfortunately there are relatively few studies dealing with immiscible polymer blends whose interfaces are stabilized by solid particles [14-17].

Nanometre inorganic compounds such as titanium dioxide (TiO_2), zinc oxide (ZnO), silica (SiO_2), aluminium dioxide (Al_2O_3), and silicon nitride (Si_3N_4) were tried as fillers in fabrics and polymers to improve the tribological properties. TiO_2 has received most of the attention because of its good thermal stability, accessibility, and catalytic properties. It is an inorganic material obtained from a variety of naturally occurring ores that contain ilmenite, rutile, anatase, and leucoxene, which are mined from deposits located throughout the world. It is generally used for various applications including photo electrochemical activity, solar energy conversion, photocatalysis, UV detection, ultrasonic sensing, and as a promising material in applications such as water or wastewater treatment. Environmental compatibility, non-toxicity and low price are some practical advantages of TiO_2 [18-23].

Few studies reported on the selective localization of inorganic nanoparticles in one of the phases in a polymer blend, or at the interface between the two polymers. The filler will selectively locate itself in order to reduce interfacial tension, and to reduce free surface energy, and as a result it may improve the interfacial interaction between the two polymers. This selective localization of the filler is mainly the result of the large difference in the affinity between the filler and the two matrix components. Thermodynamically the filler will be expected to locate in the lower viscosity phase to balance the viscoelastic difference between the two matrix components, which will contribute to the compatibility and improve the desired final properties. This assumption is based on entropy effects, where the entropy will be higher in the lower viscosity polymer in the molten state due to ease of chain movement. The nanoparticles should

therefore disperse more easily in the lower viscosity polymer to balance and reduce the levels of disorder between the two polymers in the blend. It has also been reported that lower viscosity polymers has the ability to accommodate higher filler volumes [24]. Wu *et al.* [17,25] introduced multi-walled carbon nanotubes (MWCNTs) into a 30:70 w/w PLA/PCL blend. They found that the MWCNTs were selectively dispersed in the lower viscosity PCL phase and on the interface. They explained that such a selective localization of the MWCNTs not only prevented the coalescence of the discrete PLA phase, but also enhanced the interfacial adhesion. In this case the MWCNTs acted as nano-reinforcement and compatibilizer, simultaneously improving the morphology and final properties of the PLA/PCL blend. If the filler is located at the interface of the two components, it can to some degree reduce the overall free energy of blending, leading to a thermodynamically driven compatibility. The localization of the filler is important to the final morphology and property control of immiscible blends.

Young's equation (Equation 2.1) is used to predict selective particle distribution in a polymer blend by calculating the wetting coefficient (ω_α) [26].

$$\omega_a = \frac{\gamma_{PolymerB-Filler} - \gamma_{PolymerA-Filler}}{\gamma_{PolymerA-PolymerB}} \tag{2.1}$$

where $\gamma_{polymerB\text{-}Filler}$ is the interfacial tension between polymer B and the filler, $\gamma_{polymerA\text{-}Filler}$ the interfacial tension between polymer A and the filler, and $\gamma_{polymerA\text{-}PolymerB}$ the interfacial tension between polymers A and B. The value of the wetting coefficient is normally used to determine where the filler is likely expected to disperse. If $\omega_\alpha < -1$, the particles are predicted to be localised in polymer B, if $\omega_\alpha > 1$, they are dispersed in polymer A, and if the value of ω_α is between -1 and 1, the nanoparticles are likely dispersed on the interface between the two polymers in the blend [12]. In rare cases where the particles are dispersed in both the interface and one of the phases, the third condition does not apply, so that a negative ω_α indicates dispersion of the particles in polymer B as well as the interface, and a positive ω_α indicates dispersion of the particles in polymer A and on the interface [27-28].

Both PLA and PHBV are biodegradable polymers. Blending of PLA with PHBV could provide a practical way of improving or tailoring the structure and properties of the material, without compromising the biodegradability. Another important aspect of blending these two

polymers is that the crystallinity of the blend will be improved since PHBV is highly crystalline when compared to PLA. A number of studies reported on the preparation of PLA/PHBV blends by solvent casting processes. This method was reported to improve the intimacy between the components in the blends. Although it has the important advantage of improving the mixing and interaction between the components in a blend, solution mixing is a very expensive method for preparation of blend samples, and it is not industrially viable because solvents are expensive and difficult to dispose of in an environmentally friendly way. Therefore the use of melt-mixing is considered as a more acceptable way of sample preparation [10,29-32].

In the present work the effect of blending of PLA with PHBV in the presence of TiO_2 nanoparticles as filler on the thermal stability and degradation behaviour of PLA/PHBV/TiO_2 nanocomposites was studied. The structure and properties of the blend nanocomposites were also studied and related to the thermal behaviour of the samples.

2.2. Experimental

2.2.1. Materials

The polylactic acid (PLA) used in the study is a commercial grade (PLA 2002D), obtained from Natureworks, LLC. (USA). It has a D-isomer content of 4%, a density of 1.24 g cm^{-3}, a glass transition temperature of ~53 °C, a melting temperature of ~153 °C, with a degree of crystallinity of 33%. The poly(hydroxy-butyrate-co-valerate) (PHBV) biopolymer used was purchased from Goodfellow, Huntington, UK with a 12% PHV content, density of 1.25 g cm^{-3}, a melting temperature of ~150 °C, and a degree of crystallinity of 59%. Anatase titanium(IV)oxide (TiO_2) with particle sizes < 25 nm and 99.7% purity was supplied by Sigma-Aldrich.

2.2.2. Preparation method

The samples were prepared *via* melt-mixing using a Brabender Plastograph. PLA and PHBV were dried in an oven at 80 °C for four hours prior to mixing, and TiO_2 was used as received. 30/70, 50/50, and 70/30 w/w PLA/PHBV blends and their nanocomposites with 1, 3 and 5 wt% of TiO_2 were mixed at 170 °C for ten minutes. The samples were compression moulded into 2

mm thick sheets at the same temperature for 5 minutes using a hydraulic press at a pressure of 50 bar, after which they were removed and left to cool under ambient conditions.

2.2.3. Characterization

Size exclusion chromatography (SEC) measurements were performed on a PL Olexis column (Polymer Laboratories). Chloroform was used as mobile phase at a flow rate of 1.00 mL min^{-1}. The samples were prepared at a concentration of 2 mg mL^{-1}. The column was calibrated with polystyrene (PS) standards from Polymer Laboratories (Church Stretton, Shropshire, UK). The chromatograph comprised of a Waters 1515 isocratic pump, a Waters inline degasser AF, and a Waters 717 Plus auto sampler with a 100 µL sample loop. The system was connected to an evaporative light scattering detector (PL-ELS 1000). Nitrogen was used as carrier gas in the ELSD, at a flow rate of 1.5 SLM. The evaporator and nebulizer temperatures were set at 100 and 40 °C, respectively.

The melt flow index of the two polymers in the blend was determined using a CEAST Melt Flow Junior. Ten samples each of both polymers were analysed at 180 °C. The amount of sample which flowed through the die over a period of 10 minutes under 2.16 kg weight was determined in each case.

Differential scanning calorimetry (DSC) was used to determine the polymers' degree of crystallinity. The analyses were performed under nitrogen flow (20 ml min^{-1}) from 0 to 170 °C at 10 °C min^{-1}. The melting enthalpies of the polymers were determined, and Equation 2.2 was used to calculate their crystallinities.

$$X_C(\%) = \left(\frac{\Delta H_m}{\Delta H_m^o} \right) \times 100\% \qquad (2.2)$$

where ΔH_m is the melting enthalpy, ΔH_m^0 is the melting enthalpy of the 100% crystalline polymer. Values of 93.7 J g^{-1} [3] and 109 J g^{-1} [3,31] were used for PLA and PHBV respectively, and the results are included in the methods section .

A Tescan VEGA3 scanning electron microscope (SEM) was used to study the surface dispersion of the TiO_2 nanoparticles in the PLA/PHBV blends. The liquid nitrogen fractured

samples were spatter coated with gold for 30 seconds to eliminate sample charging, and analyses were performed at three different magnifications.

The morphologies of the nanocomposites were characterised by transmission electron microscopy (TEM). Images were obtained using a 200 kV FEI Tecnai 20 TEM fitted with Gatan Tridiem. The 50/50 w/w PLA/PHBV blend with 5 wt% TiO_2 nanoparticles was trimmed and sectioned to fit the ultra-microtome, since they were hard enough to cut without cooling. 100-150 nm thin sections were collected on copper grids and viewed. Staining was not necessary as the different phases could easily be distinguished. For TEM-EDS analyses the samples were sectioned at 150 nm using a Leica UC7 (Vienna, Austria) ultramicrotome, and examined with a Philips (FEI) (Eindhoven, The Netherlands) CM100 transmission electron microscope at 60 keV. EDS spectra were obtained with an Oxford X-Max (80 mm^2) analyser (Wycombe, UK).

The contact angle measurements of the samples were conducted at room temperature on a surface energy evaluation system, based on the sessile drop method. At least 5 replicates were analysed for each sample to ensure reproducibility of the results. The contact angles and surface energies of TiO_2 were acquired from the literature [34]. Distilled water (H_2O), and diiodomethane (CH_2I_2) were used as polar and non-polar solvents, respectively. The literature values of their surface energies are: (H_2O: γ^p = 50.7 mJ m^{-2} and γ^d = 22.1 mJ m^{-2}; CH_2I_2: γ^p = 6.7 mJ m^{-2} and γ^d = 44.1 mJ m^{-2}). The contact angles, total surface energies, as well as their dispersive and polar surface components, were calculated using the Owens-Wendt method (Equations 2.3 and 2.4) [12,34,35].

$$\gamma_s = \gamma_s^{\,d} + \gamma_s^{\,p} \tag{2.3}$$

$$\gamma_1\left(1+\cos\theta\right) = 2\sqrt{\gamma_s^{\,d}.\gamma_l^{\,d} + \gamma_s^{\,p}.\gamma_l^{\,p}} \tag{2.4}$$

where θ is the contact angle, γ is the surface energy, the subscripts ‘s’ and ‘l’ indicate solid and liquid respectively, while ‘d’ and ‘p’ indicate the dispersive and polar components, respectively. If the contact angle of at least two liquids, usually a polar and nonpolar with known γ_l^d and γ_l^p values, are measured on a solid surface, the γ_s^d and γ_s^p and the total surface energy (γ_s) of the solid can be calculated by combining Equations 2 and 3 [36]. The interfacial tensions between the

components in a blend were calculated from the contact angle measurement results using the geometric mean equation (Equation 2.5) [12,27].

$$\gamma_{12} = \gamma_1 + \gamma_2 - \sqrt[2]{\gamma_1^{\,d}.\gamma_2^{\,d} + \gamma_1^{\,p}.\gamma_2^{\,p}} \qquad (2.5)$$

where γ_{12} = interfacial tension between components 1 and 2 in the blend, γ_1 and γ_2 are the total surface energies of components 1 and 2, γ_1^{d} and γ_2^{d} are the dispersive surface energies of components 1 and 2, and γ_1^{p} and γ_2^{p} are the polar surface energies of the components in the nanocomposites.

A Perkin-Elmer STA6000 thermogravimetric analyser (TGA) was used to analyse the thermal degradation behaviour of the samples. The analyses were done from 30 to 600 °C at a heating rate of 10 °C min^{-1} under nitrogen atmosphere. The sample masses were ~24 mg. The samples for thermal degradation kinetics were run at 3, 5, 7, 9 and 15 °C min^{-1} heating rates under nitrogen atmosphere, and the TGA's integrated kinetics software (based on the Flynn-Ozawa-Wall method (Equation 2.6)) was used to calculate the activation energies:

$$\ln \beta = c - 1.052\left(\frac{E_a}{RT}\right) \qquad (2.6)$$

where β = heating rate in K min^{-1}, c is a constant, E_α = activation energy in kJ mol^{-1}, R = universal gas constant, and T = temperature in K. The plot of ln β vs. 1/T, obtained from the TGA curves recorded at several heating rates, should be a straight line. The activation energy was evaluated from its slope. The TGA was also connected to a Perkin-Elmer Spectrum 100 Fourier-transform infrared (FTIR) spectrometer to analyse the thermal degradation volatiles. The same temperature range and heating rate were used, and the volatiles were transferred to FTIR by a Perkin-Elmer TL 8000 balanced flow FT-IR EGA system at 200ºC and a flow rate of 150 ml min^{-1}. Spectra were collected at five different temperatures during the degradation process.

2.3. Results and discussion

2.3.1 Molar mass analysis by SEC

The SEC results in Table 2.1 show that PLA has a higher molar mass and dispersity than PHBV. These results will be used later in this paper when the morphologies of the blend nanocomposites are discussed.

Table 2.1 Summary of molar masses, melt flow index and surface properties of PLA, PHBV and titania

	Contact angle / deg		**Surface energy / mN m^{-1}**			**Molar mass / g mol^{-1}**		**D**	**MFI / (g/10 min)**
	H_2O	**CH_2I_2**	**γ**	**γ^d**	**γ^p**	**M_n**	**M_w**		
PLA	44.7 ± 1.0	35.4 ± 0.0	62.0	41.8	20.2	55047	142500	2.6	2.8
PHBV	54.7 ± 0.5	35.6 ± 0.7	56.3	41.7	14.6	36710	77537	2.1	8.1
TiO_2	19.7	10.1	80.7	46.4	34.3				

γ = surface energy, γ^d = dispersive component of surface energy, γ^p = polar component of surface energy, M_n = number average molar mass, M_w = weight average molar mass, D = dispersity index, MFI = melt flow index

2.3.2 Morphology

Figure 2.1 shows the SEM micrographs of the 50/50 w/w PLA/PHBV blend nanocomposites with 5 wt% TiO_2. In order to achieve good material properties the reinforcement or filler should be well dispersed and should have good interaction with the matrix. In this system no chemical interaction was expected, so only physical interactions were studied. The small particulate objects (shown with arrows and in the circle in Figure 2.1) are TiO_2 nanoparticles in the blend; they seem to be well dispersed and embedded in the polymer matrices.

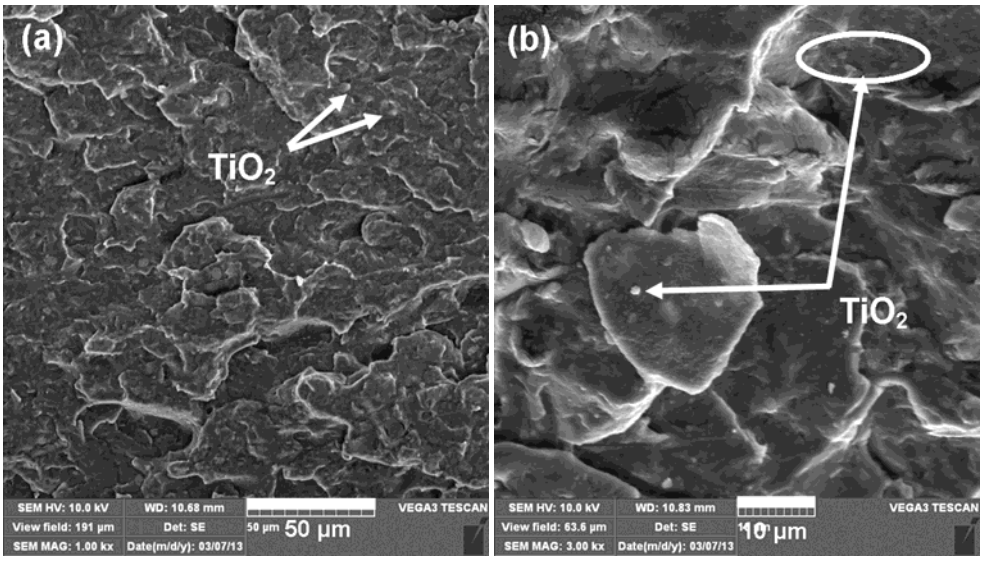

Figure 2.1 SEM micrographs of 50/50 w/w PLA/PHBVwith 5wt% TiO_2 at (a) 1000x and (b) 3000x magnifications

Most polymer blends are thermodynamically immiscible, and consequently a multi-phase phase morphology is usually observed. The two polymers can be clearly distinguished in Figure 2, and a co-continuous morphology is observed. The darker phase in the TEM photos is PHBV, and the TiO_2 nanoparticles are clearly visible. They are well dispersed in the PLA phase and on the PLA-PHBV interface, with some agglomerates. A very small number of agglomerates are visible in the PHBV phase. One would expect this selective localization of the nanoparticles in the PLA phase, and on the interface between PLA and PHBV, to be the result of the difference in molar mass, viscosity and crystallinity of these two polymers. According to the SEC results in Table 2.1 the PLA has a higher molar mass and a much higher melt viscosity (lower melt flow index) than PHBV. The nanoparticles would be expected to diffuse into the lower viscosity polymer in order to balance the viscoelastic properties. In this case, however, the nanoparticles are dispersed in the PLA phase. The crystallinity difference between the polymers could have been the driving force for the nanoparticles to select a polymer, since the inorganic nanoparticles would tend to locate themselves in the amorphous phase of a polymer. The PLA with its lower crystallinity (33% compared to 59% for PHBV) will in this respect be better suited as matrix for the nanoparticles. Another factor that could have influenced the selective localization of the nanoparticles is the difference in the surface energy between the components in the nanocomposite. If there are no specific interactions, this should determine how strong the

nanoparticles will interact with a specific polymer. In this case the PLA has a surface energy (62.0 mN m^{-1}) which is closer to that of TiO_2 (80.7 mN m^{-1}) than PHBV (56.3 mN m^{-1}**),** and the polar characters of PLA and TiO_2 (20.2 and 34.3 mN m^{-1} respectively) are closer to each other than those of PHBV and TiO_2 (14.6 and 34.3 mN m^{-1}) (see Table 2.1). These surface energy values were determined at room temperature, but they may be different from the values at the mixing temperature we used, and therefore we can only assume that the values in Table 2.1 are not too much different from what the values would have been if the surface energies were determined at 170 °C.

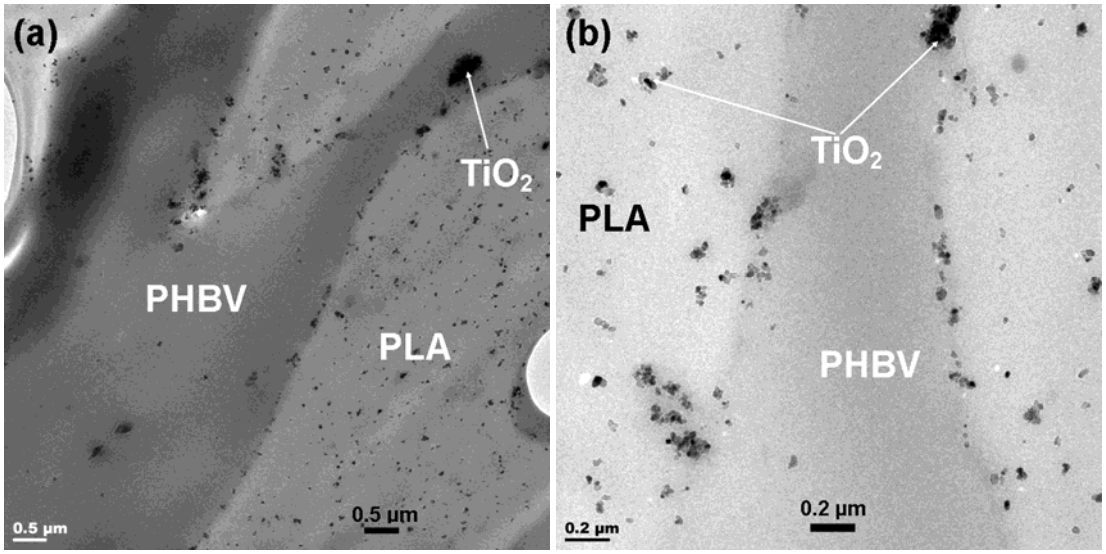

Figure 2.2 TEM micrographs of 50/50 w/w PLA/PHBV with 5 wt% TiO_2 at (a) 5700× and (b) 19000× magnifications

TEM-EDS analysis of the blend nanocomposite clearly shows that the filler is finely dispersed in the PLA phase, while some large agglomerates are visible in the PHBV phase (Figure 2.3). Figure 3a shows a continuous PLA phase with the PHBV phase dispersed in it, although the morphology is clearly close to co-continuity. The EDS elemental analysis (Figure 2.3b) shows that there is no dispersed titania in the PHBV phase (solid ellipse), but only large agglomerates (dashed ellipse) that are almost pure titania, while the PLA phase clearly contains titania which is visible as small, finely dispersed particles (dotted ellipse). These particles also form a well-defined border on the inter-phase between the two polymers (see arrows in Figures 2.3b and 2.3c).

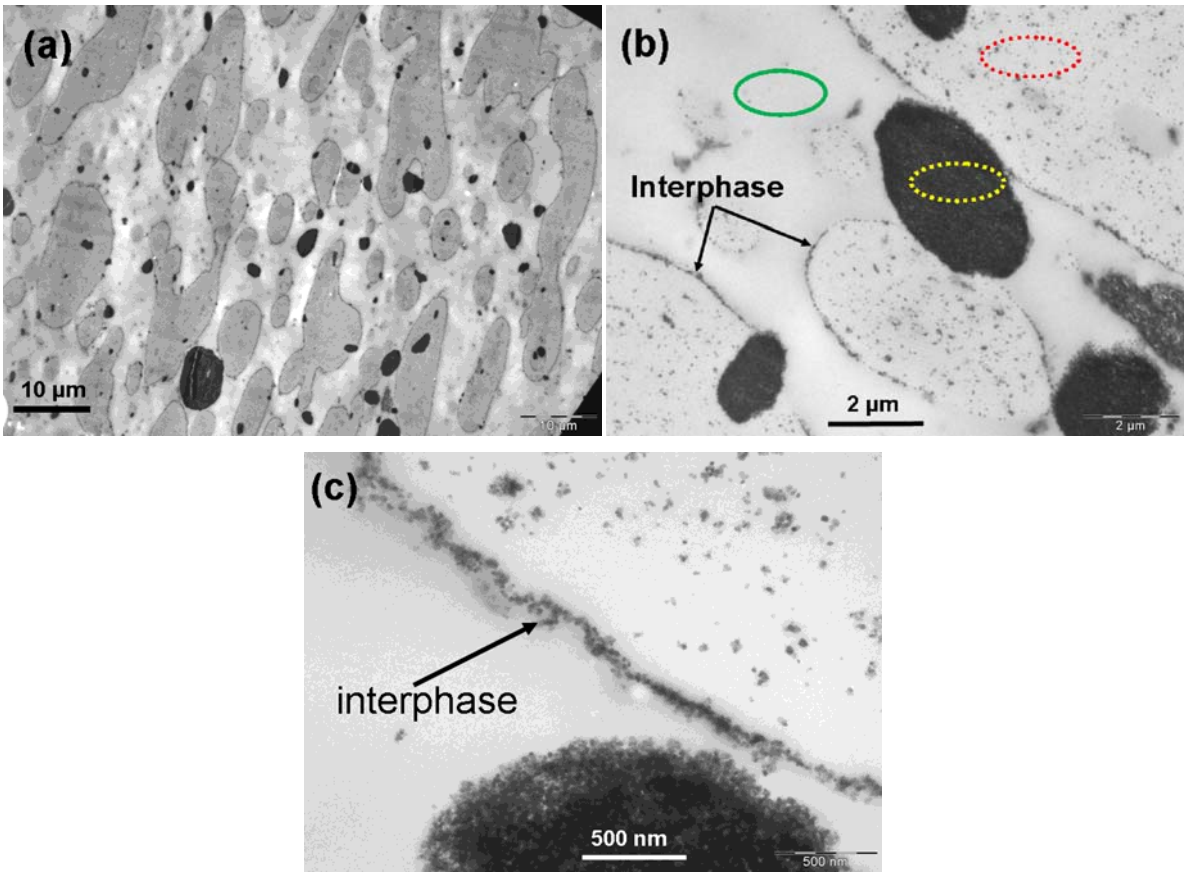

Figure 2.3 TEM-EDS micrographs of 50/50 w/wPLA/PHBV with 5 wt% of TiO_2 to illustrate the localization of nanoparticles in the different phases of the blend, showing (a) the morphology, (b) positions for the elemental analyses, and (c) a detailed view of the filler particle distribution

The wetting coefficient model [12,26-28] was applied to confirm the TEM and TEM-EDS results. The contact angles and surface energies of PLA, PHBV and TiO_2 are presented in Table 2.1, and the interfacial tensions and wetting coefficient are summarised in Table 2.2. The wetting coefficient value of 5.09 indicates that the nanoparticles should be situated in PLA and maybe on the interface. There are two factors involved in determining the selective localisation of the TiO_2 nanoparticles in a two-phase polymer blend, and those are thermodynamic and kinetic effects. Thermodynamically the particles interact more favourably with one of the polymers in order to decrease the system's free energy, and they will tend to locate in such a way to minimize the

interfacial tension between the polymers, and hence improve the interfacial adhesion between the two phases. This happens mostly when the particles are located at the interface between the two components [25]. At equilibrium the particles will likely disperse in the phase where the affinity between the polymer and the nanoparticles is high. The calculated interfacial tensions from the surface energy results indicate that the interfacial tension between PHBV and TiO_2 (4.27 mN m^{-1}) is higher than that between PLA and TiO_2 (1.98 mN m^{-1}). This explains why they preferably disperse in the PLA phase.

Table 2.2 Interfacial tensions and wetting coefficient of the investigated materials

Component couple	Interfacial tension / mN m^{-1} and wetting coefficient
PLA/PHBV	0.45
PLA/TiO_2	1.98
PHBV/TiO_2	4.27
ω_α	5.09

ω_α= wetting coefficient

Thermodymically, melt mixing of the two polymers with a significant difference in molar mass, viscosity and crystallinity, would give rise to the selective localization of the third component, which is TiO_2 nanoparticles in this case. PLA has a higher molar mass and viscosity than PHBV (Table 2.1). One would therefore expect the TiO_2 nanoparticles to more easily disperse in the PHBV phase, which is not the case as could be seen from the TEM and TEM-EDS results. However, differences in crystallinity could have played a role. Although both polymers are completely amorphous in the molten state where mixing takes place, it would be expected that during cooling when the polymers crystallize, the nanoparticles would be forced out of the more highly crystalline polymer because they would preferably tend to be in the amorphous phase of a polymer, unless the interaction between the nanoparticles and the polymer is strong enough that the nanoparticles can act as nucleating sites for the polymer. Because of the much higher crystallinity of PHBV and the much lower interfacial tension between PLA and TiO_2, it could be expected with some certainty that the nanoparticles would locate in the PLA phase and even to some extent act as nucleation sites for the crystallization of PLA. This again can be attributed to enhanced shearing forces in the higher viscosity PLA melt, that disperse the solid

TiO_2 particles. The strong interfacial tension between PHBV and TiO_2 also explains the large nanoparticles agglomerates in the PHBV phase, because the nanoparticles clearly have a higher affinity for each other than for the PHBV chains, and the melt-mixing torque was probably not enough to break up these agglomerates and re-disperse the particles in the PLA phase and on the interface. The relatively high melt viscosity of PLA, and the not-so-low PLA-TiO_2 interfacial tension, to some extent explains why a large number of nanoparticles are located at the PLA/PHBV interface.

2.3.3 Thermogravimetric analysis (TGA)

The good distribution of the filler in one of the polymers and on the interface should improve some properties in the PLA/PHBV blend nanocomposites, one of which is the thermal stability. Thermal degradation will reduce the usability of a polymer, especially in the case of recycling where the polymer undergoes several cycles of high and low temperatures. We used TGA and thermal degradation kinetics analyses to study the thermal degradation of the blends and their nanocomposites. Figures 2.4 to 2.6 show the effect of varying filler content on the mass loss curves of the blends at constant PLA/PHBV ratios. It is clear that the two polymers degrade separately, confirming their immiscibility. The temperature for 50% PHBV degradation was 280 °C, while that for 50% PLA degradation was 364 °C. This difference in thermal stability of PLA and PHBV is due to the structural difference between the two polymers. The PLA degradation proceeds according to a back-biting ester interchange reaction which takes place through a non-radical mechanism involving the –OH chain ends. The products vary with the reaction point in the backbone and can be lactide molecules, oligomeric rings, or acetaldehyde plus carbon monoxide. The thermal degradation of PHBV follows a random chain scission mechanism involving a β-hydrogen elimination process (six-membered ring ester decomposition process) to form substrate olefins and oligomers [10,37].

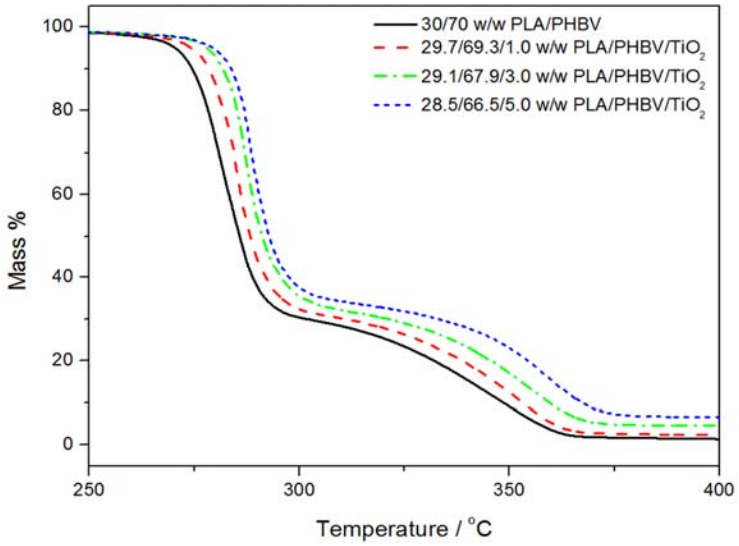

Figure 2.4 TGA curves of 30/70 w/w PLA/PHBV with different amounts of TiO_2

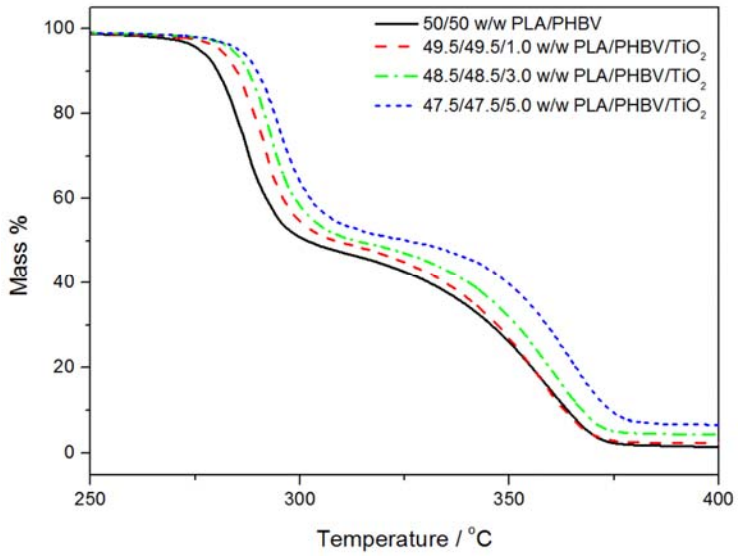

Figure 2.5 TGA curves of 50/50 w/w PLA/PHBV with different amounts of TiO_2

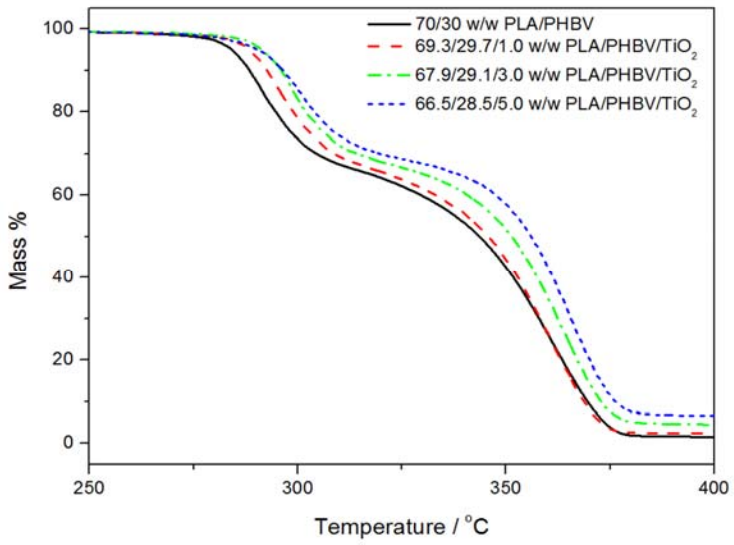

Figure 2.6 TGA curves of 70/30 w/w PLA/PHBV with different amounts of TiO_2

The thermal stability of PHBV observably improved (temperature at which 50% polymer degraded increased from about 280 to about 291°C) with an increase in PLA content in the blends, and further increased to 302°C in the presence of the nanoparticles; this is because PLA and TiO_2also absorb heat energy and because they have higher thermal stabilities than PHBV, they insulate the PHBV so that it starts to degrade at higher temperatures. On the other hand, the temperature at 50% mass loss of PLA decreased from 364 to 349 °C with increasing PHBV content in the blend, but again increased to the same level as that of pure PLA with increasing nanoparticle content. The influence of the nanoparticles on the thermal stabilities of the polymers can be attributed to the shielding effect of the nanoparticles [37-38], and/or a retardation effect of the nanoparticles on the movement of free radicals and volatile degradation products [34].This becomes clear when comparing the extent to which the thermal stability of the two polymers improved in the presence of TiO_2. The increase in degradation temperature was more significant in the case of PLA, which can be explained by the fact that nanosized particles were well dispersed in PLA which resulted in stronger and more effective interaction compared to PHBV. The % residue at 400 °C is about 1.5% for all the blends, which indicates a low level of char formation by the polymers themselves. If this percentage is subtracted from the values observed for the blend nanocomposites, the differences are almost exactly equal to the amount of titania

originally mixed into the blends. This indicates a fair dispersion of the filler in the blends, as was observed from the morphological analysis.

Figures 2.7 and 2.8 show the temperatures at 50% degradation of each component in the blends as function of titania content in the nanocomposites. These figures represent both the effect of blending and filler loading on the thermal stability of each polymer in the blends. Figure 2.7 was plotted with the temperatures calculated from the thermal degradation step of PHBV, and it clearly shows that when the PLA content increases the thermal stability of PHBV also increases, and that the stability even further improves with an increase in filler content. The degradation of PLA, on the other hand, decreases with increasing PHBV content, but the filler has a much stronger stabilizing effect on the degradation of PLA (Figure 2.8). This is a typical example where blending averages the properties of the two polymers in the blend, and where a well-dispersed inorganic filler retards the degradation of the polymer matrix in which it is dispersed. As discussed earlier, there are more filler particles well dispersed in the PLA, and therefore the filler has a stronger stabilizing effect on PLA degradation than on PHBV degradation.

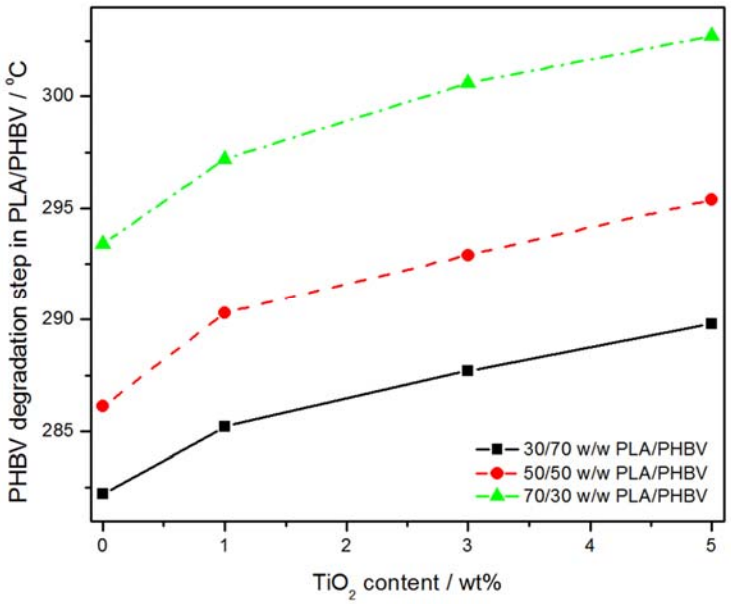

Figure 2.7 Effect of blending and filler addition on the temperature at 50% mass loss of PHBV in the PLA/PHBV blends and nanocomposites

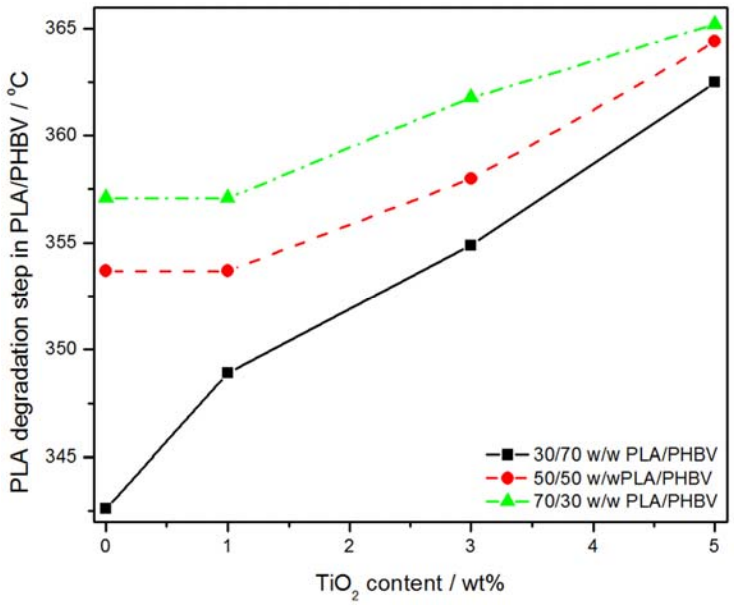

Figure 2.8 Effect of blending and filler addition on the temperature at 50% mass loss of PLA in the PLA/PHBV blends and nanocomposites

2.3.4 Degradation kinetics

Degradation kinetics analyses may assist in explaining the degradation behaviour of the polymers in the different samples. Figures 2.9 to 2.16 show the degradation kinetics results for the individual polymers without and with filler, and of their blends without and with TiO_2. The activation energy (E_α) of degradation of PLA slightly increased with extent of degradation at low conversions, but decreased quite significantly as the degradation proceeded (Figure 2.9). This indicates an auto-acceleration effect as the degradation progresses. In the presence of TiO_2, PLA has much lower activation energies of degradation, probably because of a catalytic effect of the nanoparticles on the PLA degradation [39,40]. It does, however, still show the initial increase followed by a decrease towards higher extents of degradation. This seems to be contrary to the fact that the presence of TiO_2 nanoparticles retarded the PLA degradation, as was indicated by the TGA results. However, it is quite possible that less energy is needed to initiate the degradation in the presence of titania nanoparticles, but that the nanoparticles may retard the diffusion of the volatile degradation products out of the polymer, so that the onset of mass loss is at a higher temperature for the PLA nanocomposite [39,40]. As can be seen in Figure 2.10, the mass loss rate (slope of the mass loss step) is steeper for the nanocomposite, which means that

the evolution of the volatile degradation products was faster after the onset of mass loss.Comparison of the FTIR spectra in Figure 2.11 clearly shows much lower intensities for the CO_2 peaks between 2300 and 2400 cm^{-1}, the –C=O vibration at about 1785 cm^{-1}, and the –C-O-C at about 1120 cm^{-1} between the spectra at comparable temperatures for the PLA in the nanocomposite compared to those for neat PLA. The carbonyl peak for the nanocomposite is also at a lower wavenumber (1762 cm^{-1}) than that for neat PLA (1789 cm^{-1}). Both these observations are strong indications that the degradation interacted with the nanoparticles, and that their volatilization has been retarded as a result of this.

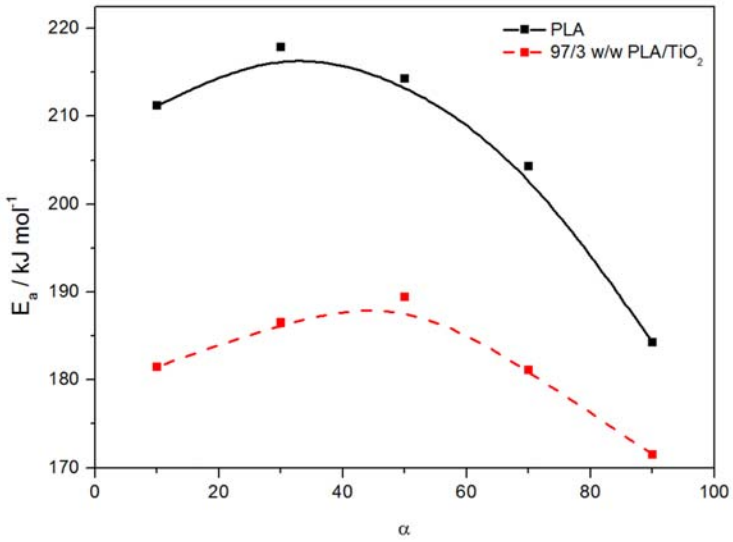

Figure 2.9 Activation energy vs. extent of degradation for PLA and PLA in the 97/3 w/w PLA/TiO_2 nanocomposite

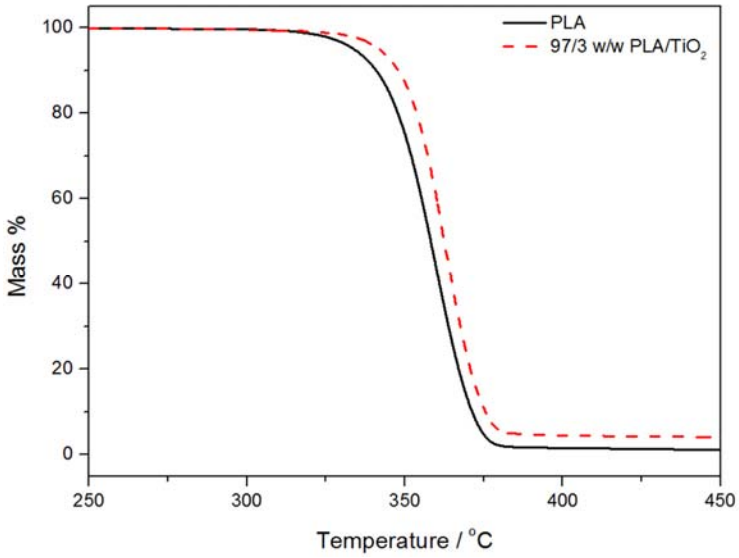

Figure 2.10 TGA curves of neat PLA and PLA in the 97/3 w/w PLA/TiO_2 nanocomposite

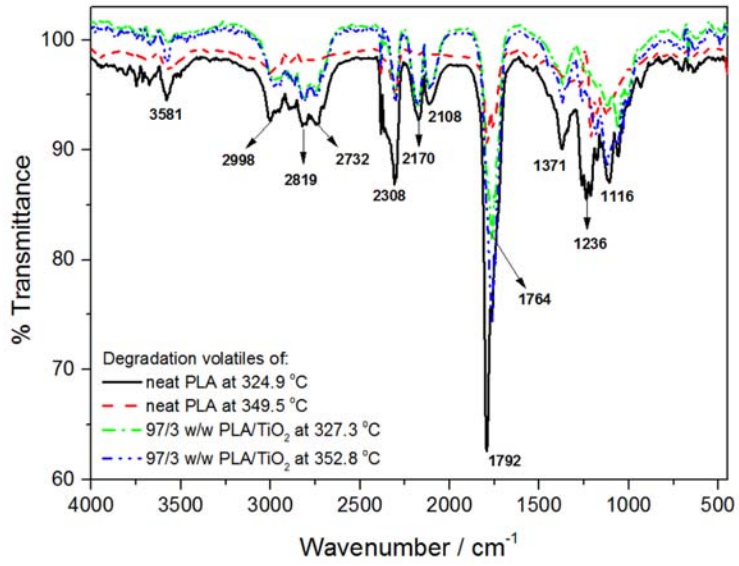

Figure 2.11 FTIR spectra of the degradation products of neat PLA and PLA in 97/3 w/w PLA/TiO_2

The activation energy of degradation of PHBV remained unchanged around 146 kJ mol^{-1} throughout the degradation process (Figure 2.12). This could mean that the degradation mechanism of pure PHBV did not change throughout the degradation process, which probably has a single rate-determining step because of the independence of E_α on the extent of degradation [39]. In the presence of TiO_2 the E_α started at 120 kJ mol^{-1} and increased almost linearly with

increasing degradation to 135 kJ mol^{-1}. The decrease in activation energy of PHBV in the presence of TiO_2 nanoparticles is initially about 25 kJ mol^{-1}, which is attributed to the lowering of the thermal stability at the initial stages of degradation. This indicates that the TiO_2 nanoparticles probably catalysed the degradation of PHBV [41,42], but that the effectiveness of this catalytic effect decreased with increasing extent of degradation, probably because the nanoparticles were much more agglomerated in PHBV than in PLA. It also seems as if the volatilization of the degradation products was initially retarded through interaction with the nanoparticles, because the onset of degradation for PHBV in the nanocomposite is clearly higher than that of neat PHBV, while the volatilization is clearly faster as can be seen from the slopes of the mass loss curves in Figure 2.13. The PHBV degradation products clearly did not interact so strongly with the nanoparticles as in the case of PLA, which is also clear from the FTIR spectra in Figure 2.14 that are almost identical for neat PHBV and PHBV in the nanocomposite at comparable temperatures. From these spectra it is also clear that the presence of the nanoparticles did not change the PHBV degradation mechanism.

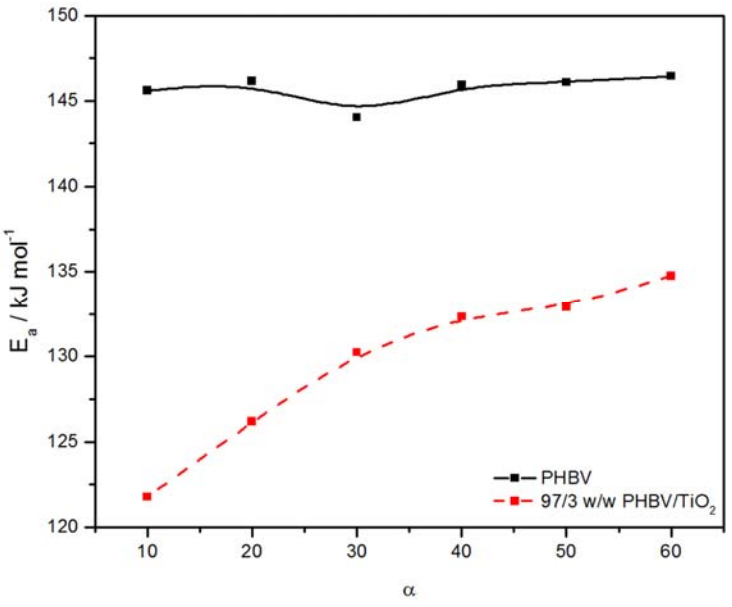

Figure 2.12 Activation energy vs. extent of degradation for PHBV and PHBV in the 97/3 w/w PHBV/TiO_2 nanocomposite

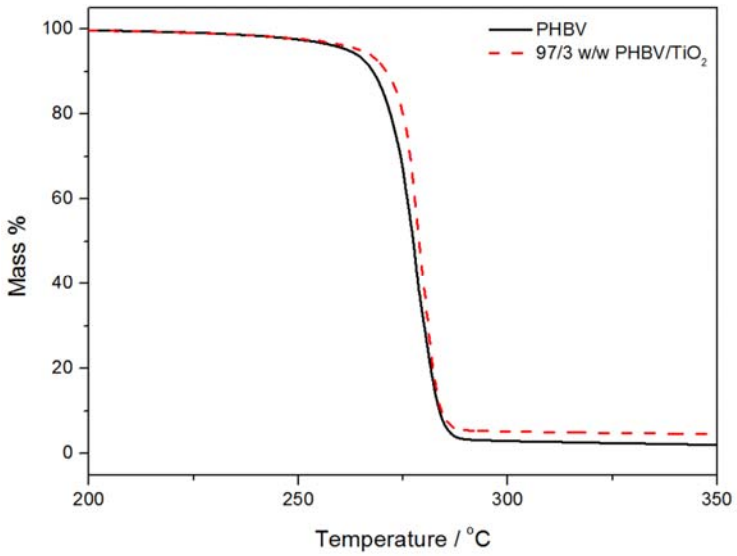

Figure 2.13 TGA curves of neat PHBV and PHBV in the 97/3 w/w PHBV/TiO_2 nanocomposite

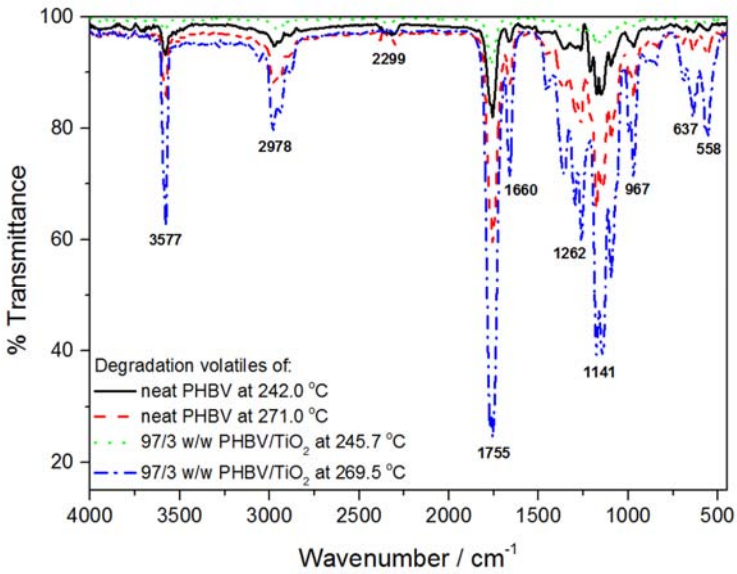

Figure 2.14 FTIR spectra of the degradation products of neat PHBV and PHBV in 97/3 w/w PHBV/TiO_2

Figure 2.15 illustrates how E_α changed with extent of degradation for the 50/50 PLA/PHBV blend and the 47.5/47.5/5.0 w/w PLA/PHBV/TiO_2 blend nanocomposite. The first part of the graph, up to about 47% mass loss, represents the activation energy for PHBV degradation. The

rest of the graph represents the activation energy for PLA degradation. The E_α of the PHBV in the blend is slightly lower than that of the pure PHBV (Figure 2.12).However, the decrease in E_α of the PHBV in the PLA/PHBV blend nanocomposite is much less significant than that of PHBV in the PHBV nanocomposite. The reason is probably that all the nanoparticles were in contact with PHBV in the PHBV nanocomposite, even if agglomerated, while most of the nanoparticles were in the PLA phase or on the interface in the blend nanocomposites. In the presence of the nanoparticles there is a very obvious decrease in the activation energy for PLA degradation, and the activation decreases with increasing extent of degradation, contrary to the increase observed for PLA in the blend. There is, however, not a clear-cut explanation for this observation. On the one hand the nanoparticles can retard the evaporation of the volatile degradation products, while on the other hand they may catalyse the degradation reaction. In this case it seems as if the catalysis effect is more dominant, and therefore the activation energy decreased with extent of degradation.

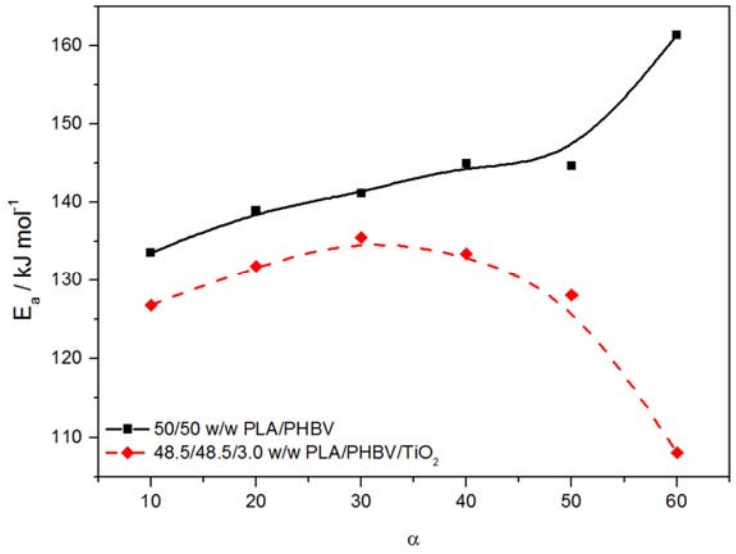

Figure 2.15 Activation energy vs. extent of degradation for a 50/50 w/w PLA/PHBV blend and its nanocomposite with 3 wt% TiO_2

The spectra of the degradation volatiles in Figure 2.16 were taken at approximately 280 °C (which falls within the PHBV degradation step) and 341 °C (which falls within the PLA degradation step. The peaks at 1660 cm^{-1} (C=C stretching), 1755 cm^{-1} (C=O stretching), 3581 and 968 cm^{-1} (O-H vibrations), and the bands in the range of 1500-800 cm^{-1} (CH_3, CH bending

vibrations and the heavily overlapped C-O-C and C-C stretching vibrations) in the 280 °C spectra (for the blend and the blend nanocomposite) indicate the presence of ester groups, carboxylic acids, and linear oligomers with crotonate end groups [10,42,44-46], that are the expected products from the degradation of PHBV, in the volatiles. Except for differences in the peak intensities, there is no difference between the spectra for PLA/PHBV and PLA/PHBV/TiO_2. This confirms that the degradation mechanism was not influenced by the presence of the nanoparticles. We did not present the FTIR curves of the volatiles at different temperatures during the degradation process, but these results show that the peaks in the PLA/PHBV spectrum reached their maximum intensity at a 10 °C lower temperature, which supports our previous observation that the TiO_2 nanoparticles probably interacted with the degradation volatiles and retarded their diffusion out of the sample.

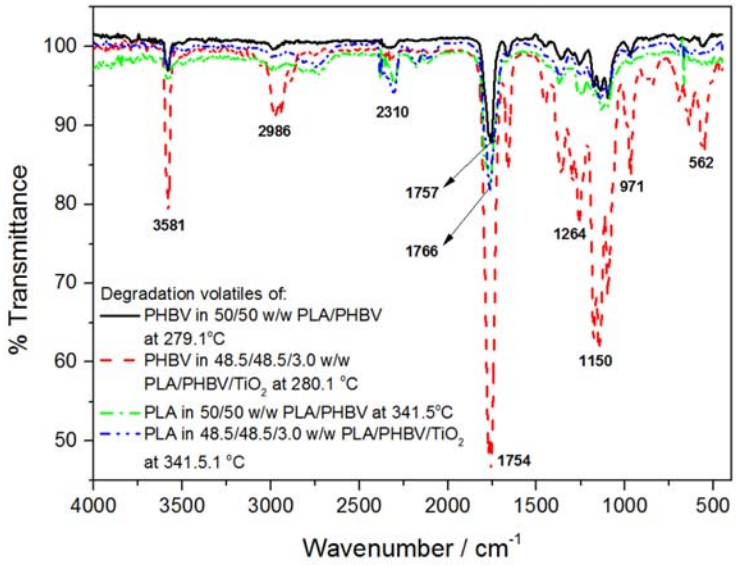

Figure 2.16 FTIR spectra of the degradation products of PHBV and PLA in 50/50 w/w PLA/PHBV and its nanocomposite with 3 wt% TiO_2

The spectra obtained at a higher temperature of 342 °C show peaks at 3580 cm^{-1} (O-H vibrations), 2997 and 2747 cm^{-1} (CH_2 stretching), 1766 cm^{-1} (C=O stretching), 1136 cm^{-} (C-O-C stretching), and 2310 cm^{-1} (CO_2 vibrations),that are characteristic of lactide molecules, oligomeric rings, and acetaldehyde plus carbon monoxide, that are the previously determined degradation products of PLA [10,37,43,46]. In this case there are also no differences between the

spectra of PLA/PHBV and PLA/PHBV/TiO_2, confirming that the presence of the nanoparticles did not change the degradation mechanism. In this case, however, the maximum peak intensities were observed at a lower temperature for PLA/PHBV/TiO_2, which is in line with the catalytic effect of the nanoparticles on the degradation of PLA, as mentioned in our degradation kinetics discussion.

2.4. Conclusions

The purpose of this work was to investigate the influence of blending and the presence of small amounts of titania nanoparticles on the thermal degradation behaviour of PLA and PHBV. The 50/50 w/w blend showed a co-continuous morphology, while the nanoparticles were selectively localised in the PLA phase and at the interface between PLA and PHBV. This was shown to be the result of differences in surface energies and interfacial tensions between the PLA, PHBV and TiO_2, as well as differences in the degree of crystallinity of PLA and PHBV. Blending of PLA with PHBV improved the thermal stability of PHBV, since PLA is more thermally stable, and the presence of the nanoparticles increased the mass loss temperatures of both polymers. This was, however, not necessarily an indication of better thermal stability, because all indications are that the well dispersed and small nanoparticles in PLA catalysed the degradation process, but also inhibited the diffusion of the degradation volatiles out of the sample. The same catalysis effect was not obvious in the case of PHBV, but the retardation of degradation product volatilization could also be seen in this case. It was further found that the presence of titania nanoparticles did not change the degradation mechanisms of the polymers.

2.5. References

1. L. As'habi, S.H. Jafari, H.A. Khonakdar, R. Boldt, U. Wagenknecht, G. Heinrich. Tuning the processability, morphology and biodegradability of clay incorporated PLA/LLDPE blends via selective localization of nanoclay induced by melt mixing sequence. eXPRESS Polymer Letters 2013; 7:21-39.
DOI:10.3144/expresspolymerlett.2013.3

2. Q. Guan, H.E. Naguib. Fabrication and characterization of PLA/PHBV-chitin nanocomposites and their foams. Journal of Polymers and the Environment 2014; 22:119-130.
DOI: 10.1007/s10924-013-0625-8
3. H. Zhao, Z. Cui, X. Wang, L.-S. Turng, X. Peng. Processing and characterization of solid and microcellular poly(lactic acid)/polyhydroxybuyrate-valerate (PLA/PHBV) and PLA/PHBV/clay nanocomposites. Composites Part B 2013; 51:79-91.
DOI: 10.1016/j.compositesb.2013.02.034
4. V. Ojijo, S.S. Ray, R. Sadiku. Role of specific interfacial area in controlling properties of immiscible blends of biodegradable polylactide and poly[(butylene succinate)-co-adipate]. Applied Materials & Interfaces 2012; 4:6690-6701.
DOI: 10.1021/am301842e
5. E. Schwach, L. Avérous. Starch-based biodegradable blends: Morphology and interface properties. Polymer International 2004; 53:2115-2124.
DOI: 10.1002/pi.1636
6. D. Cava, R. Gavara, J.M. Lagarón, A. Voelkel. Surface characterization of poly(lactic acid) and polycaprolactone by inverse gas chromatography. Journal of Chromatography A 2007; 1148:86-91.
DOI:10.1016/j.chroma.2007.02.110
7. M. Jamshidian, E.A. Tehrany, M. Imran, M. Jacquot, S. Desobry. Poly-lactic acid: Production, applications, nanocomposites, and release studies. Comprehensive Reviews in Food Science and Food Safety 2010; 9:552-571.
DOI: 10.1111/j.1541.2010.00126x
8. F. Signori, M.-B. Coltell, S. Bronco. Thermal degradation of poly(lactic acid) (PLA) and poly(butylene adipate-co-terephthalate) (PBAT) and their blends upon melt processing. Polymer Degradation and Stability 2009; 94:74-82.
DOI:10.1016/j.polymdegradstab.2008.10.004
9. H. Eslami, M.R. Kamal. Elongational rheology of biodegradable poly(lactic acid)/poly[(butylene succinate)-co-adipate] binary blends and poly(lactic acid)/poly[(butylene succinate)-co-adipate]/clay ternary nanocomposites. Journal of Applied Polymer Science 2013; 127:2290-2306.

DOI: 10.1002/app.37928

10. M.R. Nanda, M. Misra, A.K. Mohanty. The effect of process engineering on the performance of PLA and PHBV blends. Macromolecular Materials and Engineering 2011; 296:719-728.
DOI: 10.1002/mame201000417
11. Y. Tokiwa, B.P. Calabia, C.U. Ugwa, S. Aiba. Biodegradability of plastics. International Journal of Molecular Sciences 2009; 10:3722-3742.
DOI: 10.3390/ijms10093722.
12. D. Wu, D. Lin, J. Zhang, W. Zhou, M. Zhang, Y. Zhang, D. Wang, B. Lin. Selective localization of nanofillers: Effect on morphology and crystallization of PLA/PCL blends. Macromolecular Chemistry and Physics 2011; 212:613-626.
DOI: 10.1002/mapc.201000579
13. M. Martínez-Sanz, M. Villano, C. Oliveira, M.G.E. Albuquerque, M. Majone, M. Reis, A. Lopez-Rubio, J.M. Lagaron. Characterization of polyhydroxyalkanoates synthesized from microbial mixed cultures and of their nanobiocomposites with bacterial cellulose nanowhiskers. New Biotechnology 2014; 31:364-376
DOI: 10.1016/j.nbt.2013.06.003
14. M. Si, T. Araki, H. Ade, A.L.D. Kilcoyne, R. Fisher, J.C. Skolov, M.H. Rafailovich. Compatibilizing bulk polymer blends by using organoclays. Macromolecules 2006; 39:4793-4801.
DOI: 10.1021/ma060124+ CCC
15. L. Elias, F. Fenouillot, J.C. Majeste, Ph. Cassagnau. Morphology and rheology of immiscible polymer blends filled with silica nanoparticles. Polymer 2007; 48:6029-6040.
DOI: 10.1016/j.polymer.2007.07.061
16. L. Elias, F. Fenouillot, J.C. Majeste, P. Alcouffe, Ph. Cassagnau. Immiscible polymer blends stabilized with nano-silica particles: Rheology and effective interfacial tension. Polymer 2008; 49:4378-4385.
DOI: 10.1016/j.polymer.2008.07.018
17. E. Laredo, M. Grimau, A. Bello, D.F. Wu, Y.S. Zhang, D.P. Lin. AC conductivity of selectively located carbon nanotubes in poly(ε-caprolactone)/polylactide blend nanocomposites. Biomacromolecules 2010; 11:1339-1347.

DOI: 10.1021/bm100135n

18. Y. Shi, X. Feng , H. Wang, X. Lu. The effect of surface modification on the friction and wear behavior of carbon nanofiber-filled PTFE composites. Wear 2008; 264:934–939. DOI: 10.1016/j.wear.2007.06.014
19. A. Maurya, P. Chauhan. Synthesis and characterization of sol-gel derived PVA-titanium dioxide (TiO_2) nanocomposites. Polymer Bulletin 2012; 68:961-972. DOI: 10.1007/s00289-011-0589-6
20. F. Shi, Y. Ma, J. Ma, P. Wang, W. Sun. Preparation and characterization of PVDF/TiO_2 hybrid membranes with different dosage of nano-TiO_2. Journal of Membrane Science 2012; 389:522-531. DOI: 10.1016/j.memsci.2011.11.022
21. N. Nakayama, T. Hayashi. Preparation and characterization of poly(L-lactic acid)/TiO_2 nanoparticle nanocomposite films with high transparency and efficient photodegradability. Polymer Degradation and Stability 2007; 92:1255-1264. DOI: 10.1016/j.polymdegradstab.2007.03.026
22. P.M. Chou, M. Mariatti, A. Zulkifli, S. Sreekantan. Evaluation of the flexural properties and bioactivity of bioresorbable PLLA/PBSL/CNT and PLLA/PBSL/TiO_2 nanocomposites. Composites Part B 2012; 43:1374-1381. DOI: 10.1016/j.compositesb.2011.11.023
23. H. Shi, R. Magaye, V. Castranova, J. Zhao. Titanium dioxide nanoparticles: A review of current toxicological data. Particle and Fibre Toxicology 2013; 10:1-33. DOI: 10.1186/1743-8977-10-15
24. N.B. Cramer, J.W. Stansbury, C.N. Bowman. Recent advances and developments in composite dental restorative materials. International & American Associations for Dental Research 2011; 90:402-416. DOI: 10.1177/0022034510381263
25. D. Wu, Y. Zhang, M. Zhang, W. Yu. Selective localization of multiwalled carbon nanotubes in poly(ε-caprolactone)/polylactide blend. Biomacromolecules 2009; 10:417-424. DOI: 10.1021/bm801183f

26. B. Zhao, R.W. Fu, M.Q. Zhang, H. Yang, M.Z. Rong, Q. Zheng. Effect of soft segments of waterborne polyurethane on organic vapour sensitivity of carbon black filled waterborne polyurethane composites. Polymer Journal 2006; 38:799-806.
DOI: 10.1295/polymj.PJ2005202

27. X. Wang, K.-J. Xu, X.-B.Xu, S.-J. Park, S. Kim. Selective particle distribution and mechanical properties of nano-$CaCO_3$/ethylene-propylene-diene terpolymer/polypropylene composites with high content of nano-$CaCO_3$. Journal of Applied Polymer Science 2009; 113:2485-2491.
DOI: 10.1002/app.30078

28. F. Fenouillot, P. Cassagnau, J.C. Majeste. Uneven distribution of nanoparticles in immiscible fluids: Morphology development in polymer blends. Polymer 2009; 50:1333-1350.
DOI: 10.1016/j.polymer.2008.12.029

29. A.K. Bledzki, A. Jaszkiewicz. Mechanical performance of biocomposites based on PLA and PHBV reinforced with natural fibres – A comparative study to PP. Composites Science and Technology 2010; 70:1687-1696.
DOI: 10.1016/j.compscitech.2010.06.005

30. S. Modi, K. Koelling, Y. Vodovotz. Miscibility of poly(3-hydroxybutyrate-co-3-hydroxyvalerate) with high molecular weight poly(lactic acid) blends determined by thermal analysis. Journal of Applied Polymer Science 2012; 124:3074-3081.
DOI: 10.1002/app.35343

31. B.M.P. Ferreira, C.A.C. Zavaglia, E.A.R. Duek. Films of PLLA/PHBV: The thermal, morphological and mechanical characterization. Journal of Applied Polymer Science 2002; 86:2898-2906.
DOI: 10.1002/app.11334

32. L. Miao, Z. Qiu, W. Yang, T. Ikehara. Fully biodegradable poly(3-hydroxybutyrate-cohydroxyvalerate)/poly(ethylene succinate) blends: Phase behavior, crystallization and mechanical properties. Reactive & Functional Polymers 2008; 68:446-457.
DOI: 10.1016/j.reactfunctpolym.2007.11.001

33. J. Cailloux, O.O. Santana, E. Franco-Urquiza, J.J. Bou, F. Carrasco, J. Gámez-Pérez, M.L. Maspoch. Sheets of branched poly(lactic acid) obtained by one step reactive extrusion calendering process – Melt rheology analysis. eXPRESS Polymer Letters 2013; 7:304-318. DOI: 10.3144/expresspolymlett.2013.27
34. H. Xiu, H.W. Bai, C.M. Huang, C.L. Xu, X.Y. Li, Q. Fu. Selective localization of titanium dioxide nanoparticles at the interface and its effect on the impact toughness of poly(L-lactide)/poly(ether)urethane blends. eXPRESS Polymer Letters 2013; 7:261-271. DOI: 10.3144/expresspolymlett.2013.24
35. H. Yang, X. Zhang, C. Qu, B. Li, L. Zhang, Q. Zhang, Q. Fu. Largely improved toughness of PP/EPDM blends by adding nano-SiO_2 particles. Polymer 2007; 48:860-869. DOI: 10.1016/j.polymer.2006.12.022
36. D. Owens, R. Wendt. Estimation of the surface free energy of polymers. Journal of Applied Polymer Science 1969; 13:1741-1747.
37. I. McNeill, H. Leiper. Degradation studies of some polyesters and polycarbonates. 2. Polylactide: Degradation under isothermal conditions, thermal degradation mechanism and photolysis of the polymer. Polymer Degradation and Stability 1985; 11:309-326.
38. H.-T. Liao, C.-S. Wu. New biodegradable blends prepared from polylactide, titanium tetraisopropylate, and starch. Journal of Applied Polymer Science 2008; 108:2280-2289. DOI: 10.1002/app.27901
39. A.A. Vassiliou, K. Chrissafis, D.N. Bakiaris. Thermal degradation kinetics of in situ prepared PET nanocomposites with acid-treated multi-walled carbon nanotubes. Journal of Thermal Analysis and Calorimetry 2010; 100:1063-1071. DOI: 10.1007/s10973-009-0426-4
40. S. Majoni, S. Su, J.M. Hossenlopp. The effect of boron-containing layered hydroxy salt (LHS) on the thermal stability and degradation kinetics of poly(methyl methacrylate). Polymer Degradation and Stability 2010; 95:1593-1604. DOI: 10.1016/j.polymdegradstab.2010.05.033
41. H. Lin, L. Han, L. Dong. Thermal degradation behavior and gas phase flame-retardant mechanism of polylactide/PCPP blends. Journal of Applied Polymer Science 2014; 40480. DOI: 10.1002/APP.40480

42. H.-Y. Yu, Z.-Y. Qin, Y.-N. Liu, L. Chen, N. Liu, Z. Zhou. Simultaneous improvement of mechanical properties and thermal stability of bacterial polyester by cellulose nanocrystals. Carbohydrate Polymers 2012; 89:971-978.
DOI: 10.1016/j.carbpol.2012.04.053

43. H. Lin, L. Han, L. Dong. Thermal degradation behavior and gas phase flame-retardant mechanism of polylactide/PCPP blends. Journal of Applied Polymer Science 2014; 40480.
DOI: 10.1002/APP.40480

44. J. Zhang, H. Sato, I. Noda, Y. Ozaki. Conformation rearrangement and molecular dynamics of poly(3-hydroxybutyrate) during the melt-crystallization process investigated by infrared and two-dimensional infrared correlation spectroscopy. Macromolecules 2005; 38:4274–4281.
DOI: 10.1021/ma0501343 CCC

45. Q.-S. Liu, M.-F. Zhu, W.-H. Wu, Z-Y. Qin. Reducing the formation of six-membered ring ester during thermal degradation of biodegradable PHBV to enhance its thermal stability. Polymer Degradation and Stability 2009; 94:18–24.
DOI: 10.1016/j.polymdegradstab.2008.10.016

46. H. Sato, R. Murakami, A. Padermshoke, F. Hirose, K. Senda, I Noda. Infrared spectroscopy studies of CH···O hydrogen bondings and thermal behavior of biodegradable poly(hydroxyalkanoate). Macromolecules 2004; 37:7203–7213.
DOI:10.1021/ma049117o CCC

Chapter 3

Morphology and thermal degradation studies of melt-mixed PLA/PCL biodegradable polymer blend nanocomposites with TiO_2 as filler

This chapter has been submitted as a publication:
J.P. Mofokeng, A.S. Luyt. Morphology and thermal degradation studies of melt-mixed PLA/PCL biodegradable polymer blend nanocomposites with TiO_2 as filler. Polymer Testing.

Abstract

The morphology and thermal stability of melt-mixed PLA/PCL blend nanocomposites with small amounts of TiO_2 nanoparticles were investigated. The nanoparticles were well dispersed in both polymers with a small number of agglomerates. The thermal stability and degradation behaviour of the polymers, their blends and nanocomposites were studied using thermogravimetric analysis (TGA) and TGA-Fourier-transform infrared (FTIR) spectroscopy. Neat PCL showed better thermal stability than PLA, but the degradation kinetics revealed that PLA had a higher activation energy of degradation than PCL, indicating its degradation rate more strongly depends on temperature, probably because of a more complex degradation mechanism based on chain scission and re-formation. Blending of PLA and PCL reduced the thermal stabilities of both polymers, but the presence of TiO_2 nanoparticles improved their thermal stabilities. The nanoparticles also influenced the volatilization of the degradation products from the blend, acted as degradation catalyst and/or retarded the escape of volatile degradation products from the polymers or blends.

Keywords: poly(lactic acid); poly(ε-caprolactone); titania; blends; nanocomposites; thermal degradation

3.1. Introduction

The use of inorganic nanofillers to reinforce and compatibilize immiscible polymer blends has been reported in a number of papers [1-9]. In the past the compatibilizers used were graft and block copolymers or chemicals that have an affinity for the polymers in the blend, or that formed crosslinks or chemical bonds between the two components in the blend. However, with the addition of compatibilizers some important properties of one or both components in the blend are sacrificed, and a filler is therefore needed to maintain these properties [1-5]. Nanoparticles can act as a reinforcing filler and compatibilizer at the same time. They have large surface areas, and when they are homogeneously dispersed, they have the capability of reducing the interfacial tension between the components in a blend, especially if they are located at the interface. This will produce a material with a balanced morphology and other important properties from both polymers in a blend, and without deteriorating or compromising these properties [5-9].

In the past decades inorganic nanofillers have been used mainly in petroleum-based synthetic immiscible polymer blends. Their environmental unfriendliness motivated the use of biodegradable polymers, especially for packaging and short shelve-life product applications. Nanometre sized inorganic compounds such as titanium dioxide (TiO_2), zinc oxide (ZnO), silica (SiO_2), aluminium dioxide (Al_2O_3), and silicon nitride (Si_3N_4) were tried as fillers in fabrics and polymers to improve the tribological properties. TiO_2 has received most of the attention because of its good thermal stability, accessibility, and catalytic properties. It is generally used for various applications such as photo-electrochemical activity, solar energy conversion, photocatalysis, UV detection, ultrasonic sensing, and as a promising material in applications such as water or wastewater treatment. Its environmental compatibility, non-toxicity, and low price are some of its practical advantages [10-17].

Biodegradable polymers, and polymers derived from renewable resources, currently attract a lot of attention due to their environmental friendliness, since they combine biodegradability, compostability, and compatibility. They can be recycled or disposed off without harming the environment, and by using different waste forms they can be biodegraded to be used as fertilizers for crops. The use of these biodegradable polymers will not only save the environment, but will also solve the problem of possible fossil fuel shortages [18]. One such a polymer is poly(lactic acid) (PLA), which is biodegradable, bio-absorbable, and renewable thermoplastic polyester, and

which is derived mainly from corn starch and which has been extensively investigated over the past decades. It is a useful material in substituting the petroleum-based polymers used in packaging, due to its good mechanical strength, processability, and energy saving recycling in which it is degraded by addition into a suitable compost where degradation will take place at ambient temperatures. Although PLA is so attractive, it has some limitations that limit its wide-spread use. These include poor toughness, slow degradation, hydrophobicity, lack of reactive side-chain groups, and low thermal stability [19-22]. Thermal stability is an important property, because it impacts on the time and temperature associated with the processing, service lifetime, and storage of the materials. Several factors like absorbed moisture, molecular weight, residual monomers, and metal catalysts affect the thermal stability of PLA, which can be improved by blending with other thermally stable polymers or by filling it with thermally stable inorganic nanofillers [23].

Polymers can be blended to obtain materials with specific properties that are needed for certain applications. PLA can be blended with other flexible polymers that will act as plasticizers in order to improve its toughness and reduce its brittleness. One such a polymer is polycaprolactone (PCL), which is a biocompatible and biodegradable aliphatic polyester like PLA. It has good toughness, and it displays rubbery properties. PCL has low glass transition and melting temperatures (-60 and 60 ºC, respectively). It is also more thermally stable than PLA, which opens the possibility that the presence of PCL in PLA will not only improve its toughness, but also its thermal stability [20,22,24-27].

Blends of PLA and PCL have been reported to be immiscible, with poor mechanical properties because of their incompatibility [22,28,29]. Inorganic nanoparticles have lately been used to compatibilize this kind of blend, and to balance and tailor it to the desired properties needed for specific applications, mostly the thermal stability [1,2]. The thermal stability and morphology of individual PLA and PCL filled with the inorganic/organic micro- and nanofillers have been studied [13,30-33], and it was reported that the fillers deteriorate the thermal stability of the polymers by catalysing the thermal degradation. Their morphologies of the materials are controlled by whether the filler is functionalised or not. Severe aggregation of the nanofiller has been reported to decrease in thermal stability of the polymers, mostly for non-functionalised nanofillers. Nakayama *et al*. [13] prepared PLA/TiO_2 nanocomposites, and Courgneau *et al.*[31] PLA/cellulose fibre composites. Both groups found a decrease in the thermal stability of the

filled PLA, and they attributed it to a catalytic effect of the filler on the polymer degradation. Chrissafis *et al.* [33] studied the thermal degradation of PCL with organo-modified montmorillonite (MMT) and nanosilica in a nitrogen atmosphere. They reported an acceleration of PCL degradation in the presence of the fillers. However, unmodified MMT and multi-walled carbon nanotubes inhibited the thermal degradation of PCL. They also studied the degradation kinetics of PCL and found that neat PCL degrades by two consecutive mechanisms. The first step is a polymer chain cleavage via cis-elimination, and the second step is an unzipping depolymerization from the hydroxyl end of the polymer chain. They found that the nanoparticles did not affect the degradation mechanism of PCL. From this information it is clear that the presence of nanofillers did not really improve the thermal stability of PLA and PCL, and therefore we decided in this paper the influence of these two polymers on each other's thermal stability in a blend, and the influence of titania nanoparticles on their respective thermal stabilities in the same blend.

PLA/PCL blends were intensively studied over the past decade [9,20,22,25-27,34-36], and most of these studies reported a phase separated structure with discrete PLA domains in a continuous PCL phase, and in which the morphologies were stabilised by nanofillers. The nanofiller either selectively localised in one of the two phases in the blend, on the interface, or in both the interface and one of the phases. This selective localisation of the filler is determined by the large difference in the affinity, which is closely related to the surface properties of the different components, between the nanofiller and the two matrix components in the blend [37,38]. Wu *et al.* [9,34] introduced multi-walled carbon nanotubes (MWCNTs) into a 30/70 w/w PLA/PCL blend, and found that the MWCNTs were selectively dispersed in the lower viscosity PCL phase and on the interface. According to them this not only prevented the coalescence of the discrete PLA phase, but also enhanced the interfacial adhesion [39]. In this case the MWCNTs acted as nano-reinforcement and compatibilizer at the same time, adjusting the morphology and improving the final properties of the PLA/PCL blend. They also prepared 70/30 and 30/70 PLA/PCL blends with organoclay and CNTs as fillers [35], and reported that the clay was dispersed in PLA and on the interface, whereas the CNTs were dispersed in PCL and on the interface. By using surface energy results and interfacial tensions, they calculated the wetting co-efficient that proved the selective localization of the nanofillers, and attributed their observations to the difference in surface properties of the components in these blend nanocomposites. The

thermal degradation of PLA and PCL in PLA/PCL blends were investigated through basic TGA analyses [36,40]. Both the presence of PCL and the presence of clay nanoparticles were found to improve the thermal stability of PLA, but only up to 5 wt% nanoparticle content because of their agglomeration at higher contents.

The aim of the work reported in this paper was to investigate the influence of PLA/PCL blending, and the presence of TiO_2 nanofiller in the individual polymers and the blends, on the thermal stability and degradation behaviour of PLA and PCL. The blend and nanocomposite morphologies were investigated and explained, and these morphologies were used to explain the observed degradation behaviour and kinetics, that were followed through thermogravimetric analysis (TGA) and TGA-Fourier-transform infrared (FTIR) analyses.

3.2. Experimental

3.2.1 Materials

The polylactic acid (PLA) used in the study was a commercial grade (PLA 2002D), obtained from Natureworks, LLC (USA). It has a D-isomer content of 4%, density = 1.24 g cm^{-3}, glass transition temperature of ~53 ºC, and a melting temperature of ~153 ºC. The Capa™ 6500 polycaprolactone (PCL) was purchased from Southern Chemicals in Johannesburg, South Africa. It has a density of 1.1 g cm^{-3}, a glass transition temperature of -61 ºC, and a melting temperature ~60 ºC. Anatase titanium(IV)oxide (TiO_2) with particle sizes < 25 nm and 99.7% purity was supplied by Sigma-Aldrich in South Africa.

3.2.2 Blend and nanocomposite preparation

The samples were prepared *via* melt-mixing using a Brabender Plastograph. PLA was dried in an oven at 80 °C for four hours prior to mixing; PCL and TiO_2 were used as received. 30/70, 50/50, and 70/30 w/w PLA/PCL blends and their nanocomposites with 1, 3, and 5 wt% of TiO_2 were mixed at 170 ºC for ten minutes. The samples were compression moulded into 2 mm thick sheets at the same temperature for 5 minutes using a hydraulic press at a pressure of 50 bar, after which they were removed and left to cool under ambient conditions.

3.2.3 Characterization

Size exclusion chromatography (SEC) analyses performed on a PL Olexis column (Polymer Laboratories). Chloroform was used as the mobile phase at a flow rate of 1.00 mL min^{-1}. The samples were prepared at a concentration of 2 mg mL^{-1}. The column was calibrated with polystyrene (PS) standards from Polymer Laboratories (Church Stretton, Shropshire, UK). The chromatograph comprised of a Waters1515 isocratic pump, a Waters inline degasser AF, and a Waters 717 Plus auto sampler with a 100 µL sample loop. The system was connected to an evaporative light scattering detector (PL-ELS 1000). Nitrogen was used as carrier gas in the ELSD, at a flow rate of 1.5 SLM. The evaporator and nebulizer temperatures were set at 100 and 40 °C, respectively.

The melt flow index of the two polymers, used to prepare the blends and nanocomposites, was determined using a CEAST Melt Flow Junior. Ten samples each of both polymers were analysed at 180 °C. The amount of PLA which flowed through the die over a period of 10 minutes, and the amount of PCL which flowed through the die over a period of 5 minutes, under 2.16 kg weight were determined. The determined amount of PCL was multiplied by 2 to determine a comparable MFI.

A Tescan VEGA3 scanning electron microscope (SEM) was used to study the surface morphologies of the PLA/PCL blends and nanocomposites. The liquid nitrogen fractured samples were sputter coated with gold for 30 seconds to eliminate sample charging, and analyses were performed at three different magnifications.

The morphologies of the nanocomposites were characterised by transmission electron microscopy (TEM). Images were obtained using a 200 kV FEI Tecnai20 TEM fitted with Gatan Tridiem. The 50/50 w/w PLA/PCL blend with 5 wt% TiO_2 nanoparticles was trimmed and sectioned to fit the ultra-microtome, since they were hard enough to cut without cooling. Uranyl acetate was used as a staining substance for staining only PCL, to distinguish the different phases in the blend nanocomposites. The samples were sectioned at 150 nm using a Leica UC7 (Vienna, Austria) ultramicrotome, collected on copper grids, and examined with a Philips (FEI) (Eindhoven, The Netherlands) CM100 transmission electron microscope at 60 keV.

The contact angle measurements of the samples were conducted at room temperature on a surface energy evaluation system, based on the sessile drop method. At least 5 replicates were

analysed for each sample to ensure reproducibility of the results. Distilled water (H_2O) and diiodomethane (CH_2I_2) were used as polar and non-polar solvents, respectively. The literature values of their surface energies are: (H_2O: γ^p = 50.7 mJ m^{-2} and γ^d = 22.1 mJ m^{-2}; CH_2I_2: γ^p = 6.7 mJ m^{-2} and γ^d = 44.1 mJ m^{-2}). The interfacial tension between the components in a blend was calculated with the Owens-Wendt method using the geometric mean equation (Equation 3.1) [35,37,41].

$$\gamma_{12} = \gamma_1 + \gamma_2 - 2\sqrt{\gamma_1^{\,d}.\gamma_2^{\,d} + \gamma_1^{\,p}.\gamma_2^{\,p}} \qquad (3.1)$$

where γ_{12} = interfacial tension between components 1 and 2 in the blend, γ_1 and γ_2 are the total surface energies of components 1 and 2, γ_1^d and γ_2^d are the dispersive surface energies of components 1 and 2, and γ_1^p and γ_2^p are the polar surface energies of the components in the nanocomposites.

A Perkin-Elmer STA6000 thermogravimetric analyser (TGA) was used to analyse the thermal degradation behaviour of the samples. The analyses were done from 30 to 600 °C at a heating rate of 10 °C min^{-1} under nitrogen flow (20 ml min^{-1}). The sample masses were ~24 mg. The samples for thermal degradation kinetics were run at 3, 5, 7, 9, and 15 °C min^{-1} heating rates under nitrogen atmosphere, and the TGA's integrated kinetics software (based on the Flynn-Ozawa-Wall method (Equation 3.2)) was used to calculate the activation energies:

$$\ln \beta = c - 1.052\left(\frac{E_a}{RT}\right) \qquad (3.2)$$

where β = heating rate in K min^{-1}, c is a constant, E_α = activation energy in kJ mol^{-1}, R = universal gas constant, and T = temperature in K. The plot of ln β vs. 1/T, obtained from the TGA curves recorded at different heating rates, should be a straight line. The activation energy was evaluated from its slope. The TGA was also connected to a Perkin-Elmer Spectrum 100 Fourier transform infrared (FTIR) spectrometer to analyse the thermal degradation volatiles. The same temperature range and heating rate were used, and the volatiles were transferred to FTIR by a

Perkin-Elmer TL 8000 balanced flow FT-IR EGA system at 200 ºC and a flow rate of 150 ml min^{-1}. Spectra were collected at five different temperatures during the degradation process.

3.3. Results and discussion

3.3.1 Morphology

Figure 3.1 shows the SEM pictures of the 50/50 w/w PLA/PCL blend and its nanocomposite with 5 wt% TiO_2. Neither of the two pictures show separate polymer phases, but the picture of the blend nanocomposite clearly shows the TiO_2 nanoparticles fairly well dispersed in the polymer blend. It was, however, not possible to observe in this picture whether the nanoparticles were dispersed in one or both polymers. The presence of TiO_2 nanoparticles also gave rise to a much smoother surface structure (Figure 3.1(b)).

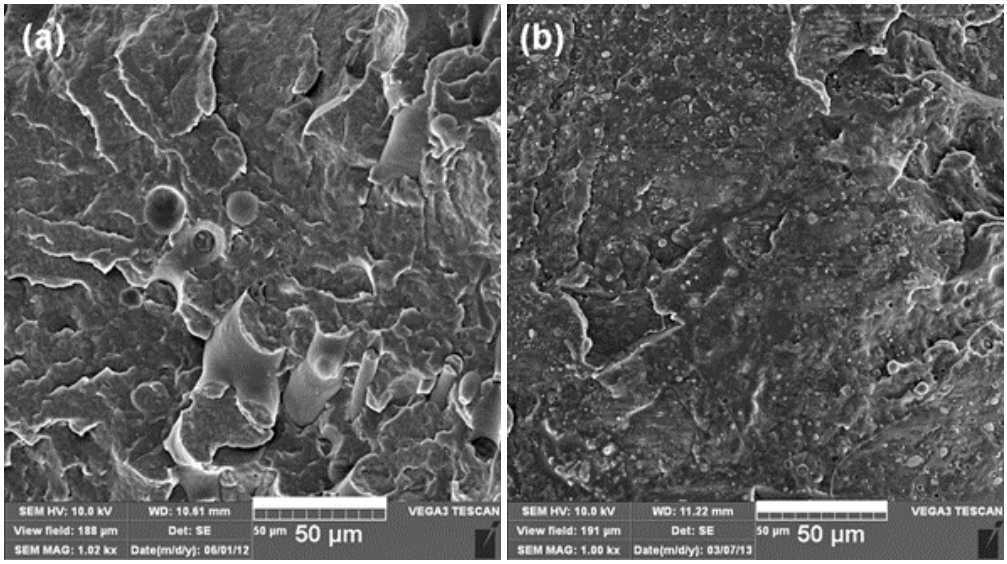

Figure 3.1 SEM pictures of the (a) 50/50 w/w PLA/PCL blend, and (b) 50/50 w/w PLA/PCL nanocomposite with 5 wt% TiO_2, both at 1000× magnification

PLA and PCL have been shown before to be immiscible with a clearly phase-separated morphology [9]. The TEM picture of a blend nanocomposite (Figure 3.2(a)) shows that the nanoparticles are homogeneously dispersed accross the whole area of the photo, but a few large agglomerates are visible. We can therefore assume that the nanoparticles equally well disperse in

both PLA and PCL. This indicates that the interaction between the nanoparticles and both polymers is fairly good. Although there seems to be a good dispersion of the nanofiller in both polymers, the different phases in the immiscible blend nanocomposite could not be seen. In order to identify the phase morphology of the blend, PCL was stained with uranyl acetate (Figure 3.2(b)). The dark phase represents the stained PCL, while the lighter phase represents the unstained PLA, and the interface between the two polymers can now be clearly identified. This picture clearly shows a co-continuous morphology, but because of the dark staining it is not possible to see the nanoparticles in both phases in order to confirm our assumption above. Normally the nanoparticles will disperse in the polymer which interacts most strongly with them, and on the interface between the polymers. In most previously investigated PLA/PCL blends the nanoparticles were selectively localised in the PCL phase or on the interfase [9,34,38], but in our case there are clear indications that the nanoparticles were equally well dispersed in both polymers.

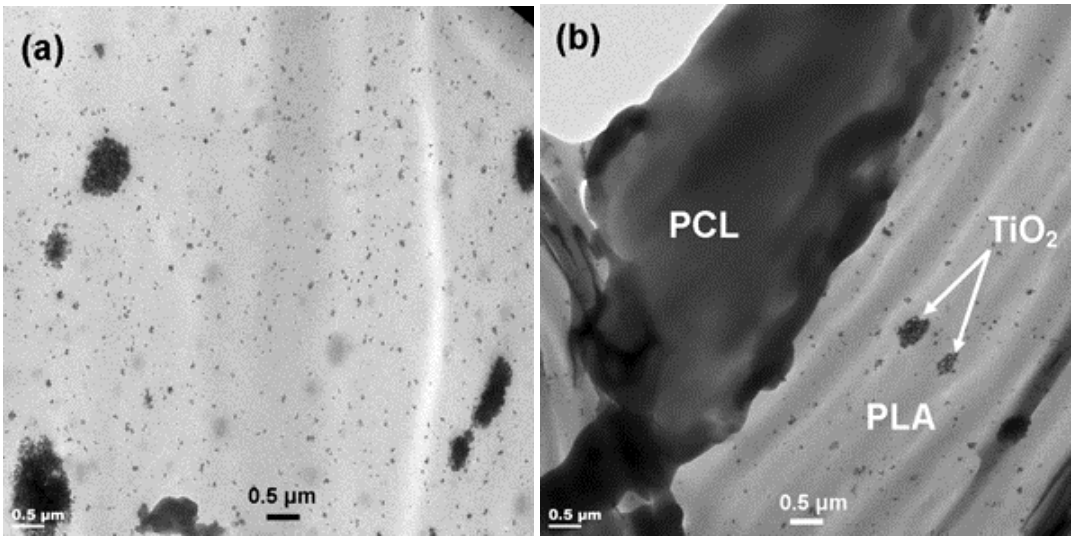

Figure 3.2 TEM pictures of 50/50 w/w PLA/PCL with 5 wt% TiO_2: (a) unstained, and (b) uranyl acetate stained, both at 5700× magnification

The fact that the titania nanoparticles dispersed equilly well in both polymers cannot be attributed to a single factor, but to a balance between the strength of the interfacial interaction and to differences in the viscosities of the two polymers. The surface properties in Tables 3.1 and 3.2 indicate that the interfacial tension between PCL and the TiO_2 nanoparticles is quite high (6.9

mN m^{-1}), probably because of the difference between the polar components of their surface free energies. When there is a large difference between the polar components of the surface free energy, the two phases will probably not be compatible and therefore the nanoparticles will preferably disperse in the phase which has a more comparable polar component, or the phase with a lower viscosity [9,32,34,35,38]. In this case, although there is more tension between PCL and the nanoparticles, the PCL is much less viscous (higher melt flow index in Table 3.3), and therefore the nanoparticles disperse in both PLA (with which it has a fairly good interfacial interaction) and PCL (which has a much lower viscosity than PLA). These surface energy values were determined at room temperature, but they may be different from the values at the mixing temperature we used, and therefore we can only assume that the values in Table 3.1 are not too much different from what the values would have been if the surface energies were determined at 170 °C.

Table 3.1 Contact angles of PLA, PCL and TiO_2. The TiO_2 contact angle was taken from the literature [37]

	Contact angle / deg		Surface energy / mN m^{-1}		
	H_2O	**CH_2I_2**	**γ**	**γ^d**	**γ^p**
PLA	44.7 ± 1.0	35.4 ± 0.0	62.0	41.8	20.2
PCL	60.2 ± 0.8	27.0 ± 0.5	55.8	45.4	10.4
TiO_2	19.7	10.1	80.7	46.4	34.3

γ = surface free energy, γ^d = dispersive component of surface free energy, γ^p = polar component of surface free energy

Table 3.2 Interfacial tension values calculated using the geometric-mean equation (Equation 3.1)

Component pair	Interfacial tension / mN m^{-1}
PLA/PCL	1.7
PLA/TiO_2	2.0
PCL/TiO_2	6.9

3.3.2 Thermogravimetric analysis (TGA)

The good dispersion of the nanofiller in the two polymers of a blend is not common in immiscible polymer blends, although it may be preferable for obtaining a certain combination of properties in the final product. We were interested in the thermal stability, because thermal degradation decreases the usability of the materials. Figure 3.3 and Table 3.4 present the TGA results of all the investigated samples. The neat PLA shows one degradation step around 365 °C, while the neat PCL shows two degradation steps around 415 and 520 °C. PCL clearly decomposes through a two-step degradation mechanism. The first step is a polymer chain cleavage *via* cis-elimination, and the second step is an unzipping depolymerization from the hydroxyl end of the polymer chain [42,43]. PLA degradation occurs according to a back-biting ester interchange reaction which takes place through a non-radical mechanism involving the –OH chain ends. The PLA/PCL blends show two clearly resolved degradation steps, and the extent of mass loss corresponds with the respective amounts of polymer in the blends, confirming their immiscibility.

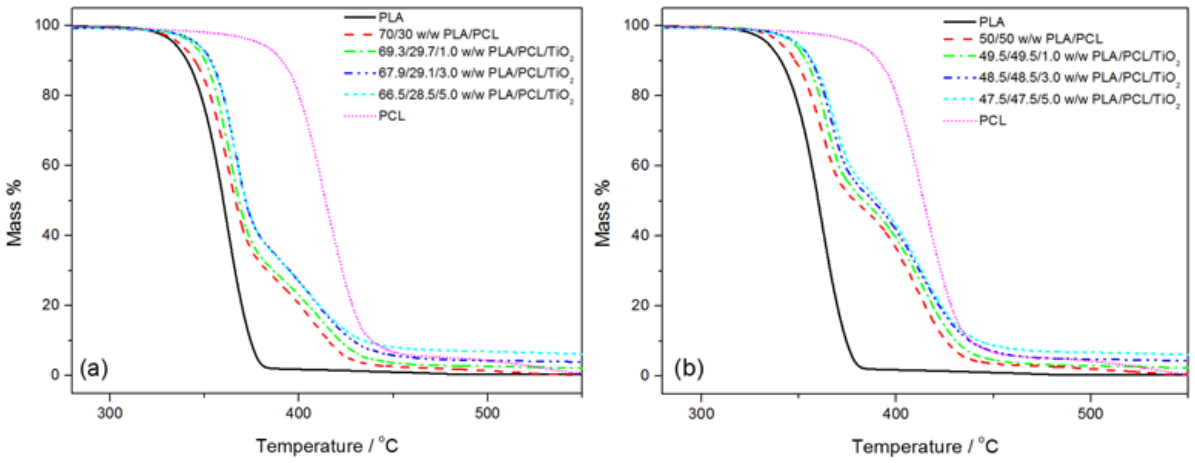

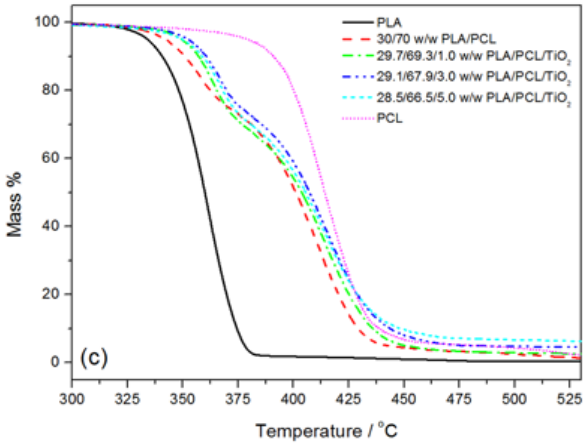

Figure 3.3 TGA curves of (a) 70/30, (b) 50/50, and (c) 30/70 w/w of PLA/PCL with 1, 3 and 5 wt% of TiO_2

Table 3.3 Molar masses, dispersity index and melt flow index of PLA and PCL

Sample	M_p	M_n	M_w	M_z	D	MFI / (g/10 min)
PLA	71960	55047	142500	352730	2.6	2.8
PCL	25828	19005	36135	55440	1.9	14.5

M_p = peak average molar mass, M_n = number average molar mass, M_w = weight average molar mass, M_z = viscosity average molar mass, D = dispersity index, MFI = melt flow index

Table 3.4 Derivative TGA peak temperatures of all the investigated samples

Sample	PLA degradation step / ºC	PCL degradation step / ºC
Neat PLA	364.4	-
70/30 w/w PLA/PCL	364.0	409.8
50/50 w/w PLA/PCL	362.8	411.6
30/70 w/w PLA/PCL	356.8	412.2
Neat PCL	-	413.9 and 521.6
69.3/29.7/1.0 w/w PLA/PCL/TiO_2	365.7	412.0
49.5/49.5/1.0 w/w PLA/PCL/TiO_2	365.3	415.4
29.7/69.3/1.0 w/w PLA/PCL/TiO_2	365.6	414.5
67.9/29.1/3.0 w/w PLA/PCL/TiO_2	368.2	411.2
48.5/48.5/3.0 w/w PLA/PCL/TiO_2	367.0	413.1
29.1/67.9/3.0 w/w PLA/PCL/TiO_2	366.2	415.2
66.5/28.5/5.0 w/w PLA/PCL/TiO_2	368.2	408.8
47.5/47.5/5.0 w/w PLA/PCL/TiO_2	370.5	414.3
28.5/66.5/5.0 w/w PLA/PCL/TiO_2	367.2	415.5

Figures 3.4 and 3.5 illustrate the effect of blending and TiO_2 nanoparticles loading on the thermal stability of the polymers in a blend. The temperatures were taken at 50% mass loss of each polymer in the blends as function of titania content in the nanocomposites. It is clear that the thermal stability of both PLA and PCL decreases (from 357 to 350 °C for PLA, and from 424 to 409 °C for PCL) with an increase in the amount of the other polymer in the blend. As already mentioned, the reason for the decrease in the thermal stability of PCL is due to the presence of the less thermally stable PLA. One would expect the thermal stability of PLA to increase in the presence of PCL, because PCL is more thermally stable than PLA. The decrease in PLA's thermal stability can therefore not be due to the presence of PCL, but is probably the result of the incompatibility of the two polymers [25]. This incompatibility restricts the balance between their properties, which may result in a poorer performance of the final product. In the presence of the TiO_2 nanoparticles the thermal stabilities, as determined from the mass loss temperatures, of both polymers in the respective blends increased (Figures 3.4 and 3.5). In the case of PLA the degradation temperature only increased up to 3 wt% nanoparticle content, with little if any further increase for the samples with 5 wt% nanoparticles. Whatever the reason for this apparent increase in thermal stability, the effect is obviously more prominent at lower nanoparticle contents when the extent of agglomeration is lower. PCL also shows some levelling off of degradation temperature with increasing nanoparticle content, but the degradation temperature increased more significantly in this case. The increased mass loss temperatures may be due to any one or a combination of the following factors: (i) The TiO_2 nanoparticles probably absorb more thermal energy than any of the polymers, at least initially; (ii) Interaction between the titania nanoparticles and the volatile degradation products probably retards their diffusion out of the sample, which will increase the onset of mass loss to higher temperatures [4,15].

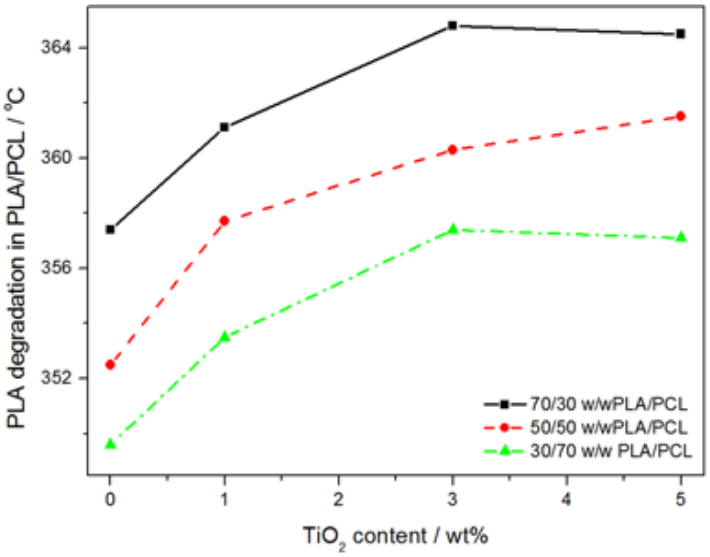

Figure 3.4 Effect of blending and filler addition on the temperature at 50% mass loss of PLA in the PLA/PCL blends and nanocomposites

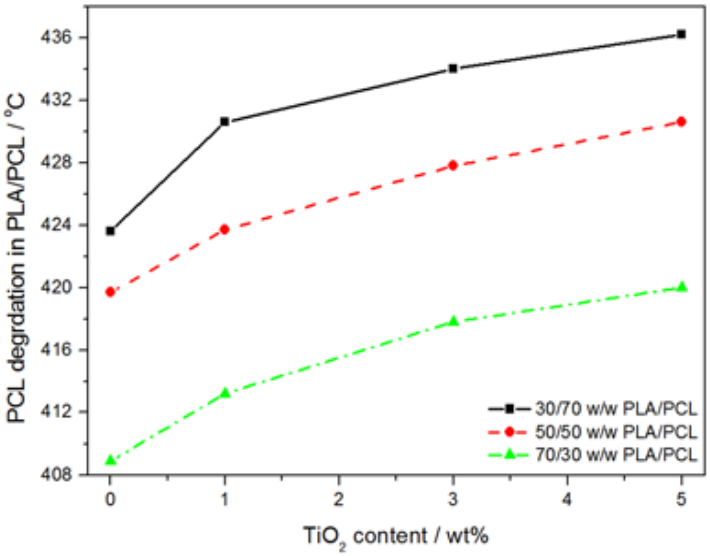

Figure 3.5 Effect of blending and filler addition on the temperature at 50% mass loss of PCL in the PLA/PCL blends and nanocomposites

3.3.3 Degradation kinetics

The activation energy (E_α) is the minimum energy required to initiate the thermal degradation process, and it is related to the temperature dependence of the rate of degradation. Figure 3.6

shows how the activation energy as function of extent of mass loss (α) of PLA and PCL compare to those of their respective nanocomposites. E_α of neat PCL increased almost linearly with extent of mass loss from 131 to 183 kJ mol^{-1}. Such an increase is E_α is said to be typical for the degradation of polymers [44]. The activation energies of PCL are significantly higher in the presence of the nanoparticles (Figure 3.6), which could signify an improvement in the thermal stability of PCL. However, it is quite possible that it is not the thermal stability which was improved, but the nanoparticles interacting with the degradation volatiles, delaying their diffusion out of the molten polymer blend [45,46].

The activation energies of PLA are much higher than those of PCL, starting at 185 kJ mol^{-1} and increasing almost linearly to 220 kJ mol^{-1} with increasing extent of mass loss. This indicates that the degradation rates of PLA have a stronger dependence on temperature than those of PCL. This is probably because the thermal degradation of PLA follows a complex route with at least six possible mechanisms [30,47]. Backbiting is one of these mechanisms, and it involves a transesterification reaction which will give rise to simultaneous bond breaking and bond formation, where the lactic acid will come back and attach itself onto the backbone again. This process will continue until all the lactide monomer molecules have been released and the thermal degradation is complete. Such a degradation mechanism will typically be more temperature dependent than a straightforward chain scission or unzipping mechanism. The presence of TiO_2 in PLA reduced the activation energy of degradation of PLA (Figure 3.6). This indicates that the TiO_2 nanoparticles must have had a catalytic effect on the degradation of PLA. However, a conclusion like this cannot be made with absolute certainty, because ‘degradation’ in this case is monitored in terms of mass loss when the volatile degradation products evaporate from the degrading sample, and the diffusion of the volatile degradation products out of the sample and their evaporation may be retarded through interaction between these degradation products and the dispersed nanoparticles.

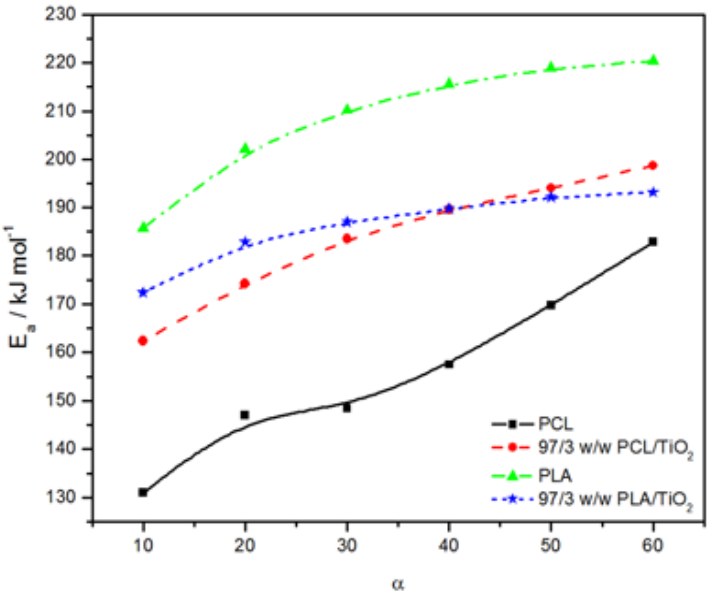

Figure 3.6 Activation energy vs. extent of degradation for PCL, PLA, 97/3 w/w PCL/TiO_2 and 97/3 w/w PLA/TiO_2

It is clear from Figure 3.7(a) that the intensities of CO_2 between 2300 and 2400 cm^{-1}, the –C=O vibration at about 1792 cm^{-1}, and the –C-O-C bands in the spectrum at about 325 °C are high. At about 350 °C the same bands have significantly lower intensities, while other peaks (2998, 2819, 2732, 2170, 2108 and 1371 cm^{-1}) disappeared completely. In the presence of TiO_2 nanoparticles, at about same temperatures, the carbonyl band shifted from 1792 to 1764 cm^{-1} and the intensity was lower than that of neat PLA, while at the higher temperatures the intensities were higher. Both these observations are a strong indication that the PLA degradation products interacted with the nanoparticles, which retarded their diffusion out of the molten polymer.

The FTIR spectra in Figure 3.7(b) show that the intensities of the hydroxyl (-OH) band around 3577 cm^{-1}, the bands between 2400 to 2300 cm^{-1} for carbon dioxide (CO_2), carbonyl band (C=O) at 1756 cm^{-1}, and the heavily overlapped C-O-C, C-O, CH, CH_2 bands between 1400-1100 cm^{-1} are lower at the higher temperature for the TiO_2 containing PCL, contrary to the higher intensities observed for neat PCL at the higher temperature. This is in line with the higher activation energies for the nanocomposites observed in the degradation kinetics investigation (Figure 3.6), and confirms that the interaction between the volatile degradation products and the nanoparticles (which retards their diffusion out of the sample) dominates any catalytic effect that the nanoparticles may have had on the PCL degradation process.

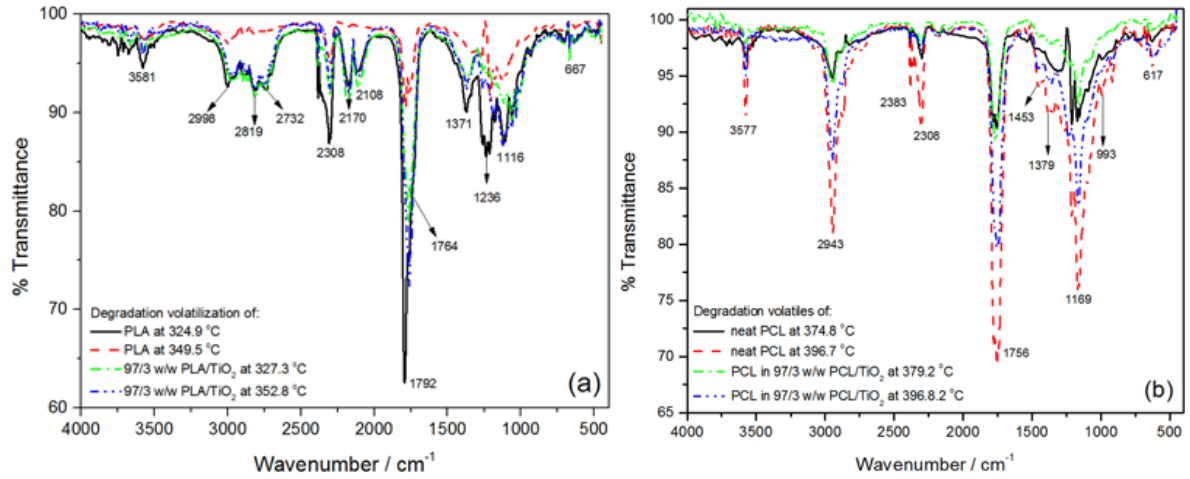

Figure 3.7 FTIR spectra of the degradation products of (a) neat PLA and 97/3 w/w PLA/TiO_2, (b) neat PCL and 97/3 w/w PCL/TiO_2

Figure 3.8 shows the activation energy versus the extent of mass loss (α) for the 50/50 w/w PLA/PCL blend and its nanocomposite with 3 wt% TiO_2. The first half of each graph is related to the PLA degradation, and the second half to that of PCL. The activation energy of degradation of the blend increased from about 141 kJ mol^{-1} to about 183 kJ mol^{-1}. The degradation activation energy for the PLA phase in the blend is therefore significantly lower than that of unblended PLA, which is in line with its reduced thermal stability in the presence of PCL, while the degradation activation energy of PCL is slightly higher than that of unblended PCL. The only reason that can be suggested at this point in time is that the co-continuous morphology of the blend, and the relatively weak interaction between the two components, in some way changed the energy requirements for the initiation and propagation of the degradation of each of the components. In the presence of the nanoparticles the activation energy is higher for the PLA in the blend, but lower for the PCL in the blend. As already discussed above, several factors may contribute to changes in the degradation kinetics of the different components in a blend and a nanocomposite. Firstly there is the catalysing effect of the nanoparticles, which we have already indicated may be more prevalent in the case of PLA. Secondly there is the interaction between the nanoparticles and the volatile degradation products, which may retard the diffusion of these products out of the sample. In this case different products may interact differently with the nanoparticles, and the adsorption of one or more of the volatile substances onto the nanoparticles

may affect the extent of influence of the nanoparticles on the other products. The evaporation of PLA degradation products may also accelerate the release of PCL degradation products.

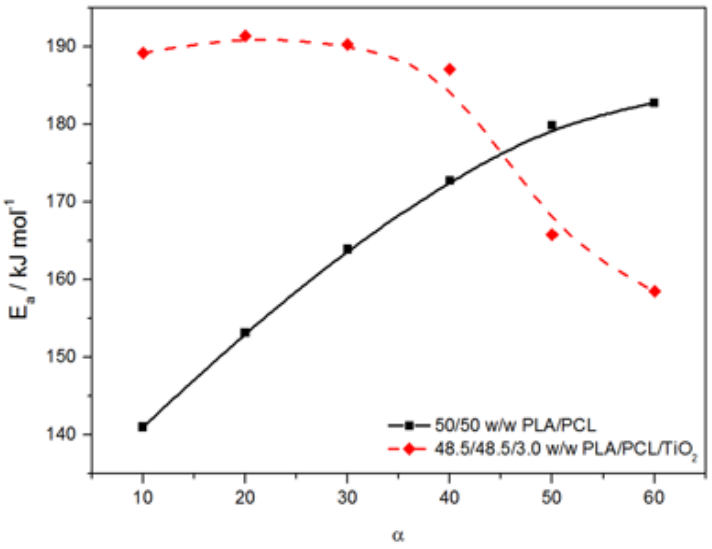

Figure 3.8 Activation energy vs. extent of degradation curves for 50/50 w/w PLA/PCL without and with 3 wt% TiO_2

The spectra of the degradation volatiles of the blend and blend nanocomposite (Figure 3.9) were obtained at around 344 °C (during the degradation step of PLA) and 396 °C (during the degradation step of PCL). The peaks indicated in the figure are characteristic of lactide molecules, oligomeric rings, and acetaldehydes plus carbon monoxide, that are the previously determined degradation products of PLA [45,46,48-50]. The carbonyl band split into two peaks (1794 and 1758 cm^{-1}) that correspond to the wavenumbers of the carbonyl bands observed in the spectra of the degradation products from neat PLA and neat PCL. Similarly the carbon dioxide band appears at two different wavenumbers (2375 and 2309 cm^{-1}). The only explanation we have for this observation is that the PCL started degrading while the degradation of PLA was still in progress, and therefore the spectra show separate carbonyl and carbon dioxide bands related to degradation products from each of the two polymers. The already discussed TGA results showed a decrease in the mass loss temperatures of both polymers when blended. It is possible that the PCL degradation products could have been drawn along during the evaporation of the PLA degradation products. This is confirmed by the fact that neat PLA shows only well-defined CO_2band around 2308 cm^{-1}, while neat PCL shows two CO_2 bands at 2383 and 2308 cm^{-1} (Figure

3.7(b)). Hoidy *el al*. [51], who also investigated the thermal degradation of PLA/PCL blends, confirmed that PCL started decomposing before the decomposition of PLA finished.

When decomposing the PLA/PCL blend in the presence of the nanoparticles, a single carbonyl band at 1762 cm^{-1} and a single CO_2 band at 2309 cm^{-1} were observed in the spectrum of the PLA degradation volatiles, contrary with the observation for the blend in the absence of nanoparticles. The positions of these bands are identical to those observed for the degradation products of neat PLA. Similarly, in the spectrum taken in the PCL degradation range, only single peaks were observed in the same positions as those from the degradation volatiles of neat PCL (Figure 3.7(b)). This confirms that in the presence of the nanoparticles the degradation products from the two polymers did not evaporate simultaneously as in the case of the blend. There are two possible reasons: (i) the catalysis effect of the nanoparticles in the case of PLA may have resulted in the degradation products of PLA evaporating before PCL really started degrading; (ii) adsorption of degradation products onto the nanoparticles may have effectively separated the volatilization of the respective polymers' degradation products.

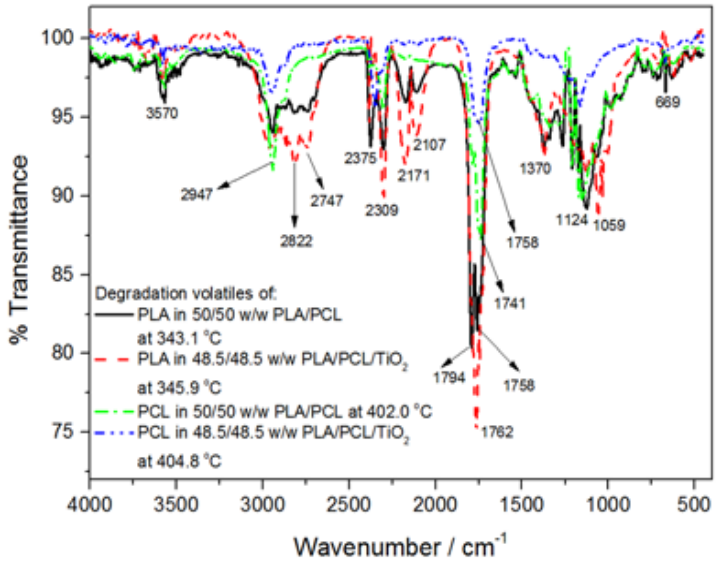

Figure 3.9 FTIR spectra of the degradation products PLA and PCL in 50/50 w/w PLA/PCL and its nanocomposites with 3 wt%

The spectra obtained at 403 °C show peaks that are characteristic of 5-hexanoic acid/ε-caprolactone, carbon dioxide, water, and methyl pentanoate [40,41,52-54] that are the typical thermal decomposition products for PCL. Although it is not obvious from the presented spectra,

the spectra we took of the blend at different temperatures during the PCL degradation step show the highest peak intensities at 381 °C, while for the nanocomposite the highest peak intensities were observed in the 375 °C spectrum. There is not much difference between these two temperatures taking into account the experimental setup for the determination of these spectra, which means that the titania nanoparticles had little effect on the degradation of PCL in the blend. This is contrary to some of our previous observations, but since spectra could not be taken at a larger number of temperatures with smaller temperature intervals, it is probably better not to use this data as conclusive evidence.

3.4. Conclusions

The purpose in this work was to investigate the effect of blending and the presence of low contents of titania nanoparticles on the thermal degradation behaviour of PLA and PCL. The nanoparticles were evenly dispersed in the PLA/PCL blends. This was attributed to (i) affinity because of small differences between the relative polarities of the nanoparticles and PLA, and (ii) the lower viscosity of PCL which caused it to easily accommodate the nanoparticles during melt-mixing. Neat PLA had a lower thermal stability than PCL, but a higher activation energy of degradation. This was attributed to the more complex degradation mechanism(s) of PLA. Blending seemingly decreased the thermal stability of both polymers, but an explanation for this observation is not immediately obvious. It is possible that, since 'degradation' in this case was monitored through TGA analysis, the escape of the volatile degradation products of one polymer could have been influenced by presence of the other polymer. The presence of the TiO_2 nanoparticles improved the thermal stabilities of both polymers in the blends, and influenced the volatilization of the degradation products. This influence was attributed to a combination of the catalytic effect of the nanoparticles and their interaction with the volatile degradation products.

3.5. References

1. J.-M. Raquez, Y. Habibi, M. Murariu, P. Dubois. Polylactide (PLA)-based nanocomposites. Progress in Polymer Science 2013; 38:1504-1542.
DOI: 10.1016/j.progpolymsci.2013.05.014

2. B. Akbari, R. Bagheri. Influence of compatibilizer and processing conditions on morphology, mechanical properties, and deformation mechanism of PP/clay nanocomposite. Journal of Nanomaterials 2012; 810623.
DOI: 10.1155/2012/810623
3. D.R. Paul, L.M. Robeson. Polymer nanotechnology: Nanocomposites. Polymer 2008; 49:3187-3204.
DOI: 10.1016/j.polymer.2008.04.017
4. P.J. Jandas, S. Mohanty, S.K. Nayak. Morphology and thermal properties of renewable resource-based polymer blend nanocomposites influenced by a reactive compatibilizer. Sustainable Chemistry & Engineering 2014; 2:377386.
DOI: 10.1021/sc400395s
5. Y. Cao, J. Zhang, J. Feng, P. Wu. Compatibilization of immiscible polymer blends using graphene oxide sheets. ACS Nano 2011; 5:5920-5927.
DOI: 10.1021/nn201717a
6. M. Si, T. Araki, H. Ade, A.L.D. Kilcoyne, R. Fisher, J.C. Skolov, M.H. Rafailovich. Compatibilizing bulk polymer blends by using organoclays. Macromolecules 2006; 39:4793-4801.
DOI: 10.1021/ma060124+ CCC
7. L. Elias, F. Fenouillot, J.C. Majeste, Ph. Cassagnau. Morphology and rheology of immiscible polymer blends filled with silica nanoparticles. Polymer 2007; 48:6029-6040.
DOI: 10.1016/j.polymer.2007.07.061
8. L. Elias, F. Fenouillot, J.C. Majeste, P. Alcouffe, Ph. Cassagnau. Immiscible polymer blends stabilized with nano-silica particles: Rheology and effective interfacial tension. Polymer 2008; 49:4378-4385.
DOI: 10.1016/j.polymer.2008.07.018
9. E. Laredo, M. Grimau, A. Bello, D.F. Wu, Y.S. Zhang, D.P. Lin. AC conductivity of selectively located carbon nanotubes in poly(ε-caprolactone)/polylactide blend nanocomposites. Biomacromolecules 2010; 11:1339-1347.
DOI: 10.1021/bm100135n
10. Y. Shi , X. Feng , H. Wang, X. Lu. The effect of surface modification on the friction and wear behavior of carbon nanofiber-filled PTFE composites. Wear 2008; 264:934–939.

DOI: 10.1016/j.wear.2007.06.014

11. A. Maurya, P. Chauhan. Synthesis and characterization of sol-gel derived PVA-titanium dioxide (TiO_2) nanocomposites. Polymer Bulletin 2012; 68:961-972.
DOI: 10.1007/s00289-011-0589-6
12. F. Shi, Y. Ma, J. Ma, P. Wang, W. Sun. Preparation and characterization of PVDF/TiO_2 hybrid membranes with different dosage of nano-TiO_2. Journal of Membrane Science 2012; 389:522-531.
DOI: 10.1016/j.memsci.2011.11.022
13. N. Nakayama, T. Hayashi. Preparation and characterization of poly(L-lactic acid)/TiO_2 nanoparticle nanocomposites films with high transparency and efficient photodegradability. Polymer Degradation and Stability 2007; 92:1255-1264.
DOI: 10.1016/j.polymdegradstab.2007.03.026
14. P.M. Chou, M. Mariatti, A. Zulkifli, S. Sreekantan. Evaluation of the flexural properties and bioactivity of bioresorbable PLLA/PBSL/CNT and PLLA/PBSL/TiO_2 nanocomposites. Composites: Part B 2012; 43:1374-1381.
DOI: 10.1016/j.compositesb.2011.11.023
15. H. Shi, R. Magaye, V. Castranova, J. Zhao. Titanium dioxide nanoparticles: A review of current toxicological data. Particle and Fibre Toxicology 2013; 10:1-33.
DOI: 10.1186/1743-8977-10-15
16. K. Zhang, A.K. Mohanty, M. Misra. Fully biodegradable and biorenewable ternary blends from polylactide, poly(3-hydroxybutyrate-co-hydroxyvalerate) and poly(butylene succinate) with balanced properties. ACS Applied Materials & Interfaces 2012; 4:3091-3101.
DOI: 10.1021/am3004522
17. A. Buzarovska, A. Grozdanov, M. Avella, G. Gentile, M. Errico. Poly(hydroxybutyrate-co-hydroxyvalerate)/titanium dioxide nanocomposites: A degradation study. Journal of Applied Polymer Science 2009; 114:3118-3124.
DOI: 10.1002/app.30867
18. M. Jamshidian, E.A. Tehrany, M. Imran, M. Jacquot, S. Desobry. Poly-lactic acid: Production, applications, nanocomposites, and release studies. Comprehensive Reviews in Food Science and Food Safety 2010; 9:552-571.

DOI: 10.1111/j.1541.2010.00126x

19. R.M. Rasal, A.V. Janorkar, D.E. Hirt. Poly(lactic acid) modifications. Progress in Polymer Science 2010; 35:338-356.
DOI: 10.1016/j.progpolymsci.2009.12.003

20. L. Cabedo, J.L. Feijoo, M.P. Villanueva, J.M. Lagarón, E. Giménez. Optimization of biodegradable nanocomposites based on a PLA/PCL blends for food packaging applications. Macromolecular Symposia 2006; 233:191-197.
DOI: 10.1002/masy.200650124.

21. F. Carrasco, P. Pagès, J. Gámez-Pérez, O.O. Santana, M.L. Maspoch. Processing of poly(lactic acid): Characterization of chemical structure, thermal stability and mechanical properties. Polymer Degradation and Stability 2010; 95:116-125.
DOI: 10.1016/j.polymdegradstab.2009.11.045

22. S. Jain, M.M. Reddy, A.K. Mohanty, M. Misra, A.K. Ghosh. A new biodegradable flexible composite sheet from poly(lactic acid)/poly(ε-caprolactone)blends and micro-talc. Macromolecular Materials and Engineering 2010; 295:750-762.
DOI: 10.1002/mame.201000063

23. Y. Fan, H. Nishida, Y. Shirai, T. Endo. Thermal stability of poly(l-lactide): Influence of end protection by acetyl group. Polymer Degradation and Stability 2004; 84:143-149.
DOI: 10.1016/j.polymdegradstab.2003.10.004

24. H. Peng, Y. Han, T. Liu, W. C. Tjiu, C. He. Morphology and thermal degradation behavior of highly exfoliated CoAl-layered double hydroxide/polycaprolactone nanocomposites prepared by simple solution intercalation. Thermochimica Acta 2010; 502:1-7.
DOI: 10.1016/j.tca.2010.01.009

25. T. Patrício, P. Bártolo. Thermal stability of PCL/PLA blends produced by physical blending process. Procedia Engineering 2013; 59:292-297.
DOI: 10.1016/j.proeng.2013.05.124

26. F. Tuba, L. Oláh, P. Nagy. Characterization of reactively compatibilized poly(D,L-lactide)/poly(ε-caprolactone) biodegradable blends by essential work of fracture method. Engineering Fracture Mechanics 2011; 78:3123-3133.
DOI: 10.1016/j.engfracmech.2011.09.010.

27. M. Amirian, A.N. Chakoli, W. Cai, J.H. Sui. In vitro degradation of poly(L-lactide)/poly(ε-caprolactone) blend reinforced with MWCNTs. Iranian Polymer Journal 2012; 21:165-174. DOI: 10.1007/s13726-012-0014-5
28. C.C. Eng, N.A. Ibrahim, N. Zainuddin, H. Ariffin, W.M.Z.W. Yunus, Y.Y. Then. C.C. Teh. Enhancement of mechanical and thermal properties of polylactic acid/polycaprolactone blends by hydrophilic nanoclay.Indian Journal of Materials Science 2013; 816503. DOI: 10.1155/2013/816503
29. Z. Xu, Y. Zhang, Z. Wang, N. Sun, H. Li. Enhancement of electrical conductivity by changing phase morphology for composites consisting of polylactide and poly(ε-caprolactone) filled with acid-oxidized multiwalled carbon nanotubes. Applied Materials & Interfaces 2011; 3:4858-4864. DOI: 10.1021/am201355j
30. Q. Zhou, M. Xanthos. Nanosize and microsize clay effects on the kinetics of the thermal degradation of polylactides. Polymer Degradation and Stability 2009; 94:327–338. DOI: 10.1016/j.polymdegradstab.2008.12.009
31. C. Courgneau, D. Rusu, C. Henneuse, V. Ducruet, M.-F. Lacrampe, P. Krawczak. Characterisation of low-odour emissive polylactide/cellulose fibre biocomposites for car interior.eXPRESS Polymer Letters 2013; 7:787-804. DOI: 10.3144/expresspolymlett.2013.76
32. B. Lepoittevin, N. Pantoustier, M. Devalckenaere, M. Alexandre, D. Kubies, C. Calberg. Poly(3-caprolactone)/clay nanocomposites by in-situ intercalative polymerization catalyzed by dibutyltindimethoxide. Macromolecules 2002; 35:8385-8390. DOI: 10.1021/ma020300w CCC
33. K. Chrissafis, G. Antoniadis, K.M. Paraskevopoulos, A. Vassiliou, D.N. Bikiaris. Comparative study of the effect of different nanoparticles on the mechanical properties and thermal degradation mechanism of in situ prepared poly(ε-caprolactone) nanocomposites. Composites Science and Technology 2007; 67:2165-2174. DOI: 10.1016/j.compscitech.2006.10.027
34. D. Wu, Y. Zhang, M. Zhang, W. Yu. Selective localization of multiwalled carbon nanotubes in poly(ε-caprolactone)/polylactide blend. Biomacromolecules 2009; 10:417-424.

DOI: 10.1021/bm801183f

35. D. Wu, D. Lin, J. Zhang, W. Zhou, M. Zhang, Y. Zhang, D. Wang, B. Lin. Selective localization of nanofillers: Effect on morphology and crystallization of PLA/PCL blends. Macromolecular Chemistry and Physics 2011; 212:613-6256.
DOI: 10.1002/mapc.201000579
36. Z. Yu, J. Yin, S. Yan, Y. Xie, J. Ma, X. Chen. Biodegradable poly(L-lactide)/poly(3-caprolactone)-modified montmorillonite nanocomposites: Preparation and characterization. Polymer 2007; 48:6439-6447.
DOI: 10.1016/j.polymer.2007.07.024
37. H. Xiu, H.W. Bai, C.M. Huang, C.L. Xu, X.Y. Li, Q. Fu. Selective localization of titanium dioxide nanoparticles at the interface and its effect on the impact toughness of poly(L-lactide)/poly(ether)urethane blends. eXPRESS Polymer Letters 2013; 7:261-271.
DOI: 10.3144/expresspolymlett.2013.24
38. D. Wu, Y. Sun, D. Lin, W. Zhou, M. Zhang, L. Yuan. Selective localization behavior of carbon nanotubes: Effect on transesterification of immiscible polyester blends. Macromolecular Chemistry and Physics 2011; 212:1700-1709.
DOI: 10.1002/macp.201100095
39. J. Chen, Y.-Y. Shi, J.-H. Yang, N. Zhang, T. Huang, Y. Wang. Improving interfacial adhesion between immiscible polymers by carbon nanotubes. Polymer 2013; 54:464-471.
DOI: 10.1016/j.polymer.2012.11.042
40. Y. Aoyagi, K. Yamashita, Y. Doi. Thermal degradation of poly[(R)-3-hydroxybutyrate], poly[ε-caprolactone], and poly[(S)-lactide]. Polymer Degradation and Stability 2002; 76:53-59.
PII: S0141-3910(01)00265-8
41. M. Monsalve, J.M. Contreras, E. Laredo, F. López-Carrasquero. Ring-opening copolymerization of (*R,S*)-β-butyrolactone and ε-caprolactone using sodium hydride as initiator. eXPRESS Polymer Letters 2010; 4:431-441.
DOI: 10.3144/expresspolymlett.2010.54
42. C.-L. Chiang, R.-C. Chang, Y.-C. Chiu. Thermal stability and degradation kinetics of novel organic/inorganic epoxy hybrid containing nitrogen/silicon/phosphorus by sol-gel method. Thermochimica Acta 2007; 453:97-104.

DOI: 10.1016/j.tca.2006.11.013

43. A.A. Vassiliou, K. Chrissafis, D.N. Bakiaris. Thermal degradation kinetics of in situ prepared PET nanocomposites with acid-treated multi-walled carbon nanotubes. Journal of Thermal Analysis and Calorimetry 2010; 100:1063-1071.
DOI: 10.1007/s10973-009-0426-4
44. S. Majoni, S. Su, J.M. Hossenlopp. The effect of boron-containing layered hydroxy salt (LHS) on the thermal stability and degradation kinetics of poly(methyl methacrylate). Polymer Degradation and Stability 2010; 95:1593-1604.
DOI: 10.1016/j.polymdegradstab.2010.05.033
45. M.R. Nanda, M. Misra, A.K. Mohanty. The effect of process engineering on the performance of PLA and PHBV blends. Macromolecular Materials and Engineering 2011; 296:719-728.
DOI: 10.1002/mame201000417
46. I. McNeill, H. Leiper. Degradation studies of some polyesters and polycarbonates. 2. Polylactide: Degradation under isothermal conditions, thermal degradation mechanism and photolysis of the polymer. Polymer Degradation and Stability 1985; 11:309-326.
47. M.-H. Yang, Y.-H. Lin. Measurement and simulation of thermal stability of poly(lactic acid) by thermogravimetricanalysis. Journal of Testing and Evaluation 2009; 37:1-7.
48. K.S. Muralidhara, S. Sreenivasan. Thermal degradation kinetic data of polyester, cotton and polyester-cotton blended textile material. World Applied Sciences Journal 2010; 11:184-189.
49. H. Lin, L. Han, L. Dong. Thermal degradation behavior and gas phase flame-retardant mechanism of polylactide/PCPP blends. Journal of Applied Polymer Science 2014; 40480.
DOI: 10.1002/app.40480
50. H. Sato, R. Murakami, A. Padermshoke, F. Hirose, K. Senda, I Noda. Infrared spectroscopy studies of CH···O hydrogen bondings and thermal behavior of biodegradable poly(hydroxyalkanoate). Macromolecules 2004; 37:7203-7213.
DOI: 10.1021/ma049117o CCC
51. W.H. Hoidy, M.B. Ahmad, E.A.J. Al-Mulla, N.A.B. Ibrahim. Preparation and characterization of polylactic acid/polycaprolactone clay nanocomposites. Journal of Applied Sciences 2010; 10:97-106.

ISSN: 1812-5654

52. C. Vogel, H.W. Siesler. Thermal degradation of poly(ε-caprolactone), poly(L-lactic acid) and their blends with poly(3-hydroxy-butyrate) studied by TGA/FT-IR spectroscopy. Macromolecular Symposia 2008; 265:183-194.
DOI: 10.1002/masy.200850520

53. O. Persenaire, M. Alexandre, P. Degée, P. Dubois. Mechanisms and kinetics of thermal degradation of poly(ε-caprolactone). Biomacromolecules 2001; 2:288-294.
DOI: 10.1021/bm0056310 CCC

54. M. Unger, C. Vogel, H.W. Siesler. Molecular weight dependence of the thermal degradation of poly(ε-caprolactone): A thermogravimetric differential thermal Fourier transform infrared spectroscopy study. Applied Spectroscopy 2010; 64:805-809.
DOI: 10.1366/000370210791666309

Chapter 4

Morphology and thermal degradation studies of melt-mixed PHBV/PCL biodegradable polymer blend nanocomposites with TiO_2 as filler

This chapter has been published as:
J.P. Mofokeng, A.S. Luyt. Morphology and thermal degradation studies of melt-mixed PHBV/PCL biodegradable polymer blend nanocomposites with TiO_2 as filler. Journal of Materials Science 2015; 50: 3812-3824.
DOI 10.1007/s10853-015-8950-z

Abstract

The morphology, thermal stability and thermal degradation kinetics of melt mixed PHBV/PCL blends filled with small amounts of TiO_2 nanoparticles were investigated. The nanoparticles were mostly well dispersed in both phases of the PHBV/PCL blend, which showed a co-continuous morphology at a 50/50 w/w ratio, but some large agglomerates were also observed. The equal dispersion of the TiO_2 nanoparticles in both polymers was attributed to the polymers having the same surface properties, polarities and viscosities. The thermal stability of PHBV was improved when blended with the more thermally stable PCL, but the PCL was less thermally stable. The introduction of only 1 wt% of TiO_2 nanoparticles seems to have observably improved the thermal stabilities both polymers in the blend, but it is quite possible that the nanoparticles only retarded the evolution of the degradation products through their interaction with these products. Further improvement in thermal stability at higher nanoparticle contents was insignificant, probably because of the nanoparticle agglomeration which reduced their effectiveness. Changes in the activation energies of degradation, determined through the Flynn-Wall-Ozawa model from thermogravimetric analysis (TGA) mass loss data, and differences between the Fourier-transform infrared (FTIR) spectra of the degradation volatiles obtained during the degradation process, to a large extent support the other observations.

Keywords: poly(hydroxybutyrate-co-valerate)); poly(ε-caprolactone); titania; blends; nanocomposites; thermal degradation

4.1. Introduction

Poly(3-hyroxybutyrate-co-3-hydroxyvalerate) (PHBV) is a biodegradable, biocompostable polyester along with poly(lactic acid) (PLA) and polyglycolide (PGA). This polymer is used in biomedical applications, but has not been widely used in the packaging industry. This is because it has a few shortcomings, of which low thermal stability and brittleness are the most disturbing. The brittleness is caused by its high degree of crystallinity [1], and this property limits its use in most packaging applications. To overcome these shortcomings, PHBV can be blended with other rubbery biodegradable polymers to improve its toughness without compromising its biodegradability [2]. The usual objective for preparing a blend of two or more polymers is not to significantly change the properties of the components, but to capitalize on the maximum possible performance of the blend. In this case the choice of polymer to blend with PHBV should only be to overcome the brittleness and improve the thermal stability. One such a polymer is poly(ε-caprolactone) (PCL) [3].

PCL belongs to the category of biocompatible, biodegradable and nontoxic polyesters with excellent mechanical strength. It is a synthetic semicrystalline polyester, also considered as an interesting blend component due to its good ductility, thermal resistance and moderate degree of crystallinity [4-6]. It has a low glass transition temperature of about -60 °C, existing always in a rubbery state at room temperature, and a melting temperature of 60 °C. It has a very good toughness and thermal stability. The only limiting factor for using this polymer individually for many applications is its low melting temperature [4,7]. To overcome this it may be blended with another biopolymer which has a higher melting temperature. A blend of PHBV and PCL should produce a balanced final product with the toughness and thermal stability of PHBV being improved by the presence of PCL, and the disadvantage of PCL's low melting temperature being improved. Although the melting temperature of PCL is significantly lower than that of PHBV, PCL does not degrade at lower temperatures and it can therefore be processed at temperatures well above its melting temperature [8,9].

Blends of PHBV and PCL have not been extensively studied, although there are some papers [10-15], mostly on biomedical applications and on the thermal properties of the blends. Chun *et al*. [15] focused on the effect of PCL on the melting behaviour of PHBV, and reported that PCL did not change the shape and position of the PHBV melting peak, whereas the PHBV

crystallization temperature was 8–12 °C lower in the PHBV/PCL blends. This shows that there is still a possibility to utilise this kind of material in the packaging industry, mostly for food packaging. No previous study reported on the thermal degradation of PHBV/PCL blends or nanocomposites, while a few only mentioned the thermal degradation of these blends used in medical applications [16-18]. These reports mostly concentrated on the thermal stability of PHBV in the blend, and found an improvement in its thermal stability in the presence of PCL. Liu *et al*. [19], however, worked with block co-polymers of PHBV and PCL, and they found that the presence of PCL in the co-polymer improved the thermal stability of PHBV, while the thermal stability of PCL was compromised. They further reported a reduction in the activation energy of the PHBV block, and an increase in that of the PCL block.

The use of inorganic micro or nanoparticles may improve the thermal stabilities of both polymers in the blend, since most previous studies showed this to be the case for various polymers [19-22].TiO_2 received a lot of attention as nanofiller in polymers because of its good thermal stability, accessibility, and catalytic properties. TiO_2 is an inorganic material obtained from a variety of naturally occurring ores that contain ilmenite, rutile, anatase, and leucoxene, and it is generally used for various applications such as photo electrochemical activity, solar energy conversion, photocatalysis, UV detection, ultrasonic sensing, and as a promising material in applications such as water or wastewater treatment. Its environmental compatibility, non-toxicity and low price are some practical advantages of TiO_2 [23-28]. Its presence in biodegradable polymer composites may contribute in accelerating the photo-degradation of these polymers.

In the present work the effect of blending of PHBV with PCL, and the addition of TiO_2 nanoparticles as inorganic nanofiller, on the thermal stability and degradation behaviour of PHBV/PCL/TiO_2 nanocomposites were studied. The structure and properties of the blends and nanocomposites were also studies and related to the thermal degradation behaviour of the samples.

4.2. Experimental

4.2.1 Materials

The PHBV biopolymer used was purchased from Goodfellow, Huntington, UK. It has a 12% hydroxyvalerate content, a density of 1.25 g cm^{-3}, a melting temperature of ~150 °C, and a degree of crystallinity of ~59%. PCL Capa™ 6500 was purchased from Southern Chemicals, Johannesburg, South Africa. It has a density of 1.1 g cm^{-3}, a glass transition temperature of approximately -61 ºC, a melting temperature of ~60 ºC, and a degree of crystallinity of ~35%. Anatase titanium(IV)oxide (TiO_2) with particle sizes < 25 nm and 99.7% purity was supplied by Sigma-Aldrich in South Africa.

4.2.2 Preparation of blends and nanocomposites

The samples were prepared *via* melt-mixing using a Brabender Plastograph. PHBV was dried in an oven at 80 °C for four hours prior to mixing, and PCL and TiO_2 were used as received. 30/70, 50/50 and 70/30 w/w PHBV/PCL blends and their nanocomposites with 1, 3 and 5 wt% of TiO_2 were mixed at 170 °C for ten minutes. The samples were compression moulded into 2 mm thick sheets at the same temperature for 5 minutes using a hydraulic press at a pressure of 50 bar, after which they were removed and left to cool under ambient conditions.

4.2.3 Characterization

Size exclusion chromatography (SEC) measurements were performed on a PL Olexis column (Polymer Laboratories). Chloroform was used as mobile phase at a flow rate of 1.00 mL min^{-1}. The samples were prepared at a concentration of 2 mg mL^{-1}. The column was calibrated with polystyrene (PS) standards from Polymer Laboratories (Church Stretton, Shropshire, UK). The chromatograph comprised of a Waters 1515 isocratic pump, a Waters inline degasser AF, and a Waters 717 Plus auto sampler with a 100 µL sample loop. The system was connected to an evaporative light scattering detector (PL-ELS 1000). Nitrogen was used as carrier gas in the

ELSD, at a flow rate of 1.5 SLM. The evaporator and nebulizer temperatures were set at 100 and 40 °C, respectively.

The melt flow index of the two polymers used in the blend was determined using a CEAST Melt Flow Junior. Ten samples each of both polymers were analysed at 180 °C. The amount of PHBV which flowed through the die over a period of 10 minutes, and the amount of PCL which flowed through the die over a period of 5 minutes, under 2.16 kg weight were determined. The determined amount of PCL was multiplied by 2 to determine a comparable MFI.

A Tescan VEGA3 scanning electron microscope (SEM) was used to study the surface dispersion of the TiO_2 nanoparticles in the PHBV/PCL blends. The liquid nitrogen fractured samples were sputter coated with gold for 30 seconds to eliminate sample charging, and analyses were performed at three different magnifications.

The morphologies of the nanocomposites were characterised by transmission electron microscopy (TEM). Images were obtained using a 200 kV FEI Tecnai 20 TEM fitted with Gatan Tridiem. The 50/50 w/w PHBV/PCL blend with 5 wt% TiO_2 nanoparticles was trimmed and sectioned to fit the ultra-microtome, since they were hard enough to cut without cooling. 100-150 nm thin sections were collected on copper grids and viewed. Uranyl acetate was used to stain PCL in the blend to identify the different phases.

The contact angles of the samples were determined at room temperature on a surface energy evaluation system, based on the sessile drop method. At least 10 replicates of each sample were analysed to ensure reproducibility of the results. Distilled water (H_2O), and diiodomethane (CH_2I_2) were used as polar and non-polar solvents, respectively. The literature values of their surface energies are: (H_2O: $\gamma^p = 50.7$ mJ m^{-2} and $\gamma^d = 22.1$ mJ m^{-2}; CH_2I_2: $\gamma^p = 6.7$ mJ m^{-2} and $\gamma^d = 44.1$mJ m^{-2}). The contact angles, total surface energies, as well as their dispersive and polar components are reported. The interfacial tension between the components in a blend was calculated with the Owens-Wendt method using the geometric equation (Equation 4.1) [29-31].

$$\gamma_{12} = \gamma_1 + \gamma_2 - 2\sqrt{\gamma_1^{\,d}.\gamma_2^{\,d} + \gamma_1^{\,p}.\gamma_2^{\,p}} \qquad (4.1)$$

where γ_{12} = interfacial tension between components 1 and 2 in the blend, γ_1 and $\gamma_2$are the total surface energies of components 1 and 2, γ_1^d and γ_2^d are the dispersive surface energies of

components 1 and 2, and γ_1^p and γ_2^p are the polar surface energies of the components in the nanocomposites.

Differential scanning calorimetry (DSC) was used to determine the degrees of crystallinity of the polymers. The analyses were performed under nitrogen atmosphere at 10 °C min^{-1}. The melting enthalpies of PHBV and PCL were determined from the curves, and Equation 2 was used to calculate the degrees of crystallinity, where ΔH_m is the measured melting enthalpy and ΔH_m^o is the enthalpy of melting of the 100% crystalline polymers, with values of 139 J g^{-1} for PCL [6,32] and 109 J g^{-1} for PHBV [33,34].

$$X_C(\%) = \left(\frac{\Delta H_m}{\Delta H_m^o} \right) \times 100\% \qquad (4.2)$$

A Perkin-Elmer STA6000 thermogravimetric analyser (TGA) was used to analyse the thermal degradation behaviour of the samples. The analyses were done from 30 to 600 °C at a heating rate of 10 °C min^{-1} under nitrogen atmosphere. The sample masses were ~24 mg. The samples for thermal degradation kinetics were run at 3, 5, 7, 9 and 15 °C min^{-1} heating rates under nitrogen atmosphere, and the TGA's integrated kinetics software (based on the Flynn-Ozawa-Wall method (Equation 4.3)) was used to calculate the activation energies:

$$\ln \beta = c - 1.052 \left(\frac{E_a}{RT} \right) \qquad (4.3)$$

where β is the heating rate in K min^{-1}, c is a constant, E_α is the activation energy in kJ mol^{-1}, R is the universal gas constant, and T is the temperature in K. The plot of ln β vs. 1/T, obtained from the TGA curves recorded at several heating rates, should be a straight line. The activation energy was evaluated from its slope. The TGA was also connected to a Perkin-Elmer Spectrum 100 Fourier-transform infrared (FTIR) spectrometer to analyse the thermal degradation volatiles. The same temperature range and heating rate were used, and the volatiles were transferred to FTIR through a Perkin-Elmer TL 8000 balanced flow FT-IR EGA system at 200 ºC and a flow rate of 150 ml min^{-1}. Spectra were collected at five different temperatures during the degradation process.

4.3. Results and discussion

4.3.1 Morphology investigation

Scanning electron microscopy (SEM) was initially used to observe the dispersion of the TiO_2 nanoparticles in the immiscible PHBV/PCL blend. Figure 1 illustrates the 50/50 w/w PHBV/PCL blend with 5 wt% TiO_2 nanoparticles, at two different magnifications. It was not easy to observe any nanoparticles in Figure 4.1(a), but close inspection does show some white dots that may indicate dispersed nanoparticles. Although slightly out of focus, Figure 4.1(b) more clearly shows the well dispersed nanoparticles.

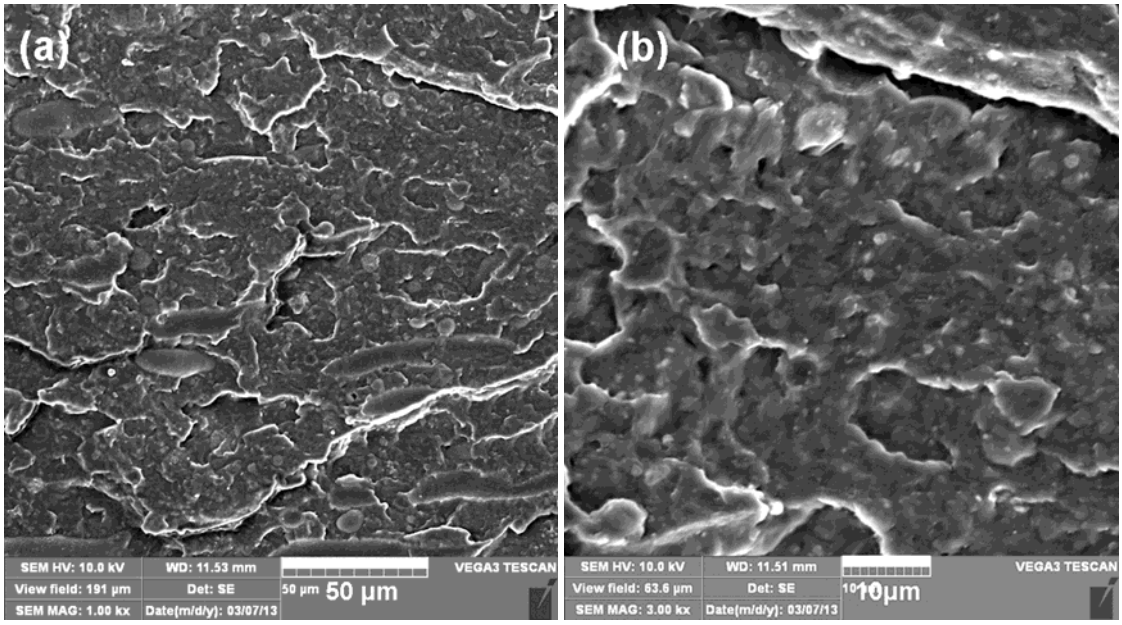

Figure 4.1 SEM micrographs of 50/50 w/w PHBV/PCL ratios with 5 wt% TiO_2: (a) 1000x and (b) 3000x magnification

The TEM analysis of the same sample confirms the good dispersion of the TiO_2 nanoparticles (Figure 4.2), but a mixture of small, well dispersed particles and agglomerates are visible in these pictures. Although we did not include all the pictures in this paper, pictures taken at different locations in the same sample showed similar nanoparticle dispersions. Even though the nanoparticles seem to be well dispersed, the different polymer phases cannot be distinguished in Figure 4.2(a), and therefore staining of one phase was required in order to distinguish the

phases in the blend. In this work uranyl acetate was used to selectively stain the PCL. The dark phase in Figure 4.2(b) is therefore the stained PCL phase, and the lighter phase the PHBV phase. Although the two polymers in the blend and their interface are clearly visible, it is not possible to see whether there are nanoparticles in the stained PCL phase, but we assume that they are there, based on our observation from Figure 4.2(a). Figure 4.2(b) further confirms the co-continuous morphology of the blend.

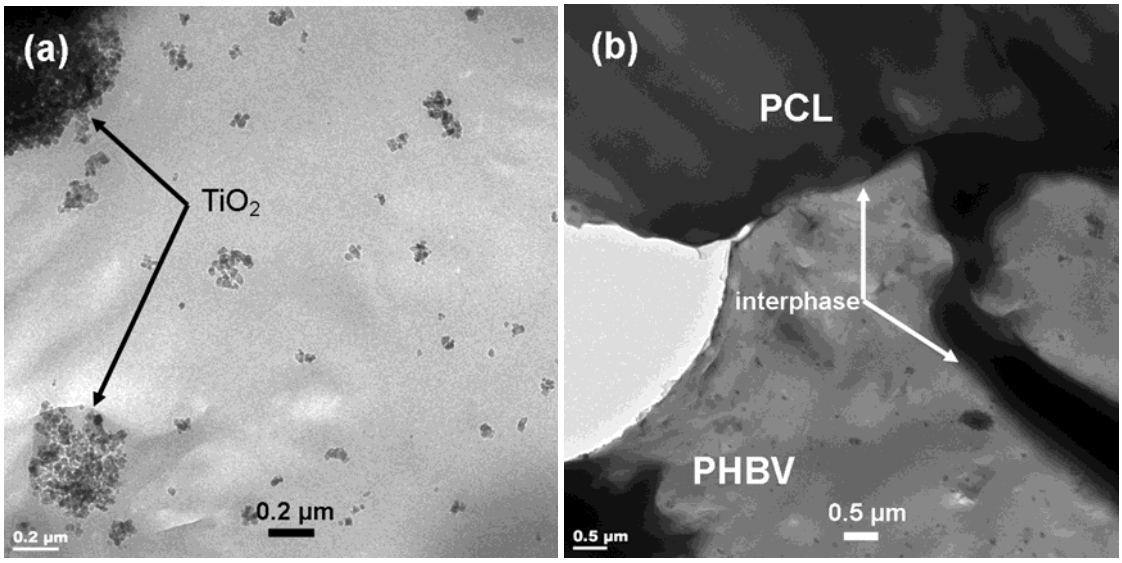

Figure 4.2 TEM pictures of (a) unstained and (b) uranyl acetate stained 50/50 w/w PHBV/PCL with 5 wt% TiO_2 both at 19000× magnification

One would expect that melt mixing of two polymers with a significant difference in molar mass, viscosity and crystallinity with an inorganic filler would give rise to the selective localization of the filler. The results in Table 4.1 show that PHBV has a much higher molar mass and degree of crystallinity, but a much lower melt flow index (much higher viscosity) than PCL. The surface energies of PHBV and PCL are very similar, and so are their dispersive and polar parts (Table 4.2). There is also very little difference between the PHBV/TiO_2 and PCL/TiO_2 interfacial tensions (Table 4.3), which further confirms that there was really no reason why the nanoparticles should selectively locate in any one of the two polymers. These surface energy values were determined at room temperature, but they may be different from the values at the mixing temperature we used, and therefore we can only assume that the values in Table 4.2 are not too much different from what the values would have been if the surface energies were

determined at 170 °C. The differences in molar mass, degree of crystallinity and viscosity should have been enough reason for the nanoparticles to selectively locate in the PCL phase [35-37], but in this case the similar surface energies and interfacial tensions probably played a much bigger role in determining the localization and dispersion of the TiO_2 nanoparticles.

Table 4.1 Summary of molar masses, degrees of crystallinity, and melt flow index values of PHBV and PCL

Sample	M_n	M_w	M_z	D	DC / %	MFI / (g/10 min)
PHBV	36710	77537	150310	2.1	69	8.1
PCL	19005	36135	55440	1.9	48	14.5

M_n = number average molar mass, M_w = weight average molar mass, M_z = viscosity average molar mass, D = dispersity index, DC = degree of crystallinity, MFI = melt flow index

Table 4.2 Contact angles of PLA, PCL and TiO_2. The TiO_2 contact angle was found in the literature [29]

	Contact angle / deg		Surface energy / mN m^{-1}		
	H_2O	CH_2I_2	γ	γ^d	γ^p
PHBV	54.7 ± 1.0	35.6 ± 0.0	56.3	41.7	14.6
PCL	60.2 ± 0.8	27.0 ± 0.5	55.8	45.4	10.4
TiO_2	19.7	10.1	80.7	46.4	34.3

γ = surface energy, γ^d = dispersive component of surface energy, γ^p = polar component of surface energy

4.3.2 Thermogravimetric analysis (TGA)

Figure 4.3 shows the TGA curves of all the investigated samples. PHBV degrades around 280 °C and PCL around 415 °C. The two polymers degrade separately, in the blend, confirming their immiscibility. The first mass loss step represents the degradation of PHBV, and the second step that of PCL. Blending PHBV with PCL seems to improve the themal stability of PHBV (Figure 4.3 and Table 4.4), since PCL is more thermally stable, but PHBV seems to decrease the thermal stability of PCL. It is known that the thermal degradation of PHBV follows a random chain

scission mechanism involving a β-hydrogen elimination process (six-membered ring ester decomposition process) to form substrate olefins and oligomers [34,38], while PCL decomposes through a two-step degradation mechanism, the first step being a polymer chain cleavage *via* cis-elimination and the second step an unzipping depolymerization from the hydroxyl end of the polymer chain [39,40].

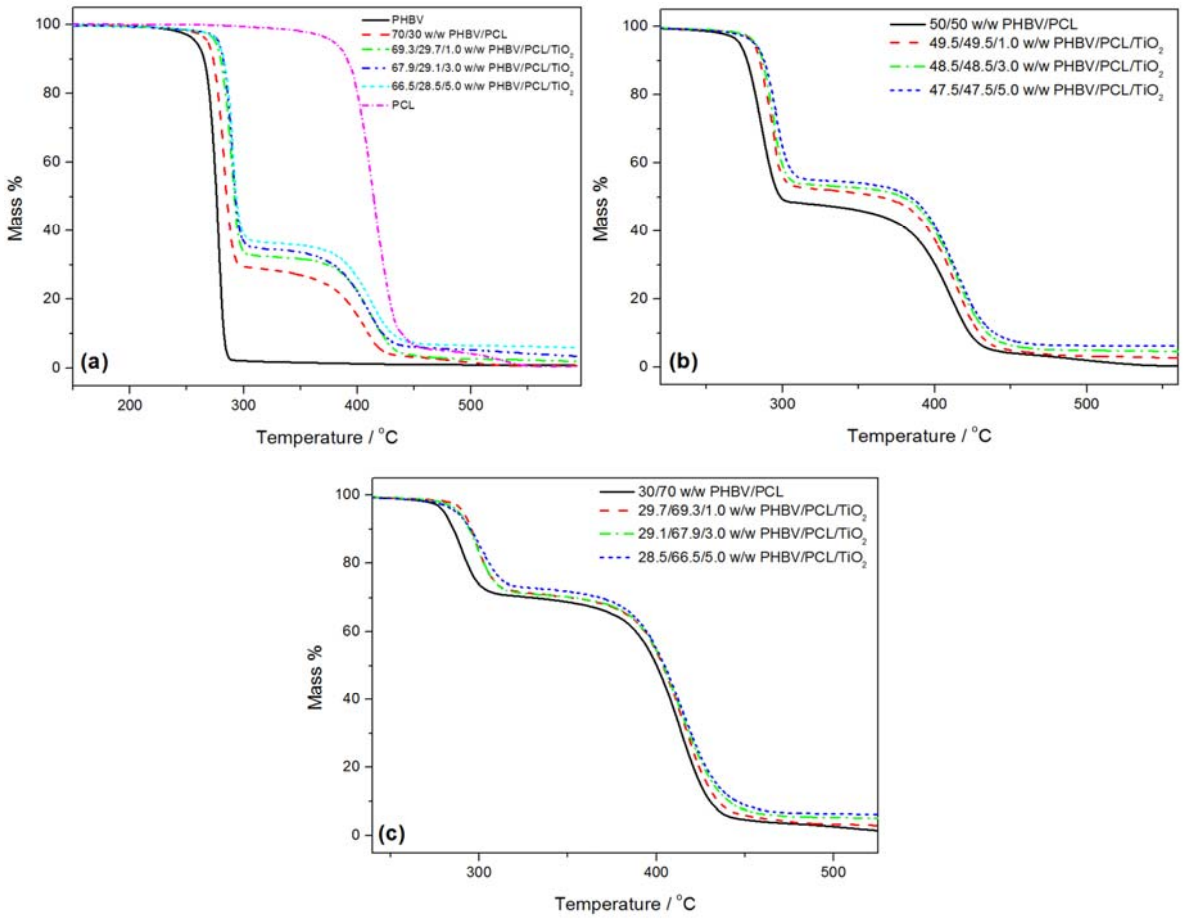

Figure 4.3 TGA curves of (a) 70/30 w/w, (b) 50/50 w/w, and (c) 30/70 w/w PHBV/PCL with 1, 3 and 5 wt% of TiO_2

Table 4.3 Interfacial tensions calculated using the geometric-mean equation (Equation 2)

Component couple	Interfacial tension / mN m^{-1}
PHBV/PCL	0.43
PHBV/TiO_2	4.27
PCL/TiO_2	6.93

Table 4.4 Derivative TGA peak temperatures of all the investigated samples

Sample	PHBV degradation step / °C	PCL degradation step / °C
Neat PHBV	280.1	-
70/30 w/w PHBV/PCL	283.4	409.0
50/50 w/w PHBV/PCL	287.7	410.9
30/70 w/w PHBV/PCL	291.1	415.4
Neat PCL	-	414.1 and 529.4
69.3/29.7/1.0 w/w PHBV/PCL/TiO_2	292.5	413.1
49.5/49.5/1.0 w/w PHBV/PCL/TiO_2	294.6	418.3
29.7/69.3/1.0 w/w PHBV/PCL/TiO_2	299.3	418.0
67.9/29.1/3.0 w/w PHBV/PCL/TiO_2	291.5	407.3
48.5/48.5/3.0 w/w PHBV/PCL/TiO_2	294.0	416.0
29.1/67.9/3.0 w/w PHBV/PCL/TiO_2	298.8	415.3
66.5/28.5/5.0 w/w PHBV/PCL/TiO_2	289.8	413.4
47.5/47.5/5.0 w/w PHBV/PCL/TiO_2	295.8	413.4
28.5/66.5/5.0 w/w PHBV/PCL/TiO_2	304.0	415.6

Figures 4.4 and 4.5 show the temperatures at 50% degradation of each component in the blends as function of titania content in the nanocomposites. These figures illustrate the effect of blending and filler loading on the thermal stability of PHBV (Figure 4.4) and that of PCL (Figure 4.5). The temperatures at which PHBV mass loss occurs increased by about 14 °C for the blend containing 70% PCL. This is expected since PCL is more thermally stable than PHBV and probably absorbs quite an amount of energy during heating. The introduction of 1 wt% TiO_2 nanoparticles improved the thermal stability even further (Figure 4.4). However, larger filler contents had little or no effect on the thermal stability of PHBV. At low TiO_2 contents the filler is

well dispersed with little agglomeration, and these large surface area particles probably interact fairly strongly with the PHBV degradation products, retarding their escape from the molten blend. The insignificant change as the filler loading increased is probably related to increased levels of agglomeration so that the effective surface area, and the probable interaction with volatile degradation products, did not increase significantly.

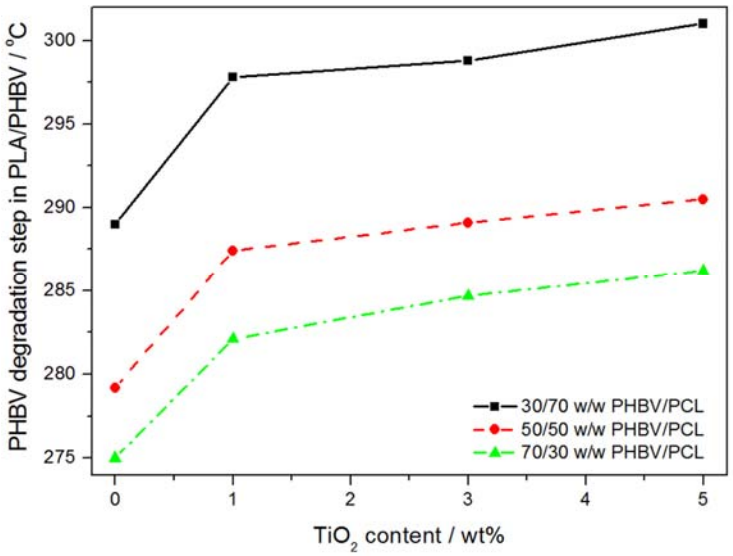

Figure 4.4 Effect of blending and filler addition on the temperature at 50% mass loss of PHBV in the PHBV/PCL blends and nanocomposites

The degradation of PCL, on the other hand, decreased when blended with low thermally stable PHBV (Figure 4.5). As in the case of PHBV, the presence of TiO_2 nanoparticles increased the mass loss temperatures of PCL, which may also be related to the interaction of the nanoparticles with the PCL degradation volatiles, and the retardation of their volatilization.

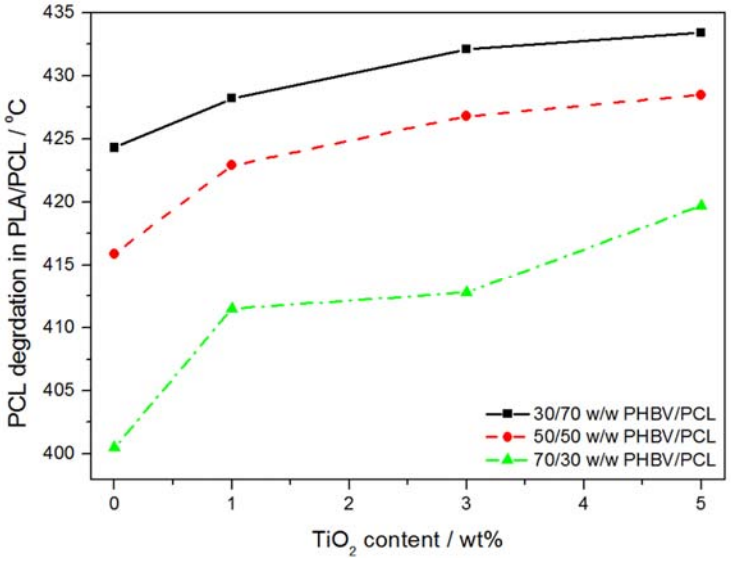

Figure 4.5 Effect of blending and filler addition on the temperature at 50% mass loss of PCL in the PHBV/PCL blends and nanocomposites

4.3.3 Degradation kinetics

The activation energy (E_α) is the minimum energy needed to initiate thermal degradation. Figure 4.6 illustrates the relationship between activation energy and the extent of mass loss (α) for neat PHBV, neat PCL and their nanocomposites with 3 wt% TiO_2 nanoparticles content. The degradation activation energy of PHBV remained unchanged around 146 kJ mol^{-1} throughout the degradation process. This could mean that the degradation mechanism of pure PHBV did not change throughout the degradation process, which probably has a single rate-determining step, because of the independence of E_α on the extent of degradation [41]. In the presence of TiO_2 the E_α started at 120 kJ mol^{-1} (26 kJ mol^{-1} lower than neat PHBV) and increased almost linearly with increasing degradation to 135 kJ mol^{-1}. This lower activation energy indicates that the rate of degradation in the presence of the nanoparticles was less dependent on temperature, which confirms that the nanoparticles probably acted as catalysts for the initiation of degradation, which is something that other authors also mentioned in related studies [41,42]. This effect was also seen in the FTIR spectra of the PHBV degradation volatiles (Figure 4.7(a)), which showed peaks for hydroxyl groups (3577 and 967 cm^{-1}), hydrocarbons (2978, and 2887 cm^{-1}), carbon dioxide (CO_2, 2300cm^{-1}), carbonyls (1755 cm^{-1}), alkenes (1660 cm^{-1}), and C-O-C (1141 cm^{-1}). PHBV is a co-polymer made up of 3-hydroxybutanoic acid (hydroxybutyrate) and 3-hydroxypentanoic acid

(hydroxyvalerate) that are connected by an ester bond. During the thermal degradation of PHBV the ester linkage is cleaved forming the individual monomers, together with other products like carbon dioxide and water due to ester breakup. Both monomers contain carbonyls, hydrocarbons, hydroxyl groups and oxygen linkages that are well described by the spectra in Figure 4.7(a). From the spectra we took of the volatiles at different temperatures during the degradation of PHBV, the spectrum at 265 °C had the most intense peaks, and in the case of PHBV/TiO_2 the most intense peaks were observed at 270 °C. This shows that, although the nanoparticles may have catalysed the degradation reaction, they also retarded the volatilization of the degradation products, which increased the temperature at which these volatiles were released from the sample.

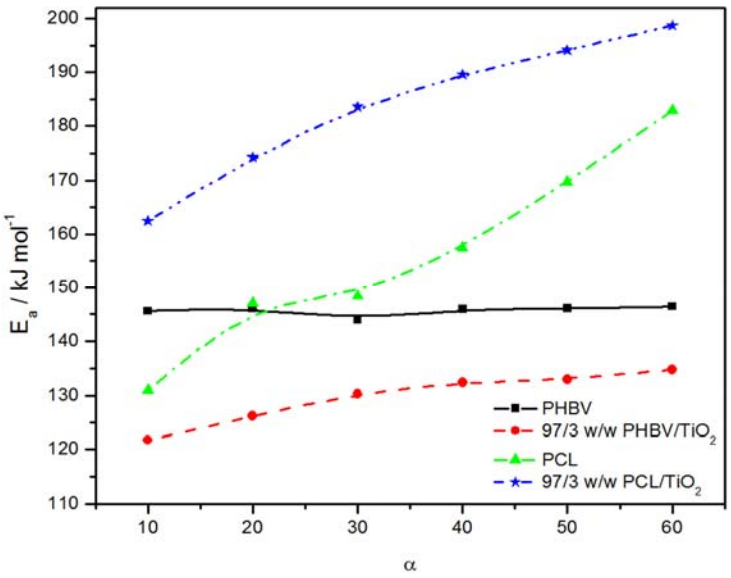

Figure 4.6 Activation energy vs. conversion of PHBV, PCL, 97/3 w/w PHBV/TiO_2 and 97/3 w/w PCL/TiO_2

The E_α of neat PCL increased with the extent of mass loss from 131 to 183 kJ mol^{-1}. Such an increase in E_α is said to be typical for the degradation of polymers [43]. This dependence on the extent of mass loss may be an indication that more than one mechanism was involved in the degradation of PCL [39,40]. The TGA results also showed that PCL underwent two degradation steps. The activation energy of PCL was higher for the sample containing TiO_2 nanoparticles, and increased from 160 kJ mol^{-1} to 200 kJ mol^{-1} with increasing extent of mass loss. This seems to

indicate an improvement in the thermal stability of PCL, because the degradation rate seems to become more temperature-dependent. However, it is quite possible that the nanoparticles retarded the diffusion of the volatile degradation products from the sample through their interaction with these volatiles, and therefore the temperature had to be increased more to obtain the same extent of mass loss.

The first step in the degradation of PCL is the elimination of β-hydrogens from which volatile products like water and carbon dioxide are formed, and this is followed by the main chain degradation which evolves carboxylic acids (5-hexenoic acid with its di- and trimers), and ε-caprolactone monomers at higher temperatures. These volatile products are characterized by the presence of carbonyl band (1756 cm^{-1}) which indicates the presence of 5-hexenoic acid and ε-caprolactone amongst the volatiles. Other bands in the FTIR spectra in Figure 4.7(b) are those of the hydroxyl group band (3577 cm^{-1}), hydrocarbons (2943 cm^{-1}), CO_2 (2400-2300 cm^{-1}), C-O (2175 and 2112 cm^{-1}), C=O (1756 cm^{-1}) and C-O-C (1250-1050 cm^{-1}), indicating the presence of *inter alia* water and carbon dioxide amongst the degradation volatiles. Vogel *et al.* [44] studied the degradation of PCL and reported that if the bands around 1778 and 2350 cm^{-1} (C=O and CO_2) are detected in FTIR spectrum of the PCL degradation volatiles, it means that 5-hexenoic acid formed before carbon dioxide. However, if the 1736 and 1778 cm^{-1} are observed in the spectrum, 5-hexenoic acid was evolved before ε-caprolactone.

The spectra we took of the degradation volatiles of neat PCL at different temperatures during the degradation process show the highest peak intensities at 386 °C, while for the nanocomposite the highest peak intensities were observed in the 397 °C spectrum. For the spectra obtained at these temperatures, the peak intensities for the nanocomposites were much lower than those for neat PCL. This observation, together with the higher degradation temperature and activation energies, confirm the retardation effect of the TiO_2 nanoparticles on the volatilization of the degradation products in the nanocomposite, which could be due to a strong interaction between the nanoparticles and the degradation volatiles.

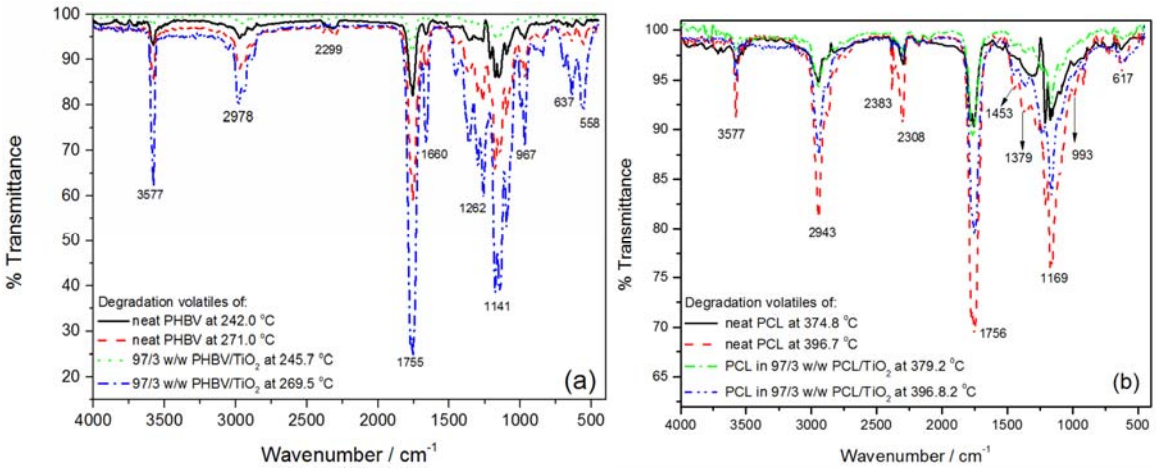

Figure 4.7 FTIR spectra of the degradation products of (a) neat PHBV and 97/3 w/w PLA/TiO_2, and (b) neat PCL and 97/3 w/w PCL/TiO_2

Figure 4.8 shows the activation energy versus extent of mass loss for 50/50 w/w PHBV/PCL blend and its nanocomposite with 3 wt% TiO_2 nanoparticles. The first half represents the degradation activation energy of PHBV, as it degrades first, and the second half represents the degradation activation energy of PCL. The activation energy of PHBV changed very little over its mass loss range, similar to what was observed for the neat polymer (Figure 4.6), but it was significantly lower than that of the neat polymer. The activation energy for the degradation of PCL in the blend was also lower than that of the neat polymer, and decreased with increasing extent of mass loss. A possible reason for this is that the co-continuous morphology of the blend, and the weak interaction between the two components, in some way changed the energy requirements for the initiation and propagation of the degradation for both components. The decrease in activation energy for PCL may also have been the result of the evaporation of PHBV degradation products that accelerated the release of the PCL degradation products.

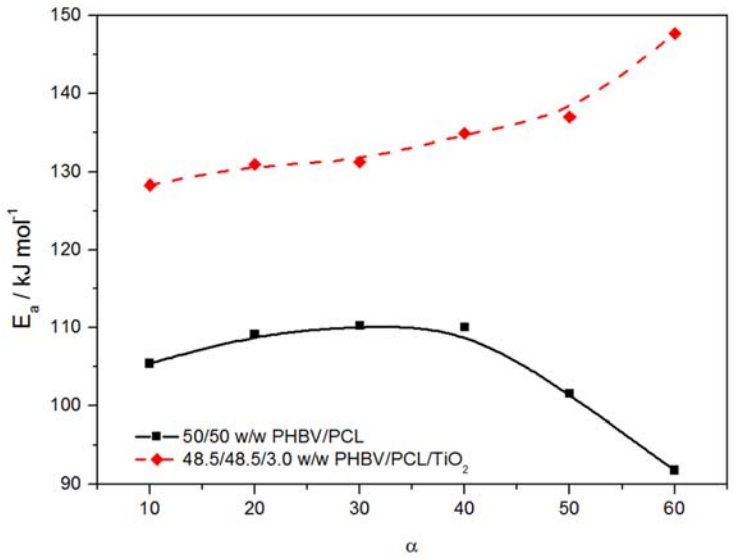

Figure 4.8 Activation energy vs. conversion of 50/50 w/w PHBV/PCL with 3 wt% TiO_2

Gaseous degradation products formed during the thermal or biodegradation of polyesters contain water and carbon dioxide in addition to other volatiles, where CO_2 is formed by the decarboxylation of carboxylic acid end groups. Water comes from the condensation reactions of hydroxyl and /or carboxylic acid functional groups formed as the temperature increases [45-47].It has been reported that the presence of moisture in biodegradable polymers causes hydrolysis of the carboxylic acids, which results in the early thermal degradation of polymers [48]. Water is one of the degradation products of PHBV, as indicated by the presence of the 967 and 3577 cm^{-1} (O-H vibration) bands in Figure 4.7(a). Since PHBV degrades first when heating a PHBV/PCL blend, the released moisture may accelerate the degradation of PCL, which could have contributed to the decrease in activation energy of the PCL phase in the neat blend.

In the presence of TiO_2 nanoparticles the activation energy was significantly higher than that in the blend, and observably increased during the PCL degradation phase (Figure 4.8). The higher activation energy for the degradation of the PHBV phase indicates that the influence of blending, as discussed earlier, has been offset by the retardation of volatilization through interaction with the nanoparticles. This is probably also the reason why the PCL phase shows an increase in activation energy compared to the decrease observed for the neat blend.

The FTIR spectra of the degradation volatiles in Figure 4.9 were obtained at approximately 278 °C (which falls within the PHBV degradation step) and 408 °C (which falls within the PCL

degradation step). The 278 °C spectra show the same peaks in the same positions as those for pure PHBV, confirming that blending with PCL did not change the degradation mechanism of PHBV, and that PHBV almost completely degraded before the onset of PCL degradation. Even though it is not clear in Figure 4.9, the spectra we took of the degradation volatiles of the blend at different temperatures during the PHBV degradation step show the most intense peaks at 271 °C for PHBV in the neat blend, and this temperature is higher than the 265 °C where the most intense peaks were observed for pure PHBV (Figure 4.7(a)). This confirms that blending with PCL improved the thermal stability of PHBV, probably by absorbing some of the heat so that higher temperatures are needed to initiate the PHBV degradation process. For the degradation of PHBV in the blend nanocomposite the most intense peaks were observed in the 277°C spectrum, confirming the additive effect of blending with PCL (which probably isolated the PHBV to some extent) and the retardation of degradation product evolution through interaction with the titania nanoparticles.

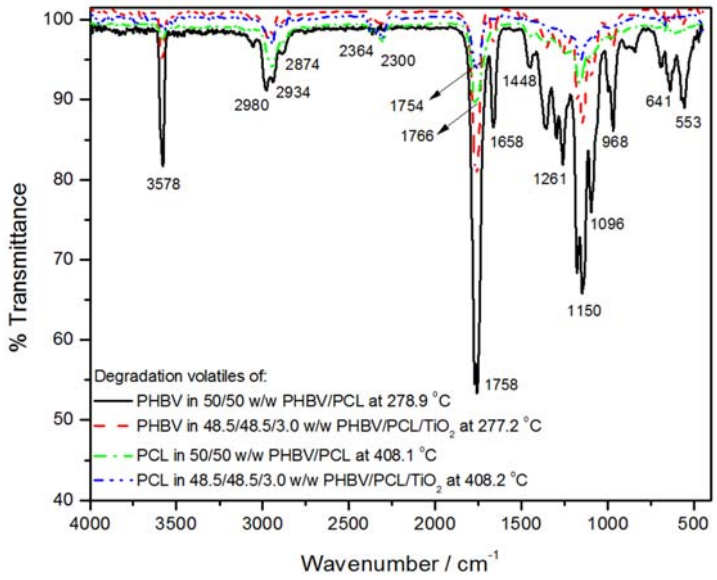

Figure 4.9 FTIR spectra of the degradation products of PHBV and PCL in 50/50 w/w PHBV/PCL and its nanocomposites with 3 wt%

The spectra obtained at 408 °C for PCL in the blend and the blend nanocomposite show identical bands to those for neat PCL and its nanocomposite (Figure 4.7(b)), confirming that there was no change in the PCL degradation mechanism and that the PHBV degradation products were

completely evolved before the onset of PCL degradation. The spectra taken at different temperatures for the degradation of PCL in the blend and the blend nanocomposite show the maximum intensities around 374 °C and 378 °C, respectively. The peak intensities in the 378 °C spectrum for the blend nanocomposite are much lower and the carbonyl band shifted from 1754 to 1766 cm^{-1}. The shift of degradation process to higher temperatures, the reduction in peak intensities for the nanocomposite, the shift of the carbonyl band, and the increased activation energy of degradation for PCL in the nanocomposite all indicate that the nanoparticles retarded the volatilization of the PCL degradation products. It therefore seems as if the volatile degradation products from both polymers interacted with the TiO_2 nanoparticles, and that the PCL in the blend to some extent protected the PHBV from degradation. However, PCL degraded more readily in the presence of PHBV, even in the presence of titania nanoparticles, although the fact that the evolution of the volatile degradation products was retarded through interaction with the nanoparticles to some extent masked this lower degradation stability.

4.4. Conclusions

The purpose of this work was to investigate the effect of blending and the presence of small amounts of titania nanoparticles on the morphology, thermal stability and degradation kinetics of PHBV/PCL blends. 50/50 w/w PHBV/PCL showed a co-continuous morphology, and the nanoparticles were well dispersed in both polymers, but some large agglomerates were also visible. The equal dispersion of the nanoparticles in both polymers in the blends was attributed to the polymers having almost the same surface energies, polar characters, viscosities, and a low interfacial tension between the polymers, although their molar masses and degrees of crystallinity were different. The thermal stability of the PHBV improved in the presence of the more thermally stable PCL, but PCL became less thermally stable. The presence of TiO_2 nanoparticles improved the thermal stabilities of both polymers, as was observed from the TGA curves, the kinetically determined activation energies of degradation, and the FTIR analysis of the degradation volatiles. We are, however, of the opinion that the degradation process as such was not really influenced by the presence of the nanoparticles, but because the degradation was followed through mass loss in a TGA, it is quite possible that interaction between the well

dispersed nanoparticles and the degradation volatiles caused a delay in the evolution of these volatiles.

4.5. References

1. Q. Guan, H.E. Naguib. Fabrication and characterization of PLA/PHBV-chitin nanocomposites and their foams. Journal of Polymers and the Environment 2014; 22:119-130.
   DOI: 10.1007/s10924-013-0625-8
2. S.S. Ray, M. Bousmina. Biodegradable polymers and their layered silicate nanocomposites: In greening the 21st century materials world. Progress in Materials Science 2005; 50:962-1079.
   DOI: 10.1016/j.pmatsci.2005.05.002
3. M.J. Jenkins, Y. Cao, L. Howell, G.A. Leeke. Miscibility in blends of poly(3-hydroxybutyrate-co-3-hydroxyvalerate) and poly(ε-caprolactone) induced by melt blending in the presence of supercritical CO_2. Polymer 2007; 48:6304-6310.
   DOI: 10.1016/j.polymer.2007.08.033
4. M.S.S.B. Monteiro, R.P.C. Neto, I.C.S. Santos, E.O. da Silva, M.I.B. Tavaras. Inorganic-organic hybrids based on poly(ε-caprolactone) and silica oxide and characterization by relaxometry applying low-field NMR. Materials Research 2012; 15:825-832.
   DOI: 10.1590/S1516-14392012005000121
5. K. Chrissafis, G. Antoniadis, K.M. Paraskevopoulos, A. Vassiliou, D.N. Bikiaris. Comparative study of the effect of different nanoparticles on the mechanical properties and thermal degradation mechanism of in situ prepared poly(ε-caprolactone) nanocomposites. Composites Science and Technology 2007; 67:2165-2174.
   DOI: 10.1016/j.compscitech.2006.10.027
6. T. Patrício, P. Bártolo. Thermal stability of PCL/PLA blends produced by physical blending process. Procedia Engineering 2013; 59:292-297.
   DOI: 10.1016/j.proeng.2013.05.124

7. A.N. Ibrahim, M.U. Wahit, A.A. Yussuf. Effect of fiber reinforcement on mechanical and thermal properties of poly(ε-caprolactone)/poly(lactic acid) blend composites. Fibers and Polymers 2014; 15:574-582.
DOI: 10.1007/s12221-014-0574-4
8. C. Hinüber, L. Häussler, R. Vogel, H. Brünig, G. Heinrich, C. Werner. Hollow fibers made from a poly(3-hydroxybutyrate)/poly-ε-caprolactone blend. eXPRESS Polymer Letters 2011; 5: 643–652.
DOI: 10.3144/expresspolymlett.2011.62
9. M.A. Woodruff, D.W. Hutmacher. The return of a forgotten polymer - Polycaprolactone in the 21st century. Progress in Polymer Science 2010; 35:1217-1256.
DOI:10.1016/j.progpolymsci.2010.04.002
10. S.P.C. Gonçalves, S.M. Martins-Franchetti. Action of soil microorganisms on PCL and PHBV blend and films. Journal of Polymers and the Environment2010; 18:714-719.
DOI: 10.1007/s10924-010-0209-9
11. J.B.E. Mendes, M.K. Riekes, V.M. de Oliveira, M. D. Michel, H. K. Stulzer, N.M. Khalil, S. F. Zawadzki, R.M. Mainardes, P.V. Farago. PHBV/PCL microparticles for controlled release of resveratrol: Physicochemical characterization, antioxidant potential, and effect on hemolysis of human erythrocytes. The Scientific World Journal 2012; 542937.
DOI: 10.1100/2012/542937
12. S.A. Casarin, S.M. Malmonge, Marcio Kobayashi, J.A.M. Agnelli. Study on in vitro degradation of bioabsorbable polymers poly(hydroxybutyrate-co-valerate) - (PHBV) and poly(caprolactone) - (PCL). Journal of Biomaterials and Nanobiotechnology 2011; 2:207-215.
DOI: 10.4236/jbnb.2011.23026
13. K. Wessler, M.H. Nishida, J. da Silva Jr, A.P.T. Pezzin, S.H. Pezzin. Thermal properties and morphology of poly(3-hydroxybutyrate-co-3-hydroxyvalerate) with poly(caprolactone triol) mixtures. Macromolecular Symposia 2006; 245-246:161–165.
DOI: 10.1002/masy.200651322
14. V. Chiono, G. Ciardelli, G. Vozzi, M. G. Sotgiu, B. Vinci, C. Domenici, P. Giusti. Poly(3-hydroxybutyrate-co-3-hydroxyvalerate)/poly(ε-caprolactone) blends for tissue engineering

applications in the form of hollow fibers. Journal of Biomedical Materials Research Part A 2008; 85A:938–953.
DOI: 10.1002/jbm.a.31513

15. Y.S. Chun, W.N. Kim. Thermal properties of poly(hydroxyutyrate-co-hydroxyvalerate) and poly(ε-caprolactone) blends. Polymer 2000; 41:2301-2308.
PII: S0032-3861(99)00534-0
16. M.K. Riekes, F.M. Barboza, D.D. Vecchia, M. Bohatch Jr., P.V. Farago, D. Fernandes, M.A.S. Silva, H.K. Stulzer. Evaluation of oral carvedilol microparticles prepared by simple emulsion technique using poly(3-hydroxybutyrate-co-3-hydroxyvalerate) and polycaprolactone as polymers. Materials Science and Engineering C 2011; 31:962-968.
DOI: 10.1016/j.msec.2011.02.017
17. F.M. Barboza, W.M. Machado, L.R.O. Junior, J.P. de Paula, S.F. Zawadzki, D. Fernandes, P.V. Farago. PCL/PHBV microparticles as innovative carriers for oral controlled release of manidipine dihydrochloride. The Scientific World Journal 2014; 268107.
DOI: 10.1155/2014/268107
18. Q. Liu, T.-W. Shyr, C.-H. Tung, B. Deng, M. Zhu. Block copolymers containing poly(3-hydroxybutyrate-co-3-hydroxyvalerate) and poly(ε-caprolactone) units: Synthesis, characterization and thermal degradation. Fibers and Polymers 2011; 12:848-856.
DOI: 10.1007/s12221-011-0848-z
19. E.G. Bajsić, V.O. Bulatović, M. Slouf, A. Šitum. Characterization of biodegradable polycaprolactone containing titanium dioxide micro and nanoparticles. International Journal of Chemical, Nuclear, Metallurgical and Materials Engineering 2014; 8:572-576.
20. M. Naffakh, A.M. Díez-Pascua. Thermoplastic polymer nanocomposites based on inorganic fullerene-like nanoparticles and inorganic nanotubes. Inorganics 2014; 2:291-312.
DOI: 10.3390/inorganics2020291
21. T. Hanemann, D.V. Szabó. Polymer-nanoparticle composites: From synthesis to modern applications. Materials 2010; 3:3468-3517.
DOI: 10.3390/ma3063468
22. A.K.F. Dyab, H.A. Al-Lohedan, H.A. Essawy, A.I.A.A. El-Mageed, F. Taha. Fabrication of core/shell hybrid organic–inorganic polymer microspheres via pickering emulsion

polymerization using laponite nanoparticles. Journal of Saudi Chemical Society 2014; 18:610-617.
DOI: 10.1016/j.jscs.2011.12.008

23. Y. Shi , X. Feng , H. Wang, X. Lu. The effect of surface modification on the friction and wear behavior of carbon nanofiber-filled PTFE composites. Wear 2008; 264:934-939.
DOI: 10.1016/j.wear.2007.06.014
24. A. Maurya, P. Chauhan. Synthesis and characterization of sol-gel derived PVA-titanium dioxide (TiO_2) nanocomposites. Polymer Bulletin 2012; 68:961-972.
DOI: 10.1007/s00289-011-0589-6
25. F. Shi, Y. Ma, J. Ma, P. Wang, W. Sun. Preparation and characterization of PVDF/TiO_2 hybrid membranes with different dosage of nano-TiO_2. Journal of Membrane Science 2012; 389:522-531.
DOI: 10.1016/j.memsci.2011.11.022
26. N. Nakayama, T. Hayashi. Preparation and characterization of poly(L-lactic acid)/TiO_2 nanoparticle nanocomposite films with high transparency and efficient photodegradability. Polymer Degradation and Stability 2007; 92:1255-1264.
DOI: 10.1016/j.polymdegradstab.2007.03.026
27. P.M. Chou, M. Mariatti, A. Zulkifli, S. Sreekantan. Evaluation of the flexural properties and bioactivity of bioresorbable PLLA/PBSL/CNT and PLLA/PBSL/TiO_2 nanocomposites. Composites Part B 2012; 43:1374-1381.
DOI: 10.1016/j.compositesb.2011.11.023
28. H. Shi, R. Magaye, V. Castranova, J. Zhao. Titanium dioxide nanoparticles: A review of current toxicological data. Particle and Fibre Toxicology 2013; 10:1-33.
DOI: 10.1186/1743-8977-10-15
29. H. Xiu, H.W. Bai, C.M. Huang, C.L. Xu, X.Y. Li, Q. Fu. Selective localization of titanium dioxide nanoparticles at the interface and its effect on the impact toughness of poly(L-lactide)/poly(ether)urethane blends. eXPRESS Polymer Letters 2013; 7:261-271.
DOI: 10.3144/expresspolymlett.2013.24
30. D. Wu, D. Lin, J. Zhang, W. Zhou, M. Zhang, Y. Zhang, D. Wang, B. Lin. Selective localization of nanofillers: Effect on morphology and crystallization of PLA/PCL blends. Macromolecular Chemistry and Physics 2011; 212:613-6256.

DOI: 10.1002/mapc.201000579

31. H. Yang, X. Zhang, C. Qu, B. Li, L. Zhang, Q. Zhang, Q. Fu. Largely improved toughness of PP/EPDM blends by adding nano-SiO_2 particles. Polymer 2007; 48:860-869.
DOI: 10.1016/j.polymer.2006.12.022
32. F. Rosário, E. Corradini, S.A. Casarin, J.A.M. Agnelli. Effect of gamma radiation on the properties of poly(3-hydroxybutyrate-co-3-hydroxyvalerate)/poly(ε-caprolactone) blends. Journal of Polymer and the Environment 2013; 21:789-794.
DOI: 10.1007/s10924-013-0573-3
33. H. Zhao, Z. Cui, X. Wang, L.-S.Turng, X. Peng. Processing and characterization of solid and microcellular poly(lactic acid)/polyhydroxybuyrate-valerate (PLA/PHBV) and PLA/PHBV/clay nanocomposites. Composites Part B 2013; 51:79-91.
DOI: 10.1016/j.compositesb.2013.02.034
34. M.R. Nanda, M. Misra, A.K. Mohanty. The effect of process engineering on the performance of PLA and PHBV blends. Macromolecular Materials and Engineering 2011; 296:719-728.
DOI: 10.1002/mame201000417
35. E. Laredo, M. Grimau, A. Bello, D.F. Wu, Y.S. Zhang, D.P. Lin. AC conductivity of selectively located carbon nanotubes in poly(ε-caprolactone)/polylactide blend nanocomposites. Biomacromolecules 2010; 11:1339-1347.
DOI: 10.1021/bm100135n
36. N.B. Cramer, J.W. Stansbury, C.N. Bowman. Recent advances and developments in composite dental restorative materials. International & American Associations for Dental Research 2011; 90:402-416.
DOI: 10.1177/0022034510381263
37. D. Wu, Y. Zhang, M. Zhang, W. Yu. Selective localization of multiwalled carbon nanotubes in poly(ε-caprolactone)/polylactide blend. Biomacromolecules 2009; 10:417-424.
DOI: 10.1021/bm801183f
38. I. McNeill, H. Leiper. Degradation studies of some polyesters and polycarbonates. 2. Polylactide: Degradation under isothermal conditions, thermal degradation mechanism and photolysis of the polymer. Polymer Degradation and Stability 1985; 11:309-326.

39. Y. Aoyagi, K. Yamashita, Y. Doi. Thermal degradation of poly[(R)-3-hydroxybutyrate], poly[ε-caprolactone], and poly[(S)-lactide]. Polymer Degradation and Stability 2002; 76:53-59.
PII: S0141-3910(01)00265-8

40. M. Monsalve, J.M. Contreras, E. Laredo, F. López-Carrasquero. Ring-opening copolymerization of (*R,S*)-β-butyrolactone and ε-caprolactone using sodium hydride as initiator. eXPRESS Polymer Letters 2010; 4:431-441.
DOI: 10.3144/expresspolymlett.2010.54

41. A.A. Vassiliou, K. Chrissafis, D.N. Bakiaris. Thermal degradation kinetics of in situ prepared PET nanocomposites with acid-treated multi-walled carbon nanotubes. Journal of Thermal Analysis and Calorimetry 2010; 100:1063-1071.
DOI: 10.1007/s10973-009-0426-4

42. S. Majoni, S. Su, J.M. Hossenlopp. The effect of boron-containing layered hydroxy salt (LHS) on the thermal stability and degradation kinetics of poly(methyl methacrylate). Polymer Degradation and Stability 2010; 95:1593-1604.
DOI: 10.1016/j.polymdegradstab.2010.05.033

43. C.-L. Chiang, R.-C. Chang, Y.-C. Chiu. Thermal stability and degradation kinetics of novel organic/inorganic epoxy hybrid containing nitrogen/silicon/phosphorus by sol-gel method. Thermochimica Acta 2007; 453:97-104.
DOI: 10.1016/j.tca.2006.11.013

44. X. Liu, S. Khor, E. Petinakis, L. Yu, G. Simon, K. Dean, S. Bateman. Effects of hydrophilic fillers on the thermal degradation of poly(lactic acid). Thermochimica Acta 2010; 509:147-151.
DOI: 10.1016/j.tca.2010.06.015

45. Y. Fan, H. Nishida, Y. Shirai, T. Endo. Thermal stability of poly(L-lactide): Influence of end protection by acetyl group. Polymer Degradation and Stability 2004; 84:143-149.
DOI: 10.1016/j.polymdegradstab.2003.10.004

46. T. Mori, H. Nishida, Y. Shirai, T. Endo. Effects of chain end structures on pyrolysis of poly(L-lactic acid) containing tin atoms. Polymer Degradation and Stability 2004; 84:243-251.
DOI: 10.1016/j.polymdegradstab.2003.11.008

47. O. Persenaire, M. Alexandre, P. Degée, P. Dubois. Mechanisms and kinetics of thermal degradation of poly(ε-caprolactone). Biomacromolecules 2001; 2:288-294.
DOI: 10.1021/bm0056310 CCC
48. H.-Y. Yu, Z.-Y.Qin, Y.-N. Liu, L. Chen, N. Liu, Z. Zhou. Simultaneous improvement of mechanical properties and thermal stability of bacterial polyester by cellulose nanocrystals. Carbohydrate Polymers 2012; 89:971-978.
DOI: 10.1016/j.carbpol.2012.04.053

Chapter 5

Dynamic mechanical properties of PLA/PHBV, PLA/PCL, PHBV/PCL blends and their nanocomposites with TiO_2 as nanofiller

This chapter has been submitted as a publication:
J.P. Mofokeng, A.S. Luyt. Dynamic mechanical properties of PLA/PHBV, PLA/PCL, PHBV/PCL blends and their nanocomposites with TiO_2 as nanofiller. Thermochimica Acta.

Abstract

The effect of blending and the addition of small amounts of TiO_2 nanoparticles on the dynamic mechanical properties of PLA/PHBV, PLA/PCL and PHBV/PCL blends is reported in this paper. The storage modulus of the PLA/PHBV blends was higher than those of both PLA and PHBV in the temperature region below the glass transition of PHBV, but the PLA/PCL and PHBV/PCL bends did not show a similar feature. The E' values between the glass transitions of PLA and PHBV depended on the blend compositions and morphologies. The presence of titania nanoparticles had little effect on the E' values of all the investigated blends. The cold crystallization transition of PLA shifted to lower temperatures in the PLA/PHBV blends, and shifts in the T_gs of the two polymers indicated partial miscibility at the polymer-polymer interfaces. This partial miscibility reduced the chain mobilities of these polymers, which could be seen in a reduction in the damping during their respective glass transitions. Blending and nanoparticle addition had little influence on the glass transition temperatures of PLA and PCL, but the glass transitions of PHBV and PCL in the PHBV/PCL blends were respectively at higher and lower temperatures than those of the neat polymers, which is a somewhat abnormal observation. The PCL glass transition peaks became broader as a result of blending, which was attributed to the incompatibility of the polymers in the blends, because blending had no influence on the PCL crystallinity.

Keywords: poly(hydroxybutyrate-co-hydroxyvalerate); poly(lactic acid); poly(ε-caprolactone); blends; nanocomposites; dynamic mechanical properties.

5.1. Introduction

The biodegradable polymers poly(hydroxybutyrate-co-hydroxyvalerate)(PHBV), poly(lactic acid) (PLA), and poly(ε-caprolactone) (PCL), have been used in many applications because of their biodegradability, biocompatibility and environmental friendliness. They are prime candidates for use in a variety of disposable materials that are used in food and medical packaging and other consumer items, since disposal is becoming difficult as a result of diminishing landfill space. However, these polymers have some drawbacks that limit their use as individual polymers. PLA, a three carbon membered thermoplastic with a hydroxyl and carbonyl at the end, has a very slow biodegradation rate, and it is brittle despite its low degree of crystallinity [1-5]. PHBV, a nine carbon membered carbon thermoplastic polymer, has been mainly used for medical applications because it is non-toxic and compatible with the human body, but it suffers from low thermal stability and brittleness due to its high degree of crystallinity. This is a limiting factor for its use in the packaging industry, because it will have to be prepared using solvents to avoid thermal degradation when processing through melt mixing [3,5-7]. PCL, a six carbon membered thermoplastic with hydroxyl terminated end groups, is a rubbery polymer with good ductility because of its low glass transition temperature of -61 °C, and a good thermal stability with a moderate degree of crystallinity [3,8-10]. Its low melting temperature (60 °C) is its main drawback. To overcome all these disadvantages, these polymers can be blended to compensate for each other's weak properties.

Blending of two or more polymers is a practical and economical way to develop new materials with unique properties such as thermal, mechanical, and dynamic mechanical properties. Dynamic mechanical analysis (DMA) gives information on the mechanical and rheological properties of materials, and is used to determine properties like glass transition temperatures, stress relaxation, dynamic fragility parameters, miscibility of polymer blends, interfacial compatibility of individual composite components, and filler effectiveness [11-18].

In recent years a new concept of compatibilisation by using inorganic nanoparticles has been introduced. Unfortunately there are relatively few studies dealing with immiscible polymer

blends whose interfaces are stabilized by solid particles [19,20]. Nanometre sized inorganic compounds such as titanium dioxide (TiO_2), zinc oxide (ZnO), silica (SiO_2), aluminium dioxide (Al_2O_3), and silicon nitride (Si_3N_4) were tried as fillers in fabrics and polymers to improve the tribological properties. TiO_2 has received most of the attention because of its good thermal stability, accessibility, and catalytic properties. It is generally used for various applications including photo electrochemical activity, solar energy conversion, photocatalysis, UV detection, ultrasonic sensing, and as a promising material in applications such as water or wastewater treatment. Environmental compatibility, non-toxicity and low price are some practical advantages of TiO_2 [22-25].

PLA/PCL blends and their nanocomposites were fairly intensively studied during the past decade [9,19-30], and most of these studies reported on the dynamic mechanical properties of these materials [27,28,31,33,36,38]. Cabedo *et al.* [27] and Jain *et al.* [28] studied the dynamic mechanical properties of PLA/PCL blends in the presence of respectively clay and micro-talc. They reported a decrease in the storage modulus (E') of PLA as a result of a plasticization effect of PCL on PLA. The storage modulus, however, increased in the presence of fillers, but was still lower than that of neat PLA. This was attributed to the inherent stiffness of talc and clay, which introduced a rigid interface in the blend. Wu *et al.* [31] reported an improvement in the miscibility between PLA and PCL when multiwalled carbon nanotubes were added, which was attributed to the emulsification that occurred at the interface in the presence of the amphiphilic carboxylic MWCNTs, leading to a thermodynamic stabilization of the interface.

PLA/PHBV blends and their blend nanocomposites were also studied, but to a lesser extend [2,38-41]. Ma *et al.* [2] reported that the storage modulus of PLA was higher than that of PHBV in the glassy state, and blending of the polymers and an increase in the PHBV content reduced the storage modulus of PLA. Ferreira *et al.* [39] found that the glass transition temperatures of both polymers shifted to higher temperatures in the presence of the other polymer, which they attributed to a restriction in the amorphous chain mobilities. Only one paper was found where the introduction of a particulate filler into the blend was studied [40]. This paper reported that the neat blend had a low glassy storage modulus, but that the presence of clay nanoparticles increased the storage modulus even in the rubbery region of PLA.

Very little information is available on the mechanical properties of PHBV/PCL blends [7,35], and none on the introduction of particulate fillers into these blends. A study of the

dynamic mechanical properties of irradiated samples of these blends showed that the glass transition temperature of PCL increased and the intensity of the tan δ peaks decreased in the presence of PHBV. This was attributed to the reduced mobility of the amorphous chains, which may have been caused by chain scission that led to increased crystallinity.

In previous studies [42-44] we prepared and investigated the morphologies, as well as the degradation behaviour and kinetics, of PLA/PHBV, PLA/PCL and PHBV/PCL blends containing TiO_2 nanoparticles. Generally we observed well dispersed nanoparticles in both polymer phases of the PLA/PCL and PHBV/PCL blends, although some agglomerates were also observed. In the PLA/PHBV system the nanoparticles were well dispersed in the PLA phase and concentrated on the interface between the two polymers, with a few agglomerates in the PHBV phase. For all three blends the TEM pictures showed immiscibility of the polymers, with co-continuous morphologies for the 50/50 w/w blends. This paper reports on the dynamic mechanical properties of the same blends and blend nanocomposites.

5.2. Experimental

5.2.1 Materials

The polylactic acid (PLA) used in this study is a commercial grade (PLA 2002D), obtained from Natureworks, LLC (USA). It has a D-isomer content of 4%, a density of 1.24 g cm^{-3}, a glass transition temperature of ~53 °C, a melting temperature of ~153 °C, and a degree of crystallinity of ~33%. The poly(hydroxybutyrate-co-hydroxyvalerate) (PHBV) biopolymer was purchased from Goodfellow, Huntingdon, UK, and it has a 12% PHV content, a density of 1.25 g cm^{-3}, a melting temperature of ~150 °C, and a degree of crystallinity of 59%. The Capa™ 6500 polycaprolactone (PCL) was purchased from Southern Chemicals in Johannesburg, South Africa. It has a density of 1.1 g cm^{-3}, a glass transition temperature of -61 ºC, a melting temperature of ~60 ºC, and a degree of crystallinity of 35%. The 99.7% pure anatase titanium(IV)oxide (TiO_2), with a nanopowder with particle sizes < 25 nm, was supplied by Sigma-Aldrich in South Africa.

5.2.2 Sample preparation

The samples were prepared *via* melt-mixing using a Brabender Plastograph. PLA and PHBV were dried in an oven at 80 °C for four hours prior to mixing, and TiO_2 was used as received. 30/70, 50/50 and 70/30 w/w PLA/PHBV, PLA/PCL and PHBV/PCL blends and their nanocomposites with 1, 3 and 5 wt% of TiO_2 were prepared through mixing at 170 °C for ten minutes at the speed of 50 rpm. The samples were compression moulded into 2 mm thick sheets at the same temperature for 5 minutes using a hydraulic press at a pressure of 50 bars, after which they were removed and left to cool under ambient conditions.

5.2.3 Characterization

The dynamic mechanical properties of the samples were tested using a Perkin Elmer Diamond DMA dynamic mechanical analyser. The testing was performed in bending mode at a frequency of 1 Hz and a heating rate of 3 °C min^{-1} under nitrogen atmosphere. The samples were heated from -80 °C, and the end temperatures were 140°C for the PLA/PHBV samples, and 58°C for the PLA/PCL and PHBV/PCL samples because of the low melting temperature of PCL.

Differential scanning calorimetry (DSC) was used to determine the polymers' degree of crystallinity. The analyses were performed under nitrogen atmosphere, from 0 to 170 °C at a rate of 10°C min^{-1}. The melting enthalpies of the three polymers were determined, and Equation 5.1 was used to calculate their crystallinities. Equation 5.2 was used to calculate the crystallinity of PCL in the blends.

$$X_C(\%) = \left(\frac{\Delta H_m}{\Delta H_m^o} \right) \times 100\% \qquad (5.1)$$

$$X_C(\%) = \left(\frac{\Delta H_m(PCL)}{W \Delta H_m^o(PCL)} \right) \times 100\% \qquad (5.2)$$

where ΔH_m is the enthalpy of melting, $\Delta H_m^0$is the enthalpy of melting of the 100% crystalline polymer, and W is the weight fraction of PCL in the blends. Values of 93.7 J g^{-1} [40], 139 J g^{-1} [7,9] and 109 J g^{-1} [39,40] were respectively used for PLA, PCL and PHBV.

A Tescan VEGA3 scanning electron microscope (SEM) was used to study the surface dispersion of the TiO_2 nanoparticles in the blends. The liquid nitrogen fractured samples were sputter coated with gold for 30 seconds to eliminate sample charging, and the analyses were performed at 1000× magnification.

5.3. Results and discussion

5.3.1 DMA analysis of PLA/PHBV blends and their nanocomposites with 1, 3, and 5 wt% TiO_2 nanoparticles.

The storage moduli for all the blends and nanocomposites, below the glass transitions of PLA and PHBV, are higher than those of both the neat polymers (Figure 5.1). There is not much change in these values for the nanocomposites, and there is also no trend with respect to the amount of polymer in the blend and the amount of filler in the nanocomposites. Between the two polymers' glass transitions there is a very clear influence of the amount of each polymer on the storage modulus, which shows that the phase morphology played a role in determining the stiffness of the respective samples. It is, however, difficult to distinguish between the two polymers in the blend on the scanning electron microscopy (SEM) photos in Figure 5.2, but our previously reported transmission electron microscopy (TEM) photos [42] clearly showed a co-continuous morphology for the 50/50 w/w blend, and we can therefore assume that the 30/70 and 70/30 w/w PLA/PHBV blends respectively had PLA and PHBV dispersed as spheres in a matrix of the other component. Again the presence and amount of nanoparticles had a small influence, and no trend was observed. The reason for this is that the nanoparticle contents were relatively low, and they were dispersed in the stiffer PLA phase and on the interface [42], so their influence on the modulus of the composites was insignificant. The glass transitions of respectively PHBV and PCL are clearly visible around 3 and 65 °C, and the modulus of PHBV is lower than that of PLA below the T_g of PLA. However, between the glass transition and cold crystallization (starting at about 100 °C) of PLA, PHBV has a significantly higher modulus, but the two polymers have

about the same modulus after PLA's cold crystallization, independent of the composition of the blends. The cold crystallization is the result of the recrystallization of the metastable chains formed during cooling from the melt. These chains become mobile after PLA's glass transition and re-crystallize to form more perfect crystals. The cold crystallization started at lower temperatures for the blends, that further decreased with increasing PHBV content in the blends. This was probably caused by the creation of more free volume in the presence of the more mobile PHBV chains, which made it easier for the PLA chains to come together and crystallize during the heating process.

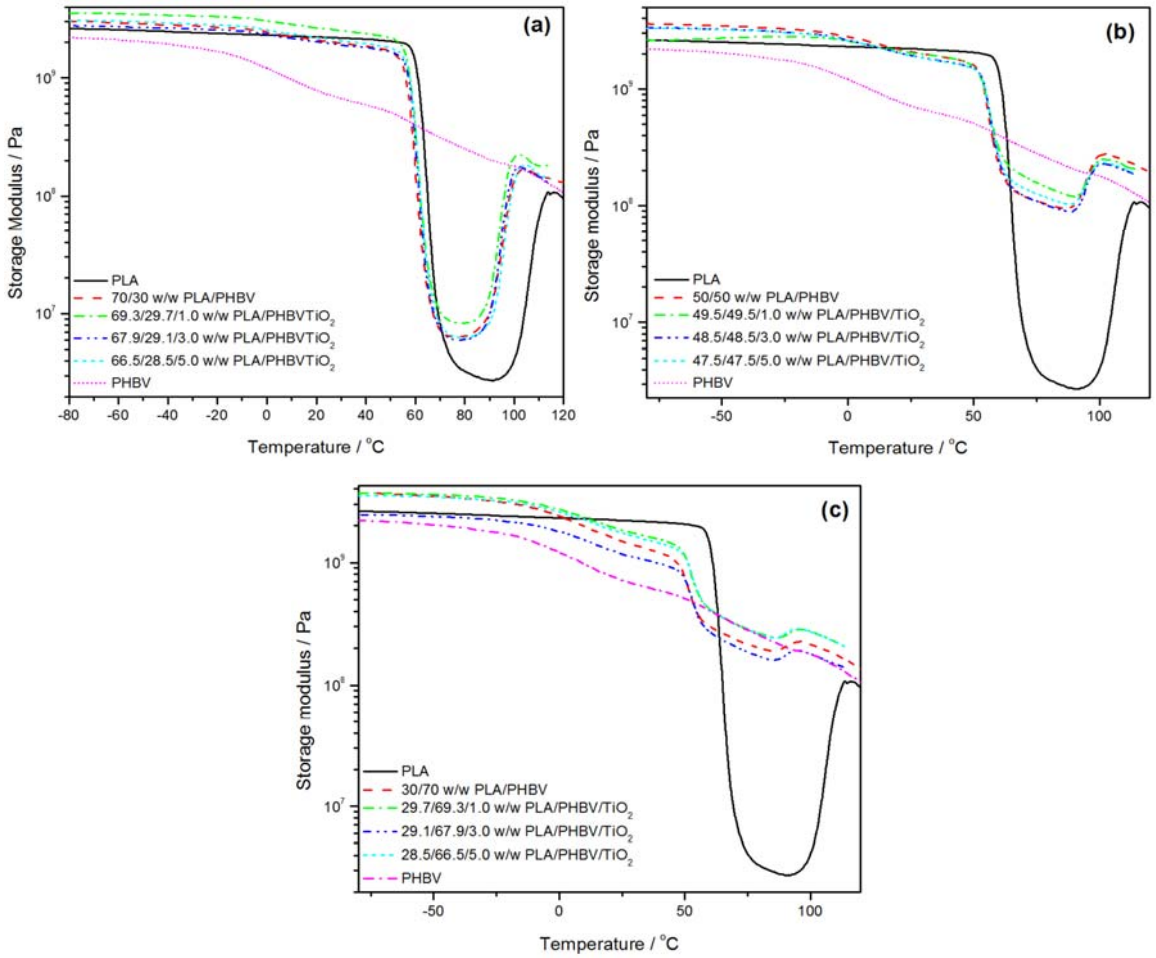

Figure 5.1 E' curves of PLA and PHBV, and the PLA/PHBV blends and PLA/PHBV/TiO_2 nanocomposites: (a) 70/30, (b) 50/50, and (c) 30/70 PLA/PHBV with 1, 3, and 5 wt% TiO_2

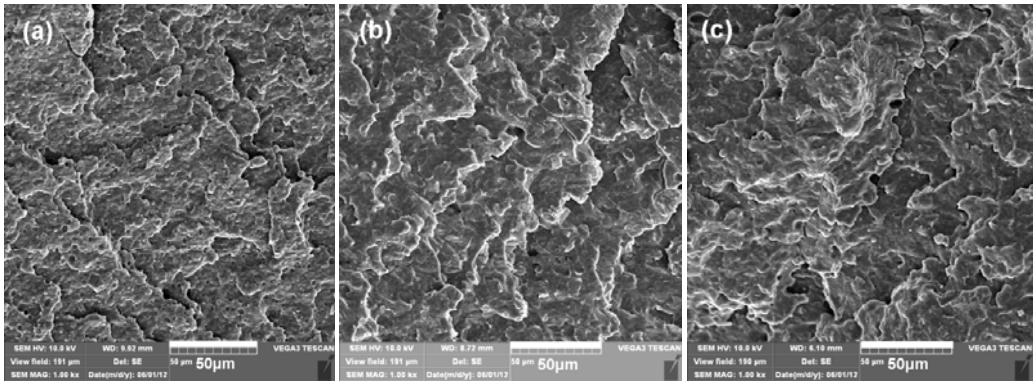

Figure 5.2 SEM pictures of PLA/PHBV blends at (a) 70/30, (b) 50/50, and 30/70 w/w ratios

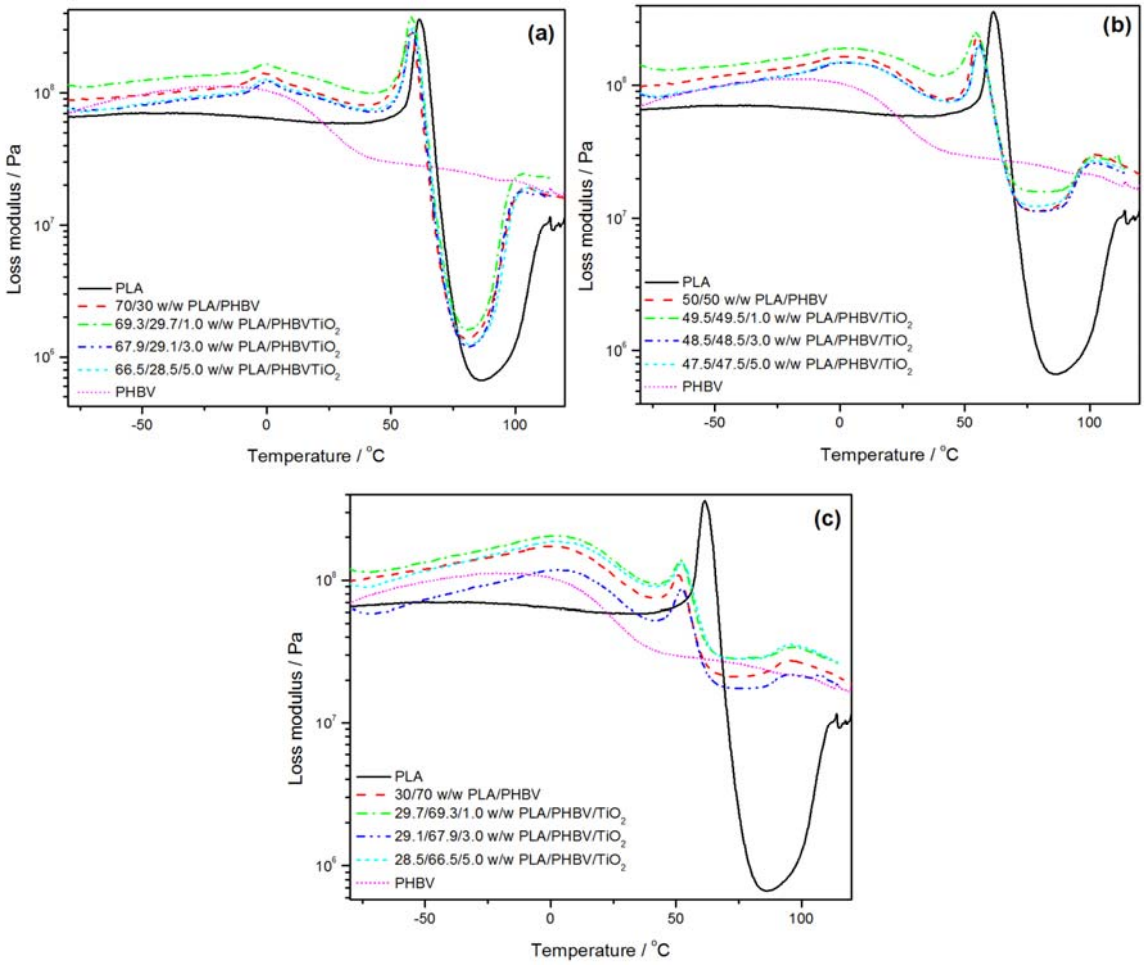

Figure 5.3 E" curves of PLA and PHBV, and the PLA/PHBV blends and PLA/PHBV/TiO_2 nanocomposites: (a) 70/30, (b) 50/50, and 30/70 PLA/PHBV with 1, 3, and 5 wt% TiO_2

The glass transition temperatures of both polymers changed when blended with each other. The T_g of PHBV increased from about -18 to about 1 °C, while that of PLA decreased from about 62 to about 55 °C for 50/50 w/w PLA/PHBV (Figure 5.3). The values in Table 5.1 show that the extent of these changes depended on the PLA:PHBV ratios in the blends. This is an indication of partial miscibility of the two polymers, at least in the interfacial areas. This partial miscibility at the interface is clear from the SEM photos in Figure 5.2, because no obvious separation between the two polymer phases can be observed from these photos. The presence of nanoparticles had very little influence on the extent of these changes, indicating that the nanoparticles did not influence the extent of miscibility at the interfaces, despite the fact that a large number of the nanoparticles were actually concentrated in the interface between the two polymers [42]. The glass transition peaks for PHBV in Figure 5.3 is very broad, indicating that the polymer is very crystalline which restricts the mobility of the chains or chain segments in the amorphous phase [12].

The glass transition peak in the tan δ curve of neat PLA is very intense, with an obvious cold crystallization peak around 100 °C, which clearly indicates that in the unblended and unfilled PLA there is a large extent of molecular motion on going from the glassy to the rubbery phase. The intensity did not reduce much for the 70/30 w/w blend and its nanocomposites, probably because PLA still formed the continuous phase and the dispersed PHBV only slightly influenced the molecular motion in the glass transition region. However, there was a significant reduction in the intensity of this peak for the 50/50 w/w and 30/70 w/w PLA/PHBV samples. The reason for this is probably the existence of a co-continuous morphology for the 50/50 w/w PLA/PHBV, and a sea-island morphology for the 30/70 w/w PLA/PHBV blend in which PLA spheres would have been dispersed in the PHBV continuous phase. This, as well as the miscibility of the two phases at the interface, could cause significant immobilization of the PLA chains in the glass transition region. The shifts in T_g values (Table 5.2) are in line with the already discussed loss modulus results.

Table 5.1 Glass transition temperatures, obtained from the DMA loss modulus and tan δ curves, of all investigated samples in the PLA/PHBV system

Sample	PLA T_g / °C from E" δ curve	PHBV T_g / °C from E" curve	PLA T_g / °C from tan δ curve	PHBV T_g / °C from tan δ curve
Neat PLA	61.8	-	67.5	-
70/30 w/w PLA/PHBV	57.6	-1.0	63.2	0.1
50/50 w/w PLA/PHBV	55.2	3.1	58.3	13.0
30/70 w/w PLA/PHBV	50.8	1.2	52.9	12.8
Neat PHBV	-	-17.6	-	10.9
69.3/29.3/1.0 w/w PLA/PHBV/TiO_2	58.0	-1.2	64.0	0.4
49.5/49.5/1.0 w/w PLA/PHBV/TiO_2	54.6	3.2	57.8	13.8
29.3/69.7/1.0 w/w PLA/PHBV/TiO_2	51.6	3.0	54.0	14.4
67.9/29.1/3.0 w/w PLA/PHBV/TiO_2	58.6	0.9	64.0	1.5
48.5/48.5/3.0 w/w PLA/PHBV/TiO_2	55.7	4.4	58.4	12.6
29.1/67.9/3.0 w/w PLA/PHBV/TiO_2	52.4	3.7	54.3	13.6
66.5/28.5/5.0 w/w PLA/PHBV/TiO_2	58.7	-0.4	64.3	0.7
47.5/47.5/5.0 w/w PLA/PHBV/TiO_2	55.5	4.2	58.5	12.6
28.5/66.5/5.0 w/w PLA/PHBV/TiO_2	52.5	2.0	54.8	14.7

T_g = glass transition, E" = loss modulus

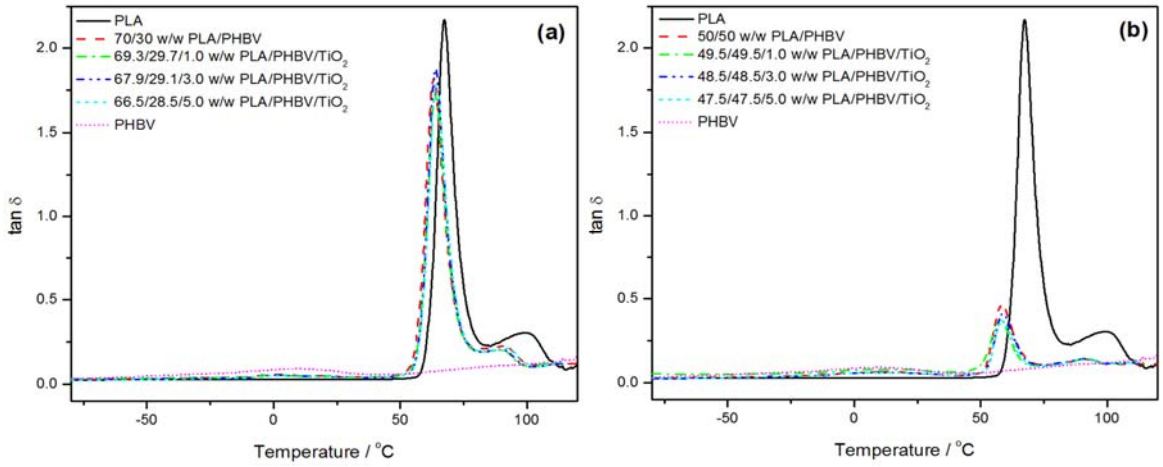

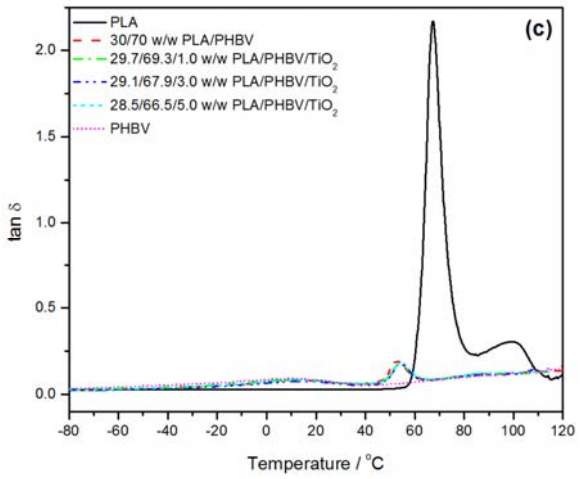

Figure 5.4 The tan δ curves of neat PLA, neat PHBV, PLA /PHBV blends and PLA/PHBV/TiO_2 nanocomposites (a) 70/30, (b) 50/50, and 30/70 PLA/PHBV with 1,3, and 5 wt% TiO_2

5.3.2 DMA analysis of PLA/PCL blends and their nanocomposites with 1, 3, and 5 wt% TiO_2 nanoparticles.

The storage moduli around -80 °C (which is below the T_gs of PLA and PCL) of all the PLA/PCL blends and nanocomposites are closely the same or lower than the storage moduli of the neat polymers (Figure 5.5). The storage modulus at 20 °C, which is between the glass transition temperatures of the two polymers in the blend, shows a decrease with an increase in the content of the lower modulus PCL in the blend (Table 5.2). This is normal for immiscible and incompatible polymer blends, which is clearly the case for the PLA/PCL blend (Figure 5.6), where certain properties of the blends are averaged over those of the individual polymers that make up the blend. The storage modulus values of the nanocomposites in Table 5.2 do not show any trend, and it is therefore not possible to describe or explain the influence of the nanoparticles on the viscoelastic properties of the blends at temperatures between the glass transitions of PCL and PLA. This is probably because the nanoparticles were dispersed in both polymer phases, but also formed agglomerates in an inconsistent way [43].

Table 5.2 Data obtained from the DMA storage modulus, loss modulus and tan δ curves for the different PLA/PCL samples

Sample	E′ at 20 °C / Pa	tan δ at peak maximum for PLA	tan δ at peak maximum for PCL
PLA	2.2×10^9	2.2	-
70/30 w/w PLA/PCL	2.0×10^9	2.4	0.05
50/50 w/w PLA/PCL	1.3×10^9	2.7	0.06
30/70 w/w PLA/PCL	8.2×10^8	-	0.08
PCL	6.5×10^8	-	0.11
69.3/29.3/1.0 w/w PLA/PCL/TiO_2	1.4×10^9	2.6	0.05
49.5/49.5/1.0 w/w PLA/PCL/TiO_2	1.1×10^9	-	0.06
29.3/69.7/1.0 w/w PLA/PCL/TiO_2	7.6×10^8	-	0.08
67.9/29.1/3.0 w/w PLA/PCL/TiO_2	7.8×10^8	-	0.04
48.5/48.5/3.0 w/w PLA/PCL/TiO_2	1.1×10^9	-	0.06
29.1/67.9/3.0 w/w PLA/PCL/TiO_2	1.9×10^9	-	0.05
66.5/28.5/5.0 w/w PLA/PCL/TiO_2	1.4×10^9	-	0.08
47.5/47.5/5.0 w/w PLA/PCL/TiO_2	1.4×10^9	-	0.06
28.5/66.5/5.0 w/w PLA/PCL/TiO_2	5.9×10^8	-	0.10

PW_{HH} is peak width at half height of PCL glass transition peak in loss modulus curves

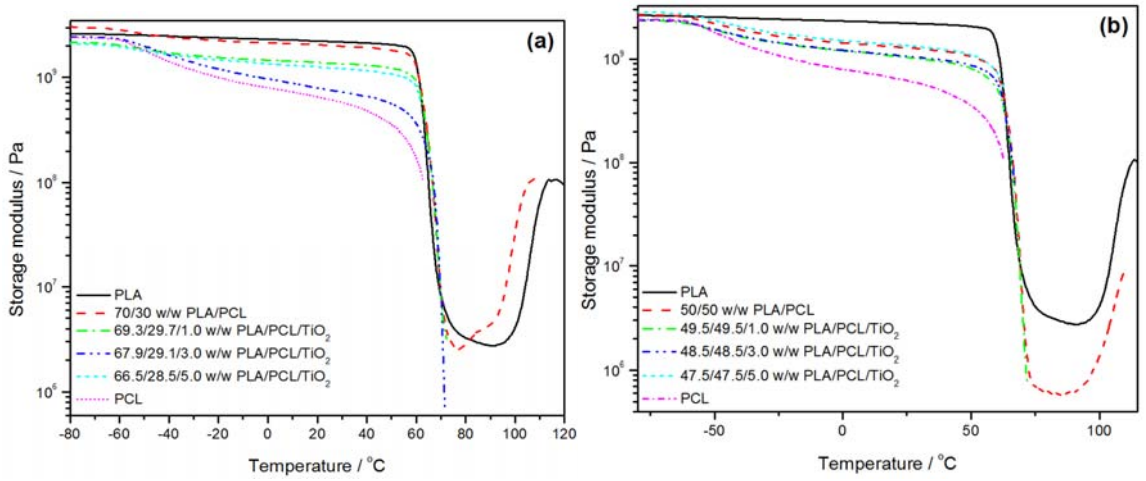

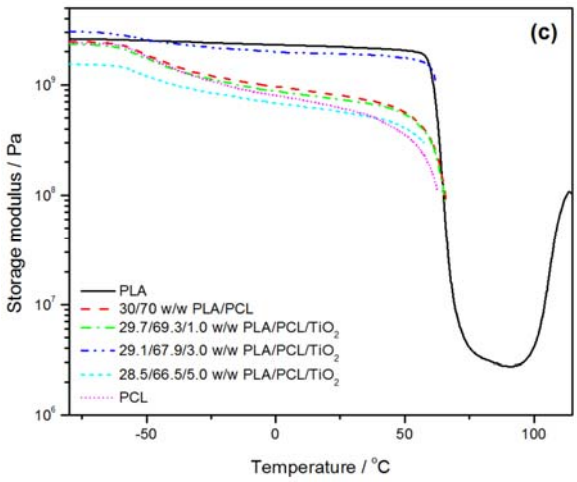

Figure 5.5 The E' curves of neat PLA, neat PCL, PLA/PCL blends and PLA/PCL/TiO_2 nanocomposites (a) 70/30, (b) 50/50, and 30/70 PLA/PCL with 1,3, and 5 wt% TiO_2

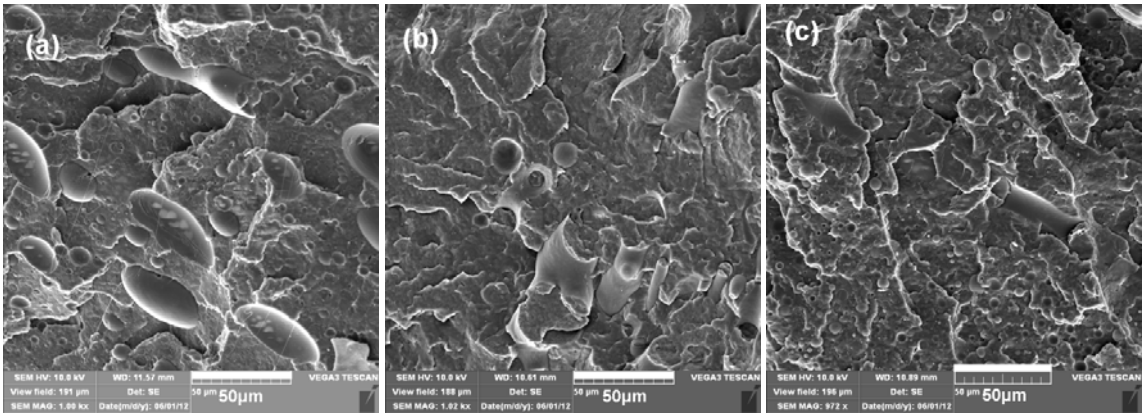

Figure 5.6 SEM pictures of PLA/PCL blends at (a) 70/30, (b) 50/50, and 30/70 w/w ratios

The loss modulus results (Figure 5.7 and Table 5.3) show that the glass transition temperatures of PLA and PCL changed very little as a result of blending. This confirms the complete immiscibility of the two polymers. The presence and content of TiO_2 nanoparticles in the blends also had little influence on the glass transition temperatures, despite the fact that they were well dispersed in both polymers [43]. This indicates that the interaction between the respective polymers and the nanoparticles were not strong enough for the nanoparticles to have any influence on the polymer chain mobility. The T_g of PLA in the 30/70 w/w PLA/PCL blend could not be determined because of PCL melting at about the same temperature.

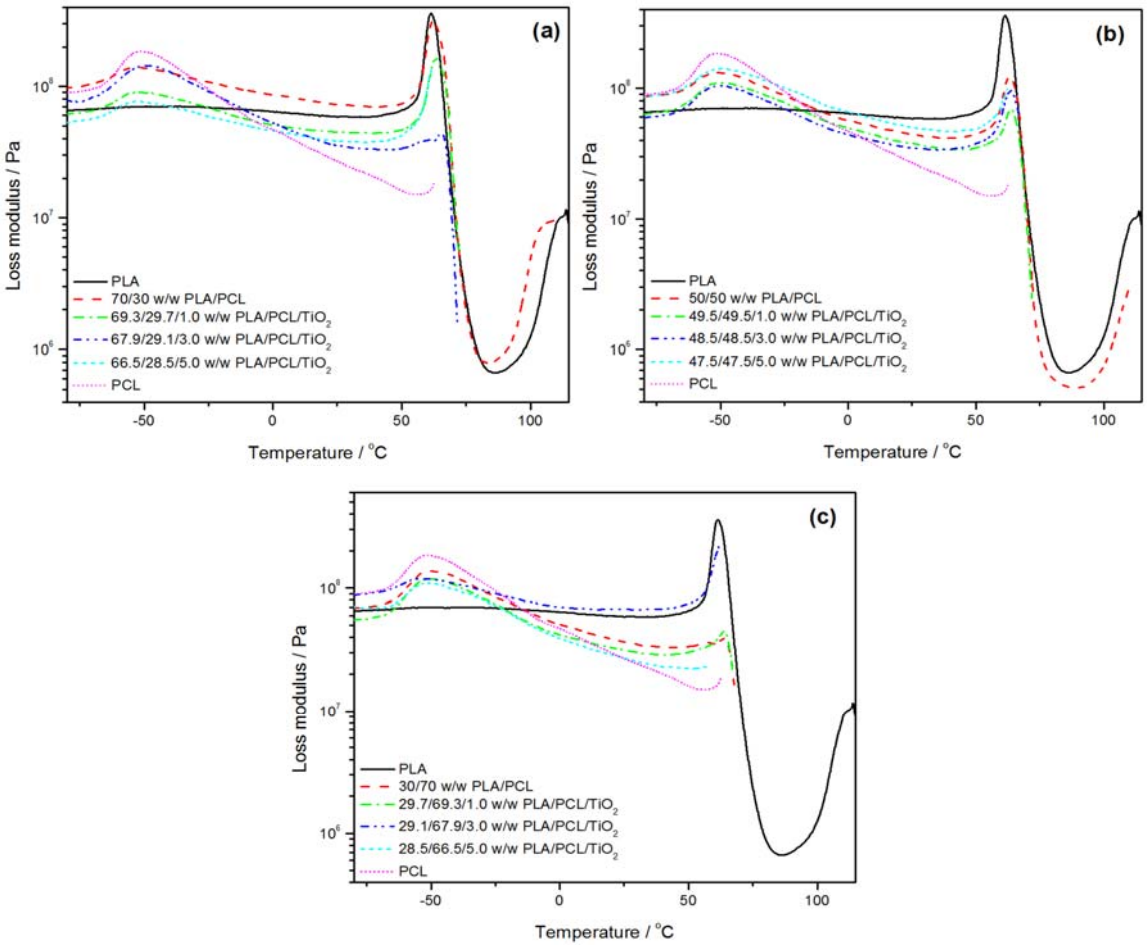

Figure 5.7 The E" curves of neat PLA, neat PCL, PLA/PCL blends and PLA/PCL/TiO_2 nanocomposites (a) 70/30, (b) 50/50, and 30/70 PLA/PCL with 1,3, and 5 wt% TiO_2

The tan δ curves (Figure 5.8) show three transitions: the first is the glass transition of PCL, the second the glass transition of PLA, and the third the cold crystallization of PLA. The loss tangent represents the damping characteristics of the material and is characteristic of the amount of mechanical energy dissipated as heat. In a tan δ curve, a peak is observed when the loss modulus increases with respect to the storage modulus as the temperature is increased. The tan δ value at the peak maximum of polymers and their blends and nanocomposites is influenced by molecular weight, crosslink density, filler content, morphology, type and distribution of fillers, filler-matrix interaction and void content. Generally, larger peak areas or increased intensities of the damping peaks, or shifts to higher temperatures, indicate better damping ability and are related to changes in the polymer chain mobility [12,45]. The intensities of the β-relaxation peaks

are lower for PCL in the blends (Figure 5.8 and Table 5.2), which was expected because of the decreasing amounts of PCL in the blends. The presence and amount of titania filler has little effect on the maximum tan δ values for PCL, and no trend is observed. This is probably because PCL anyway shows extremely low damping as a result of its fairly high chain mobility, and the interaction between the nanoparticles and the PCL chains is not strong enough to cause a significant change in the loss tangent of this polymer. The intensity of the β-relaxation peaks for PLA increases with increasing PCL content, although this peak was not completely formed for 30/70 w/w PLA/PCL because of PCL melting which interrupted the DMA analysis. This increase is the result of larger PLA chain mobility in the presence of the softer PCL. Unfortunately the effect of the nanoparticles on the PLA chain mobility could not be determined from these results because of the interruption of the DMA analyses in this temperature region.

Table 5.3 Glass transition temperatures, obtained from the DMA loss modulus and tan δ curves, of all investigated samples in the PLA/PHBV system

Sample	PLA T_g / °C from E" curve	PCL T_g / °C from E" curve	PLA T_g / °C from tan δ curve	PCL T_g / °C from tan δ curve
PLA	61.8	-	67.5	-
70/30 w/w PLA/PCL	62.0	-54.5	69.5	-47.6
50/50 w/w PLA/PCL	63.4	-51.0	71.3	-45.1
30/70 w/w PLA/PCL	-	-49.2	-	-40.7
PCL	-	-51.7	-	-43.2
69.3/29.3/1.0 w/w PLA/PCL/TiO_2	63.1	-51.8	70.1	-46.8
49.5/49.5/1.0 w/w PLA/PCL/TiO_2	64.0	-49.8	-	-42.0
29.3/69.7/1.0 w/w PLA/PCL/TiO_2	-	-50.2	-	-40.7
67.9/29.1/3.0 w/w PLA/PCL/TiO_2	63.1	-49.7	-	-41.0
48.5/48.5/3.0 w/w PLA/PCL/TiO_2	63.7	-50.0	-	-43.0
29.1/67.9/3.0 w/w PLA/PCL/TiO_2	-	-53.0	-	-47.1
66.5/28.5/5.0 w/w PLA/PCL/TiO_2	65.5	-51.5	-	-46.9
47.5/47.5/5.0 w/w PLA/PCL/TiO_2	62.7	-49.5	-	-42.7
28.5/66.5/5.0 w/w PLA/PCL/TiO_2	-	-51.6	-	-41.5

T_g = glass transition temperature, E" = loss modulus

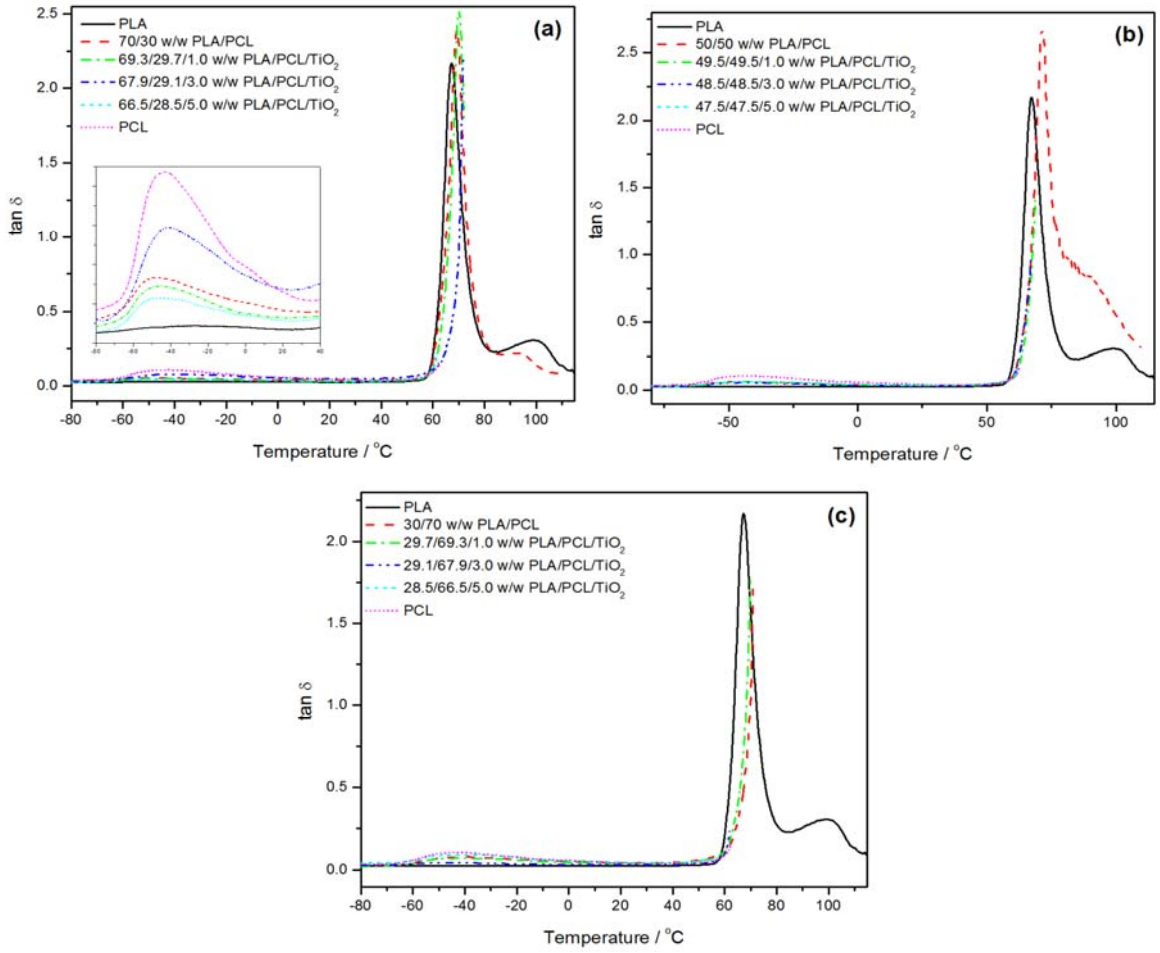

Figure 5.8 The tan δ curves of neat PLA, neat PCL, PLA/PCL blends and PLA/PCL/TiO_2 nanocomposites (a) 70/30, (b) 50/50, and 30/70 PLA/PCL with 1, 3, and 5 wt% TiO_2

5.3.3 DMA analysis of PHBV/PCL blends and their nanocomposites with 1, 3, and 5 wt% TiO_2 nanoparticles

The E' values for the investigated blends and nanocomposites do not show any trends over the whole temperature range of the analysis (Figure 5.7), and therefore no conclusion can be drawn about the influence of blending and the addition of nanoparticles on this property. The SEM pictures in Figure 5.10 clearly show a change from a sea-island morphology for the 70/30 w/w PHBV/PCL blend (in which PCL should be the dispersed phase), through a co-continuous morphology for the 50/50 w/w blend, to a sea-island morphology for the 30/70 w/w blend in which PHBV should be the dispersed phase. The lack of interaction between the two polymers,

and the absence of strong and well-defined glass transition steps, may be amongst the reasons for not observing clear trends in this case.

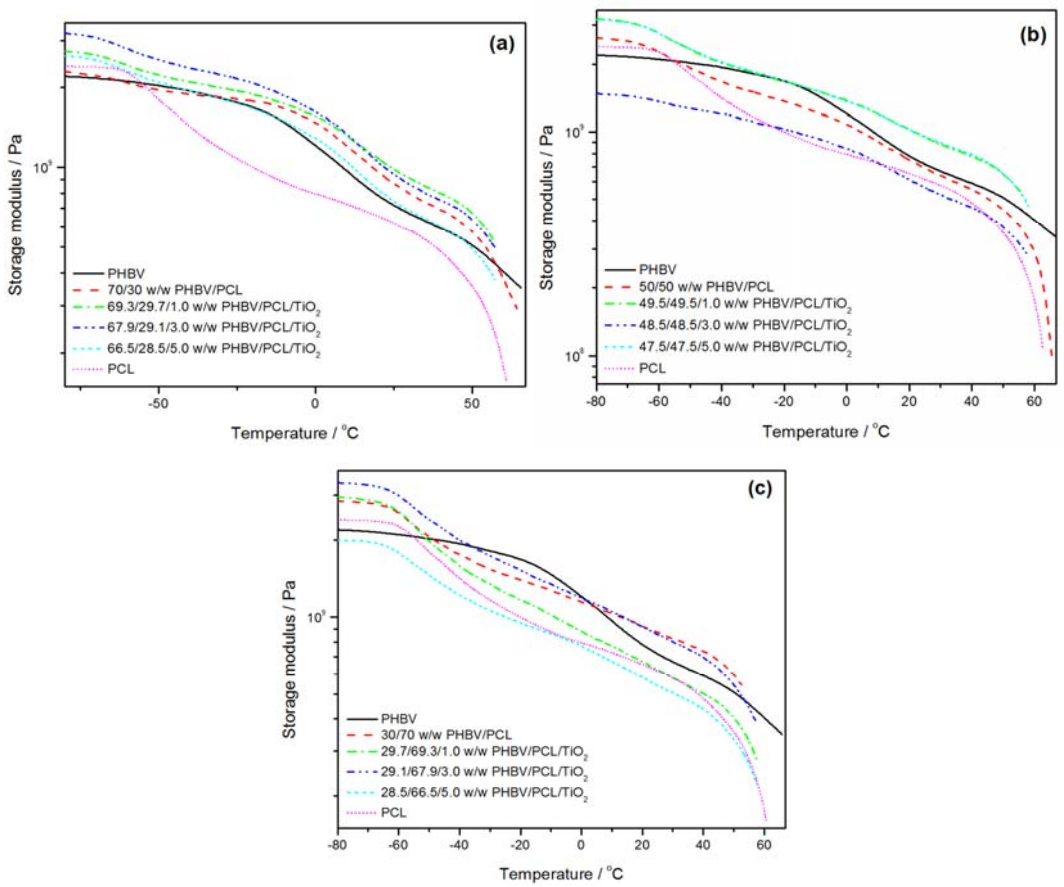

Figure 5.9 The E' curves of neat PHBV, neat PCL, PHBV/PCL blends and PHBV/PCL/TiO_2 nanocomposites (a) 70/30, (b) 50/50, and (c) 30/70 PHBV/PCL with 1,3, and 5 wt% TiO_2

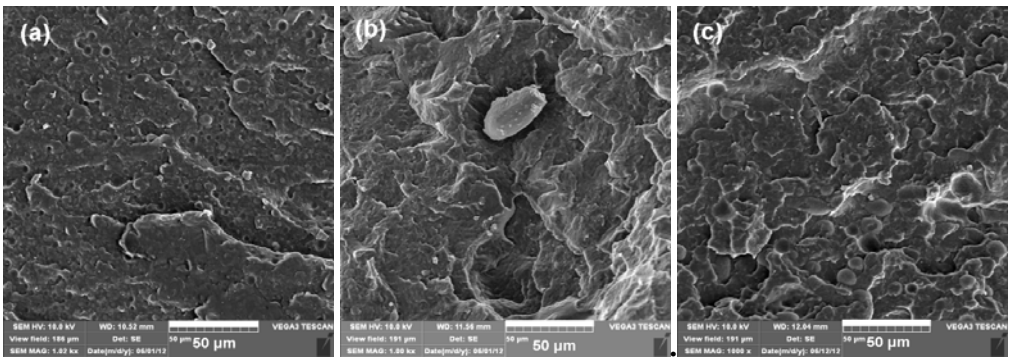

Figure 5.10 SEM pictures of PHBV/PCL blends at (a) 70/30, (b) 50/50, and 30/70 w/w ratios

The loss modulus curves of PCL and PHBV (Figure 5.11) show broad glass transitions at respectively -52 °C and -17 °C. This is in line with the fairly high degrees of crystallinity of these two polymers; PHBV, which has a very high degree of crystallinity shows a very broad, ill-defined glass transition peak. Loss modulus is the viscous response of the material, and it is associated with unrecoverable energy dissipation by the material. In semicrystalline polymers there is a mixture of amorphous and crystalline phases, intimately interconnected. This has an influence on the relaxation at the T_g, resulting in a broadening of the glass transition peak in the loss modulus curve. The broadness of the glass transition peak is influenced by a number of factors such as extent of crystallinity, crosslinking, or incompatibility/immiscibility/microphase separation in polymer blends, or microphase separation/immiscibility in polymers due to their different structures [12].The data in Table 4 show a very clear increase in the broadness of the PCL glass transition peak after blended with PHBV, which could have been the result of an increase in the PCL crystallinity after being blended with PHBV or the incompatibility/immiscibility/microphase separation in these blends, or both. DSC analyses of the blends were performed to establish whether blending with PHBV changed the degree of crystallinity of PCL. The crystallinity values of neat PCL and PCL in the blends were found to be very similar within experimental error, which means that the strong incompatibility between PCL and PHBV is the most probable reason for the increase in the broadness of the β-relaxation of PCL.

In polymers that develop a high degree of crystallinity like PHBV, the T_g is suppressed, and the glass transition in the loss modulus curve appears as a relatively minor event, and in some cases it may even be difficult to detect [12], which is exactly what we observed in our loss modulus curves (Figure 5.11). It was therefore not possible to quantify any changes in the broadness of the PHBV glass transition peak in the loss modulus curves.

The T_gs of the polymers show adverse behaviour in the blends. Normally the T_gs should be the same as those of the neat polymers if there is complete immiscibility, or move closer to each other when there is partial miscibility (Table 5.5). In this case the T_gs moved further from each other, which means the presence of PCL in some way immobilized the PHBV chains, while the presence of PHBV created more free volume in which the PCL chains can move. The presence of

the TiO_2 nanoparticles in the blends did not have a significant effect on the T_gs of the respective polymers in the blend, which is more clear from the tan δ results (Figure 5.12 and Table 5.5).

Table 5.4 Data from the DMA loss modulus and loss tangent curves of all the investigated PHBV/PCL samples

Sample	PW_{HH} / °C	tan δ at peak maximum for PHBV	tan δ at peak maximum for PCL
PHBV	-	0.09	-
70/30 w/w PHBV/PCL	21.4	0.10	0.05
50/50 w/w PHBV/PCL	43.6	0.09	0.06
30/70 w/w PHBV/PCL	37.1	-	0.10
PCL	27.3	-	0.11
69.3/29.3/1.0 w/w PHBV/PCL/TiO_2	33.1	0.10	0.06
49.5/49.5/1.0 w/w PHBV/PCL/TiO_2	35.4	0.08	0.08
29.3/69.7/1.0 w/w PHBV/PCL/TiO_2	31.9	-	0.09
67.9/29.1/3.0 w/w PHBV/PCL/TiO_2	35.4	0.09	0.05
48.5/48.5/3.0 w/w PHBV/PCL/TiO_2	54.6	0.08	0.07
29.1/67.9/3.0 w/w PHBV/PCL/TiO_2	34.1	-	0.09
66.5/28.5/5.0 w/w PHBV/PCL/TiO_2	33.5	0.09	0.04
47.5/47.5/5.0 w/w PHBV/PCL/TiO_2	42.6	0.09	0.07
28.5/66.5/5.0 w/w PHBV/PCL/TiO_2	34.5	-	0.08

PW_{HH} is the peak width at half height of the PCL glass transition peak in the loss modulus curves

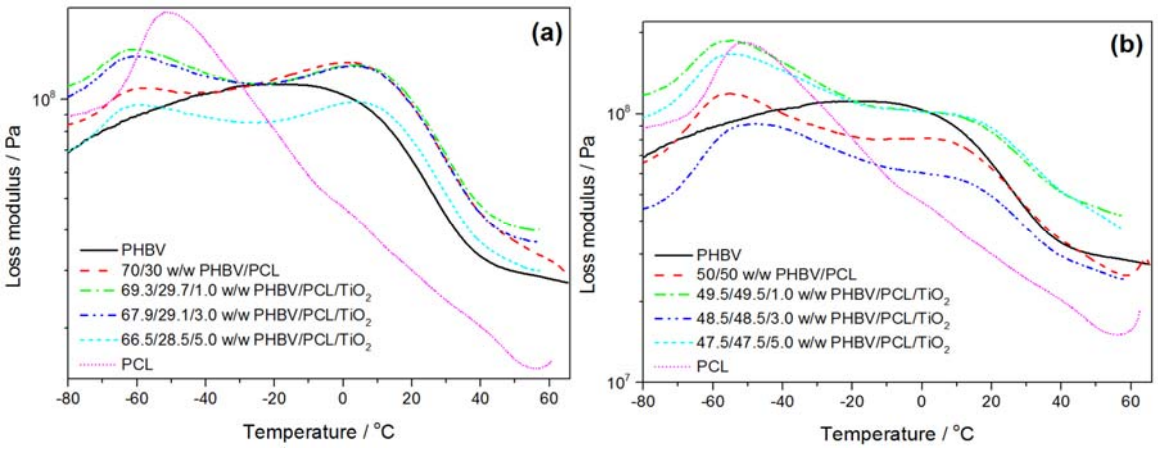

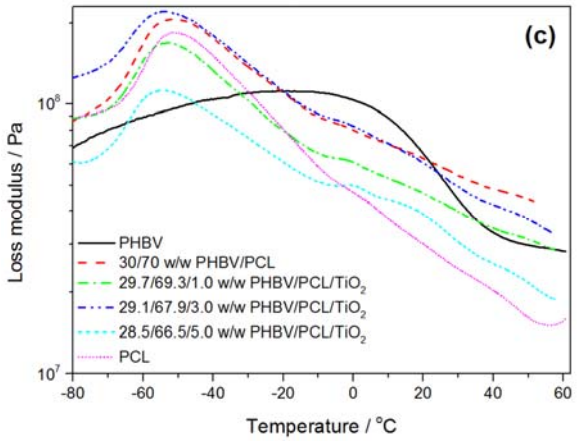

Figure 5.11 The E" curves of neat PHBV, neat PCL, PHBV/PCL blends and PHBV/PCL/TiO_2 nanocomposites (a) 70/30, (b) 50/50, and (c) 30/70 PHBV/PCL with 1,3, and 5 wt% TiO_2

Table 5.5 DMA storage modulus and glass transition temperatures of all investigated samples in PHBV/PCL system

Sample	PHBV T_g / °C from E" curve	PCL T_g / °C from E" curve	PHBV T_g / °C from tan δ curve	PCL T_g / °C from tan δ curve
Neat PHBV	-17.6	-	10.9	-
70/30 w/w PHBV/PCL	1.2	-59.2	14.8	-56.0
50/50 w/w PHBV/PCL	2.2	-57.1	13.1	-49.3
30/70 w/w PHBV/PCL	-3.4	-52.0	-2.9 /21.1	-45.6
Neat PCL	-	-51.7	-	-43.2
69.3/29.3/1.0 w/w PHBV/PCL/TiO_2	3.0	-60.7	14.6	-56.2
49.5/49.5/1.0 w/w PHBV/PCL/TiO_2	10.0	-55.4	17.1	-45.7
29.3/69.7/1.0 w/w PHBV/PCL/TiO_2	-2.0	-53.1	1.2 / 18.9	-45.6
67.9/29.1/3.0 w/w PHBV/PCL/TiO_2	2.8	-60.8	15.2	-56.3
48.5/48.5/3.0 w/w PHBV/PCL/TiO_2	11.2	-47.8	16.5	-41.8
29.1/67.9/3.0 w/w PHBV/PCL/TiO_2	-2.2	-53.5	-1.6 /18.5	-45.0
66.5/28.5/5.0 w/w PHBV/PCL/TiO_2	3.8	-59.7	15.2	-56.6
47.5/47.5/5.0 w/w PHBV/PCL/TiO_2	10.8	-54.1	17.9	-44.5
28.5/66.5/5.0 w/w PHBV/PCL/TiO_2	-1.1	-54.6	1.7 / 17.0	-46.7

T_g = glass transition temperature, E" = loss modulus

The tan δ curves (Figure 5.12) and the results in Tables 5.4 and 5.5 show that there is a reduction in the intensity of the β-relaxation of PCL in the presence of and with an increase in TiO_2 nanoparticle content in the blends, but very little change in that of the PHBV relaxation. It

seems as if the nanoparticles have a much stronger influence on the mobility of the amorphous chains in PCL than on that of PHBV, although according to the interfacial interaction data in our previous paper [44], TiO_2 should not interact more strongly with PCL than with PHBV.

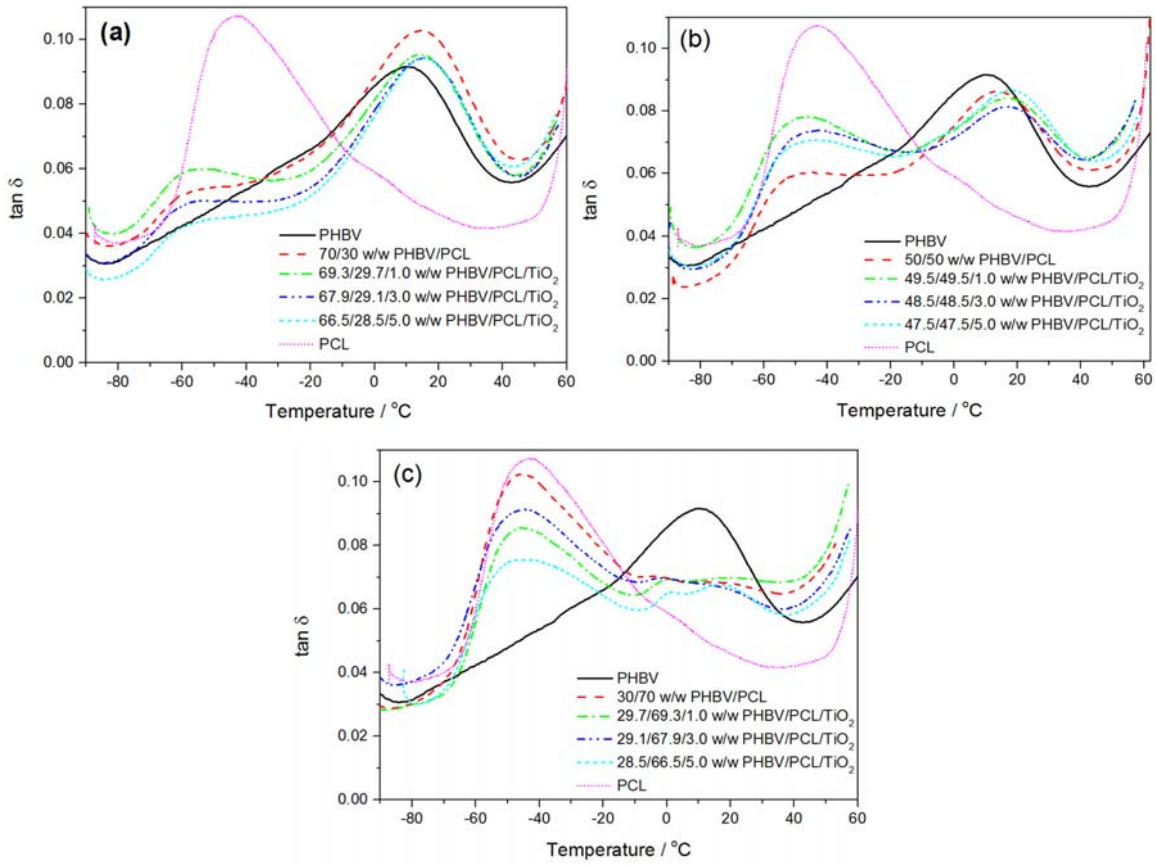

Figure 5.12 The tan δ curves of neat PHBV, neat PCL, PHBV/PCL blends and PHBV/PCL/TiO_2 nanocomposites (a) 70/30, (b) 50/50, and (c) 30/70 PHBV/PCL with 1,3, and 5 wt% TiO_2

5.4. Conclusions

The purpose of this work was to investigate the dynamic mechanical properties of melt-blended PLA/PHBV, PLA/PCL and PHBV/PCL prepared in the absence and presence of small amounts of TiO_2 nanoparticles. Blending PHBV and PLA increased the glassy modulus to values above those of the individual neat polymers, while the presence of nanoparticles had little effect. Changes in the glass transition temperatures of these two polymers in the blends indicated partial

miscibility at their interfaces, which was also observed from the reduced maximum damping values. The cold crystallization transition of PLA shifted to lower temperatures after blending with PHBV, which was attributed to more free volume created by the presence of the more mobile PHBV chains. The dynamic mechanical properties of PLA/PCL and PHBV/PCL were little influenced by blending and the presence of TiO_2 nanoparticles. The glass transitions of PHBV and PCL in the blends were, however, seen to be more separated than those of the individual neat polymers, which we explained as the immobilization of PHBV chains through the presence of PCL, and the creation of more free volume for the movement of PCL chains through the presence of PHBV. The broadness of the PCL β-relaxation peaks increased when blended with PHBV, probably because of the incompatibility between PHBV and PCL in the blends.

5.5. References

1. J. Cailloux, O.O. Santana, E. Franco-Urquiza, J.J. Bou, F. Carrasco, J. Gámez-Pérez, M.L. Maspoch. Sheets of branched poly(lactic acid) obtained by one step reactive extrusion calendering process – Melt rheology analysis. eXPRESS Polymer Letters 2013; 7:304-318. DOI: 10.3144/expresspolymlett.2013.27
2. P. Ma, A.B. Spoelstra, P. Schmit, P.J. Lemstra. Toughening of poly(lactic acid) by poly(β-hydroxybutyrateco-β-hydroxyvalerate) with high β-hydroxyvalerate content. European Polymer Journal 2013; 49:1523-1531. DOI: 10.1016/j.eurpolymj.2013.01.016
3. S. Modi, K. Koelling, Y. Vodovotz. Assessing the mechanical, phase inversion, and rheological properties of poly-[(R)-3-hydroxybutyrate-co-(R)-3-hydroxyvalerate] (PHBV) blended with poly-(L-lactic acid) (PLA). European Polymer Journal 2013; 49:3681-3690. DOI: 10.1016/j.eurpolymj.2013.07.036
4. L.-T. Lim, R. Auras, M. Rubino. Processing technologies for poly(lactic acid). Progress in Polymer Science 2008; 33:820-852. DOI: 10.1016/j.progpolymsci.2008.05.004
5. D.H.S. Ramkumar, M. Bhattacharya. Study shear and dynamic properties of biodegradable polymers. Polymer Engineering and Science 1998; 38:1428-1435.

6. Q. Guan, H.E. Naguib. Fabrication and characterization of PLA/PHBV-chitin nanocomposites and their foams. Journal of Polymers and the Environment 2014; 22:119-130.
DOI: 10.1007/s10924-013-0625-8
7. F. Rosário, E. Corradini, S.A. Casarin, J.A.M. Agnelli. Effect of gamma radiation on the properties of poly(3-hydroxybutyrate-co-3-hydroxyvalerate)/poly(ε-caprolactone) blends. Journal of Polymers and the Environment 2013; 21:789-794.
DOI: 10.1007/s10924-013-0573-3
8. K. Chrissafis, G. Antoniadis, K.M. Paraskevopoulos, A. Vassiliou, D.N. Bikiaris. Comparative study of the effect of different nanoparticles on the mechanical properties and thermal degradation mechanism of in situ prepared poly(ε-caprolactone) nanocomposites. Composites Science and Technology 2007; 67:2165-2174.
DOI: 10.1016/j.compscitech.2006.10.027
9. T. Patrício, P. Bártolo. Thermal stability of PCL/PLA blends produced by physical blending process. Procedia Engineering 2013; 59:292-297.
DOI: 10.1016/j.proeng.2013.05.124
10. M.S.S.B. Monteiro, R.P.C. Neto, I.C.S. Santos, E.O. da Silva, M.I.B. Tavaras. Inorganic-organic hybrids based on poly(ε-caprolactone) and silica oxide and characterization by relaxometry applying low-field NMR. Materials Research 2012; 15:825-832.
DOI: 10.1590/S1516-14392012005000121
11. A. Gregorova, M. Machovsky, R. Wimmer. Viscoelastic properties of mineral-filled poly(lactic acid) composites. International Journal of Polymer Science 2012; 252981.
DOI: 10.1155/2012/252981
12. R.P. Chartoff, J.D. Menczel, S. H. Dillman. Dynamic mechanical analysis (DMA). In: J.D. Menczel, R.B. Prime. Thermal Analysis of Polymers – Fundamentals and Applications. John Wiley & Sons: New Jersey (2009).
13. A.N. Frone, S. Berlioz, J.-F. Chailan, D.M. Panaitescu, D. Donescu. Cellulose fibre-reinforced polylactic acid. Polymer Composites 2011; 32:976-985
DOI: 10.1002/pc.21116
14. J.F. Mano. Study of the segmental dynamics in semicrystalline poly(lactic acid) using mechanical spectroscopies. Macromolecular Bioscience 2005; 5:337-343.

DOI: 10.1002/mabi.200400199

15. M. Hrabalova, A. Gregorova, R. Wimmer, V. Sedlarik, M. Machovsky, N. Mundigler. Effect of wood flour loading and thermal annealing on viscoelastic properties of poly(lactic acid) composite films. Journal of Applied Polymer Science 2010; 118:1534-1540.
DOI: 10.1002/app.32509
16. A. Gregorova, R. Wimmer, M. Hrabalova, M. Koller, T. Ters, N. Mundigler. Effect of surface modification of beech wood flour on mechanical and thermal properties of poly(3-hydroxybutyrate)/wood flour composites. Holzforschung 2009; 63:565-570.
DOI: 10.1515/HF.2009.098
17. A. Gregorova, M. Hrabalova, R. Kovalcik, R. Wimmer. Surface modification of spruce wood flour and effects on the dynamic fragility of PLA/wood composites. Polymer Engineering and Science 2011; 51:143-150.
DOI: 10.1002/pen.21799
18. A. Gregorova, M. Hrabalova, R. Wimmer, B. Saake, C. Altaner. Poly(lactide acid) composites reinforced with fibers obtained from different tissue types of Piceasitchensis. Journal of Applied Polymer Science 2009; 114:2616-2623.
DOI: 10.1002/app.30819
19. M. Si, T. Araki, H. Ade, A.L.D. Kilcoyne, R. Fisher, J.C. Skolov, M.H. Rafailovich. Compatibilizing bulk polymer blends by using organoclays. Macromolecules 2006; 39:4793-4801.
DOI: 10.1021/ma060124+ CCC
20. L. Elias, F. Fenouillot, J.C. Majeste, Ph. Cassagnau. Morphology and rheology of immiscible polymer blends filled with silica nanoparticles. Polymer 2007; 48:6029-6040.
DOI: 10.1016/j.polymer.2007.07.061
21. A. Maurya, P. Chauhan. Synthesis and characterization of sol-gel derived PVA-titanium dioxide (TiO_2) nanocomposites. Polymer Bulletin 2012; 68:961-972.
DOI: 10.1007/s00289-011-0589-6
22. F. Shi, Y. Ma, J. Ma, P. Wang, W. Sun. Preparation and characterization of PVDF/TiO_2 hybrid membranes with different dosage of nano-TiO_2. Journal of Membrane Science 2012; 389:522-531.
DOI: 10.1016/j.memsci.2011.11.022

23. N. Nakayama, T. Hayashi. Preparation and characterization of poly(L-lactic acid)/TiO_2 nanoparticle nanocomposite films with high transparency and efficient photodegradability. Polymer Degradation and Stability 2007; 92:1255-1264.
DOI: 10.1016/j.polymdegradstab.2007.03.026
24. P.M. Chou, M. Mariatti, A. Zulkifli, S. Sreekantan. Evaluation of the flexural properties and bioactivity of bioresorbable PLLA/PBSL/CNT and PLLA/PBSL/TiO_2 nanocomposites. Composites Part B 2012; 43:1374-1381.
DOI: 10.1016/j.compositesb.2011.11.023
25. H. Shi, R. Magaye, V. Castranova, J. Zhao. Titanium dioxide nanoparticles: A review of current toxicological data. Particle and Fibre Toxicology 2013; 10:1-33
DOI: 10.1186/1743-8977-10-15
26. E. Laredo, M. Grimau, A. Bello, D.F. Wu, Y.S. Zhang, D.P. Lin. AC conductivity of selectively located carbon nanotubes in poly(ε-caprolactone)/polylactide blend nanocomposites. Biomacromolecules 2010; 11:1339-1347.
DOI: 10.1021/bm100135n
27. L. Cabedo, J.L. Feijoo, M.P. Villanueva, J.M. Lagarón, E. Giménez. Optimization of biodegradable nanocomposites based on aPLA/PCL blends for food packaging applications. Macromolecular Symposia 2006; 233:191-197.
DOI: 10.1002/masy.200650124
28. S. Jain, M.M. Reddy, A.K. Mohanty, M. Misra, A.K. Ghosh. A new biodegradable flexible composite sheet from poly(lactic acid)/poly(ε-caprolactone)blends and micro-talc. Macromolecular Materials and Engineering 2010; 295:750-762.
DOI: 10.1002/mame.201000063
29. F. Tuba, L. Oláh, P. Nagy. Characterization of reactively compatibilized poly(D,L-lactide)/poly(ε-caprolactone) biodegradable blends by essential work of fracture method. Engineering Fracture Mechanics 2011; 78:3123-3133.
DOI: 10.1016/j.engfracmech.2011.09.010.
30. M. Amirian, A.N. Chakoli, W. Cai, J.H. Sui. In vitro degradation of poly(L-lactide)/poly(ε-caprolactone) blend reinforced with MWCNTs. Iranian Polymer Journal 2012; 21:165-174.
DOI: 10.1007/s13726-012-0014-5

31. D. Wu, Y. Zhang, M. Zhang, W. Yu. Selective localization of multiwalled carbon nanotubes in poly(ε-caprolactone)/polylactide blend. Biomacromolecules 2009; 10:417-424.
DOI: 10.1021/bm801183f

32. D. Wu, D. Lin, J. Zhang, W. Zhou, M. Zhang, Y. Zhang, D. Wang, B. Lin. Selective localization of nanofillers: Effect on morphology and crystallization of PLA/PCL blends. Macromolecular Chemistry and Physics 2011; 212:613-6256.
DOI: 10.1002/mapc.201000579

33. Z. Yu, J. Yin, S. Yan, Y. Xie, J. Ma, X. Chen. Biodegradable poly(L-lactide)/poly(ε-caprolactone)-modified montmorillonite nanocomposites: Preparation and characterization. Polymer 2007; 48:6439-6447.
DOI: 10.1016/j.polymer.2007.07.024

34. A.N. Ibrahim, M.U. Wahit, A.A. Yussuf. Effect of fiber reinforcement on mechanical and thermal properties of poly(ε-caprolactone)/poly(lactic acid) blends composites. Fibers and Polymers 2014; 15:574-582.
DOI: 10.1007/s12221-014-0574-4

35. D. Ju, L. Han, F. Li, S. Chen, L. Dong. Poly(ε-caprolactone) composites reinforced by biodegradable poly(3-hydroxybutyrate-co-3-hydroxyvalerate) fiber. International Journal of Biological Macromolecules 2014; 67:343-350.
DOI: 10.1016/j.ijbiomac.2014.03.048

36. C.C. Eng, N.A. Ibrahim, N. Zainuddin, H. Ariffin, W.M.Z.W. Yunus, Y.Y. Then. C.C. Teh. Enhancement of mechanical and thermal properties of polylactic acid/polycaprolactone blends by hydrophilic nanoclay.Indian Journal of Materials Science 2013; 816503.
DOI: 10.1155/2013/816503

37. Z. Xu, Y. Zhang, Z. Wang, N. Sun, H. Li. Enhancement of electrical conductivity by changing phase morphology for composites consisting of polylactide and poly(ε-caprolactone) filled with acid-oxidized multiwalled carbon nanotubes. Applied Materials & Interfaces 2011; 3:4858-4864.
DOI: 10.1021/am201355j

38. M.R. Nanda, M. Misra, A.K. Mohanty. The effect of process engineering on the performance of PLA and PHBV blends. Macromolecular Materials and Engineering 2011; 296:719-728.
DOI: 10.1002/mame201000417
39. B.M.P. Ferreira, C.A.C. Zavaglia, E.A.R. Duek. Films of PLLA/PHBV: The thermal, morphological and mechanical characterization. Journal of Applied Polymer Science 2002; 86:2898-2906.
DOI: 10.1002/app.11334
40. H. Zhao, Z. Cui, X. Wang, L.-S.Turng, X. Peng. Processing and characterization of solid and microcellular poly(lactic acid)/polyhydroxybutyrate-valerate (PLA/PHBV) and PLA/PHBV/clay nanocomposites. Composites Part B 2013; 51:79-91.
DOI: 10.1016/j.compositesb.2013.02.034
41. I. Zembouai, S. Bruzaud, M. Kaci, A. Benhamida, Y.-M. Corre,Y. Grohens, J.-M. Lopez-Cuesta. Synergistic effect of compatibilizer and Cloisite 30B on the functional properties of poly(3-hydroxybutyrate-co-3-hydroxyvalerate)/polylactide blends. Polymer Engineering & Science 2013; 54:2239-2251.
DOI: 10.1002/pen.23776
42. J.P. Mofokeng, A.S. Luyt. Morphology and thermal degradation studies of melt-mixed PLA/PHBV biodegradable polymer blend nanocomposites with TiO_2 as filler. Journal of Applied Polymer Science (accepted).
43. J.P. Mofokeng, A.S. Luyt. Morphology and thermal degradation studies of melt-mixed PLA/PCL biodegradable polymer blend nanocomposites with TiO_2 as filler. eXPRESS Polymer Letters (submitted).
44. J.P. Mofokeng, A.S. Luyt. Morphology and thermal degradation studies of melt-mixed PHBV/PCL biodegradable polymer blend nanocomposites with TiO_2 as filler. Journal of Materials Science (published online).
DOI: 10.1007/s10853-015-8950-z
45. H.L. Ornaghi Jr, A.S. Bolner, R. Fiorio, A.J. Zattera, S.C. Amico. Mechanical and dynamic mechanical analysis of hybrid composites molded by resin transfer molding. Journal of Applied Polymer Science 2010; 118:887-896.
DOI: 10.1002/app.32388

Chapter 6

Conclusions

The aim of this project was to prepare completely biodegradable polymer blends and blend nanocomposites from PLA, PHBV, and PCL with small amounts of titania (TiO_2) nanoparticles. This was done to contribute in combating the environmental issues associated with waste plastic management which results from short shelve life products and packaging material. PLA/PHBV, PLA/PCL and PHBV/PCL blends without and with TiO_2nanoparticles were prepared through melt-blending, and the morphologies, thermal stability, degradation kinetics and dynamic mechanical properties were investigated.

The main objective of this research was to investigate the use of TiO_2 nanofiller in biodegradable polymers to reinforce the blends, to stabilize the interface, and to positively affect the thermal stability and degradation behaviour of the different polymers in the blends. To achieve this objective, it would have been necessary that (i) the nanoparticles disperse well with no agglomeration in one or more of the polymers or on the interface, and (ii) the nanoparticles interact well with the polymer(s) they are in contact with. The melt-mixing was successful as a preparation method in this research. We did find that, even when selectively localized, the nanoparticles were well dispersed in the phase of their choice, although some agglomeration was observed. The agglomeration, which has been caused by the nanoparticles still having stronger affinity for each other than for the polymer(s), is one observation that should be attended to in future research. It may be overcome by functionalizing the nanoparticles through different methods, amongst which is the treatment with alkane phosphonic acid that will attach alkane monolayers to the titanium dioxide surfaces. Phosphonic acids are known to form strong bonds with metal oxides, and the functionalized TiO_2 nanoparticles will form chemical bonds with polymers in the blends, which should improve their dispersion in and interaction with the polymer(s). Another functionalization method that can be used is a mixture of maleic anhydride (MA) and dicarboxylic acid in the presence of toluene and ethanol. The dicarboxylic acid will form grafting sides on the TiO_2 nanoparticles, which should attach to the polymers in the blends. The advantage of the latter method is that dicarboxylic acids have biodegradable and biocompatible amino acids that make them an excellent choice as compatibilizing agents when

mixing titania into biodegradable polymers. The degree of functionalization can also be controlled by controlling the MA concentration.

To some extent we achieved our objective, although the property improvements were not always as significant as we would have liked it to be. Generally the thermal stabilities of both polymers in the blends were improved in the presence of the TiO_2 nanoparticles, although they had little effect on the viscoelastic properties and glass transition temperatures. It is also possible that the nano-filler did not really improve the thermal stabilities, but merely retarded the evolution of the volatile degradation products. Since the thermal stability and degradation kinetics were monitored through TGA analysis in which weight loss is measured as function of temperature, this would have caused weight losses to occur at higher temperatures, giving the impression of higher thermal stability. The small changes in viscoelastic properties may have been the result of low filler contents or weak interactions between the filler particles and the polymer(s). This should be further investigated through increasing the filler content and/or functionalizing the filler particles, as discussed above.

This research can also be extended to include kinetic investigations on the crystallization of the respective polymers in the blends and nanocomposites, and determination of the influence of blending and nanoparticle addition on the tensile, flexural and impact properties of these materials. There are also a number of other suitable nanoparticles, e.g. zirconia and conductive particles like nano-copper and nano-silver, that may be used in similar investigations. It will further be interesting to see if the crystal structure (anatase or rutile) of, for example, titania will have a different influence on the properties of the blends.

Acknowledgements

First of all I will like to thank **God** for giving me strength, courage, and perseverance to achieve the important milestone and dream of my life, and most importantly the gift of life, I am really grateful because You blessed me.

I also would like to express my profound gratitude and deep appreciation to my honourable supervisor **Professor Adriaan Stephanus Luyt** for his guidance, support, and enthusiastic encouragement throughout the entire period of this research that enabled me to complete this important milestone in my life, and for his efforts to explain things clearly and cleanly. I would like to thank him for his sound advice, good teaching, and lots of good ideas. His overly enthusiasm and integral view on research and his mission for providing only the best and high-quality work, has made a deep impression on me. I am very grateful that I had him as my supervisor and mentor and I learned a lot from his strong character and good conduct as well as the same treatment of all his students.

I acknowledge the University of the Free State at large for proving me with an opportunity to study, and the National Research Foundation (NRF) for providing me with financial support and affording the opportunity to obtain a Ph.D. degree.

I acknowledge Mr. Mohamed Jaffer from the University of Cape Town, and Professor Pieter van Wyk from the University of the Free State (Bloemfontein campus) for TEM analysis of my samples, I really appreciate the good work you did.

Countless thanks to my mother Mme Mmakeletso Mofokeng, and my brothers Lefu and Lebohang Mofokeng for their love and support, I am proud to be part of this beautiful family. I would also like to thank my late grandmother Mmamokgae Tibisa Mokoena for what she did for me and my brothers. I would also like to thank the entire Mokoena and Mofokeng families, without them I would not have existed.

I would like to thank the Old Apostolic Church (OAC) congregation for providing me with spiritual, emotional support and strength through difficult times, mainly Mr and Mrs Letino, Mr and Mrs Malebese, Mr and Mrs Tsotetsi, Mr and Mrs Chabane, Mr and Mrs Ramokhothoane, Mr and Mrs Nkanyane, Mr and Mrs Gosenyegang, Mr and Mrs Ntleru, Mr and Mrs Mahlohla as my leaders, and the entire OAC Phuthaditjhaba section for their great support always.

Many thanks to the Faculty of Natural and Agricultural Sciences staff, my colleagues in the department of Chemistry and my fellow polymer science research group members (Mrs Marlize Jackson, Mrs Mpho Patience Leripa, Dr. Dusko Dudic, Mr Mokgaotsa Mochane, Mr Teboho Mokhena, Ms Motshabi Sibeko, Ms Cherylann Clarke, Ms Thandi Gumede, Ms Dineo Molaba, Ms Tholloana Makhetha, Mr Teboho Motloung, Mrs Moipone Malimabe, Mr Tsietsi Tsotetsi, Mr Mfiso Mngomezulu, Mr Tyson Mosoabisane, Mr S. Jeremia Sefadi, Dr Nomampondomise Molefe, Mr Rantoa Papzen Moji), for all their help, support, interest and valuable hints.

I would also like to thank Dr Spirit Molefi, Mrs Seadimo Mojaki, Mrs Doreen Mosiangaoko, Ms Rethabile Marumo, Mrs Zanele my Zee Pasha, Dr He Wei, Mrs Itumeleng Buthelezi, Mrs Pholositswe Mpharu, Ms Makhosazana Mthembu, Dr Tshwafo Motaung, Dr Thabang Mokhothu, Dr. Essa Esmail Mohammad Ahmad, Dr Kamohelo George Tshabalala, Dr Lehlohonolo Koao, not forgetting Nkgono Mmamoloi, Mme Mmamotloung, Mme Mmakgatwe, Jabulile and Matiisetso for their inspirations, moral support and good friendship.

I would like to thank Mrs Elsa Luyt and her son Mr Ian Luyt, who have let Prof Luyt work and help all his students, even when they needed him most, I really appreciate it.

I am thankful to the maintenance staff, Mrs Mmadibuseng Lemeko, Mrs Mmaanie Motaung, Mrs Mmalehlohonolo Moremi, Mrs Mmalehlohonolo Bereng who are always making our working environment clean, and for their parental advice. Finally I would like to thank everyone who has supported me academically and emotionally throughout the entire study, may God bless you all.

Appendix

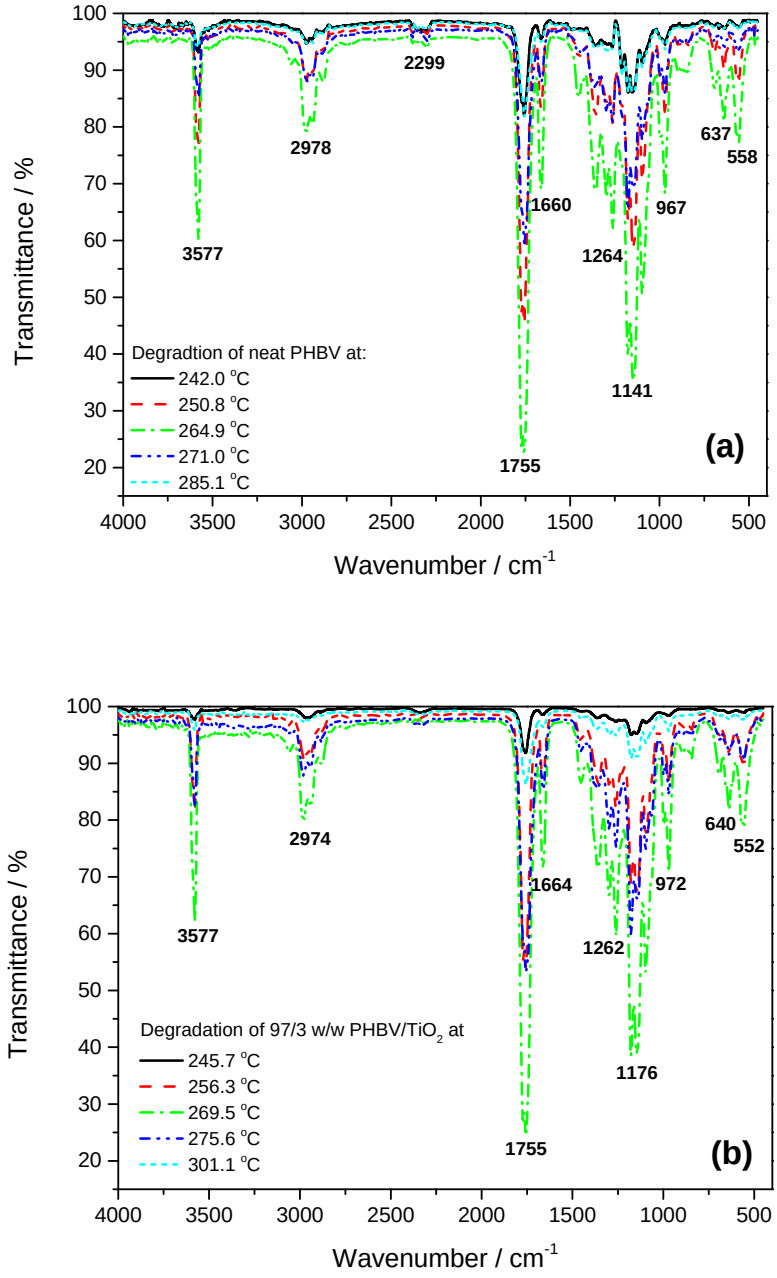

Figure A.1 TGA-FTIR spectra at different temperatures of the degradation of (a) neat PHBV, and (b) 97/3 w/w PHBV/TiO_2

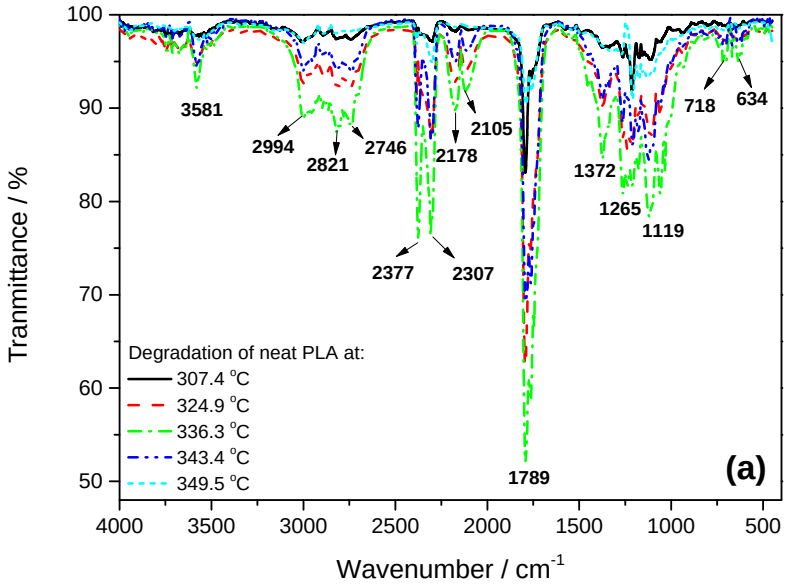
Tranmittance / %
Wavenumber / cm-1
Degradation of neat PLA at:
307.4 °C
324.9 °C
336.3 °C
343.4 °C
349.5 °C
3581
2994
2821
2746
2377
2307
2178
2105
1789
1372
1265
1119
718
634
(a)

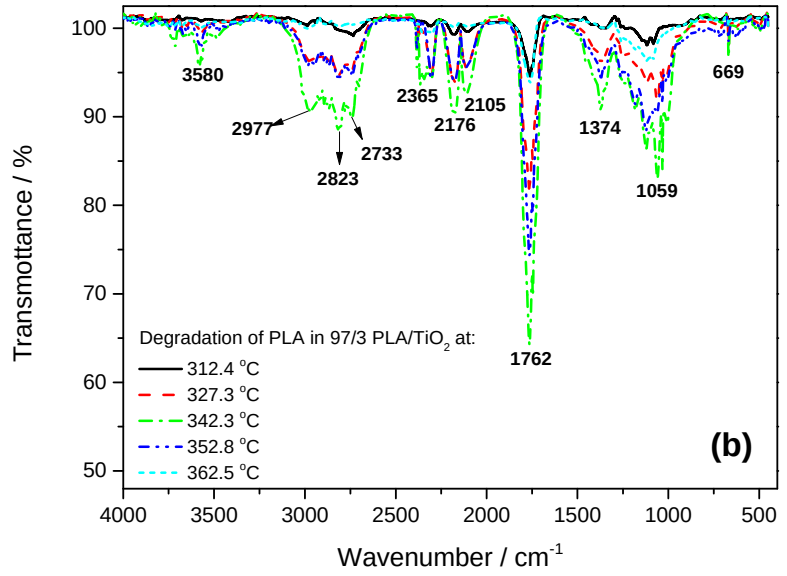
Transmottance / %
Wavenumber / cm-1
Degradation of PLA in 97/3 PLA/TiO2 at:
312.4 °C
327.3 °C
342.3 °C
352.8 °C
362.5 °C
3580
2977
2823
2733
2365
2176
2105
1762
1374
1059
669
(b)

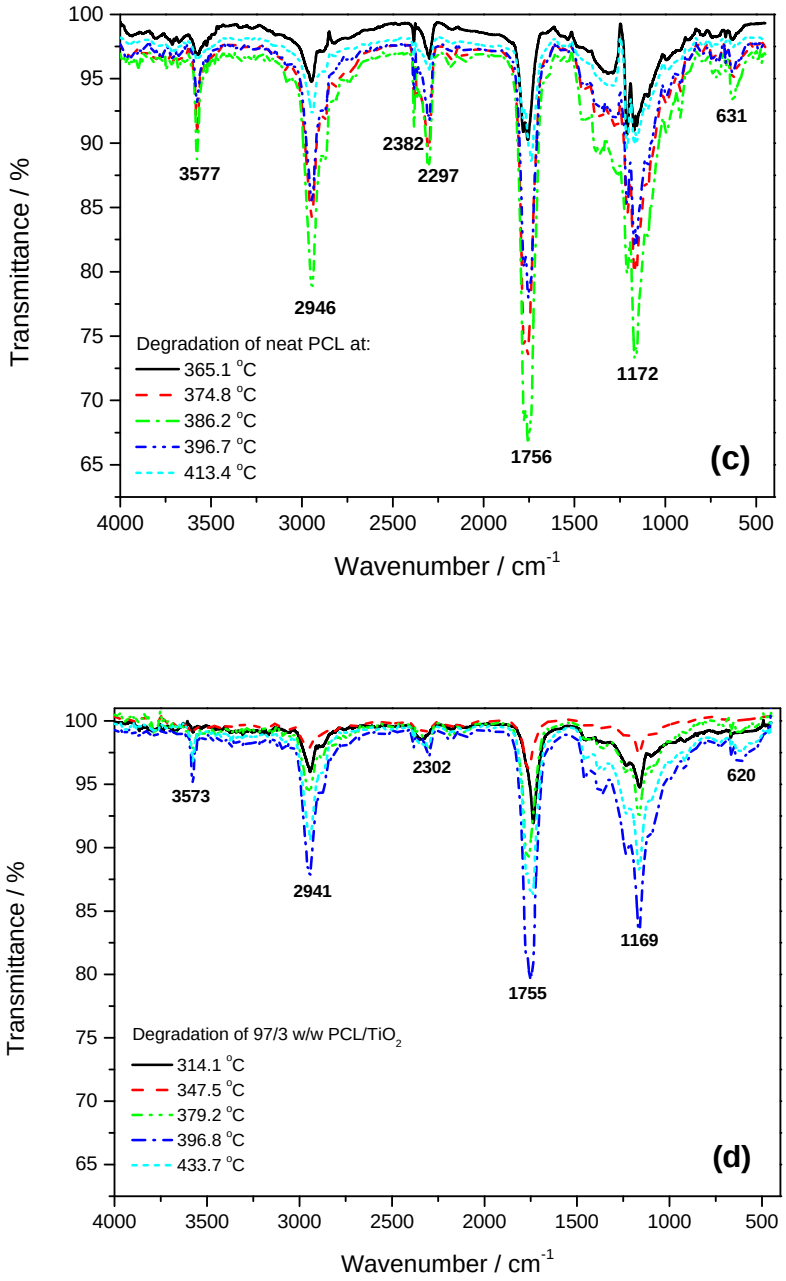

Figure A.2 TGA-FTIR spectra at different temperatures of the degradation of (a) neat PLA, (b) 97/3 w/w PLA/TiO_2,(c) neat PCL, and (d) 97/3 w/w PCL/TiO_2

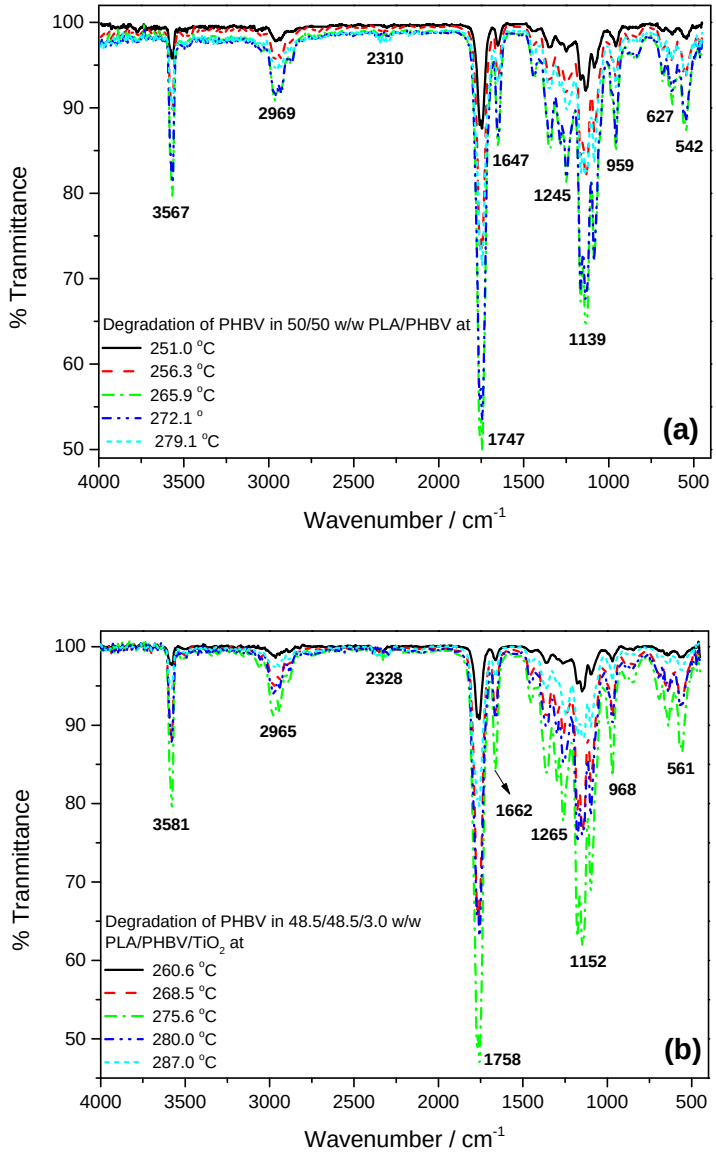

Figure A.3 TGA-FTIR spectra at different temperatures of (a) PHBV degradation in a (a) 50/50 w/w PLA/PHBV blend and (b) 48.5/48.5/3.0 w/w PLA/PHBV/TiO_2 blend nanocomposite

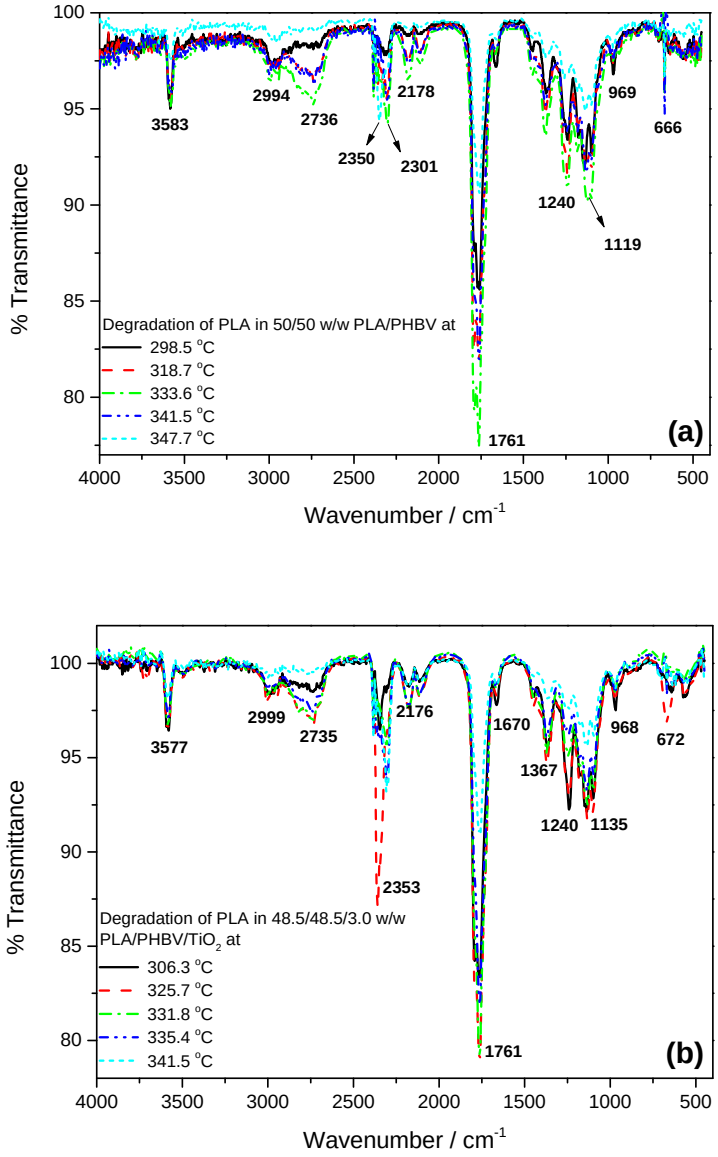

Figure A.4 TGA-FTIR spectra at different temperatures of (a) PLA degradation in 50/50 w/w PLA/PHBV blend (b) PLA degradation in a 48.5/48.5/3.0 w/w PLA/PHBV/TiO_2 blend nanocomposite

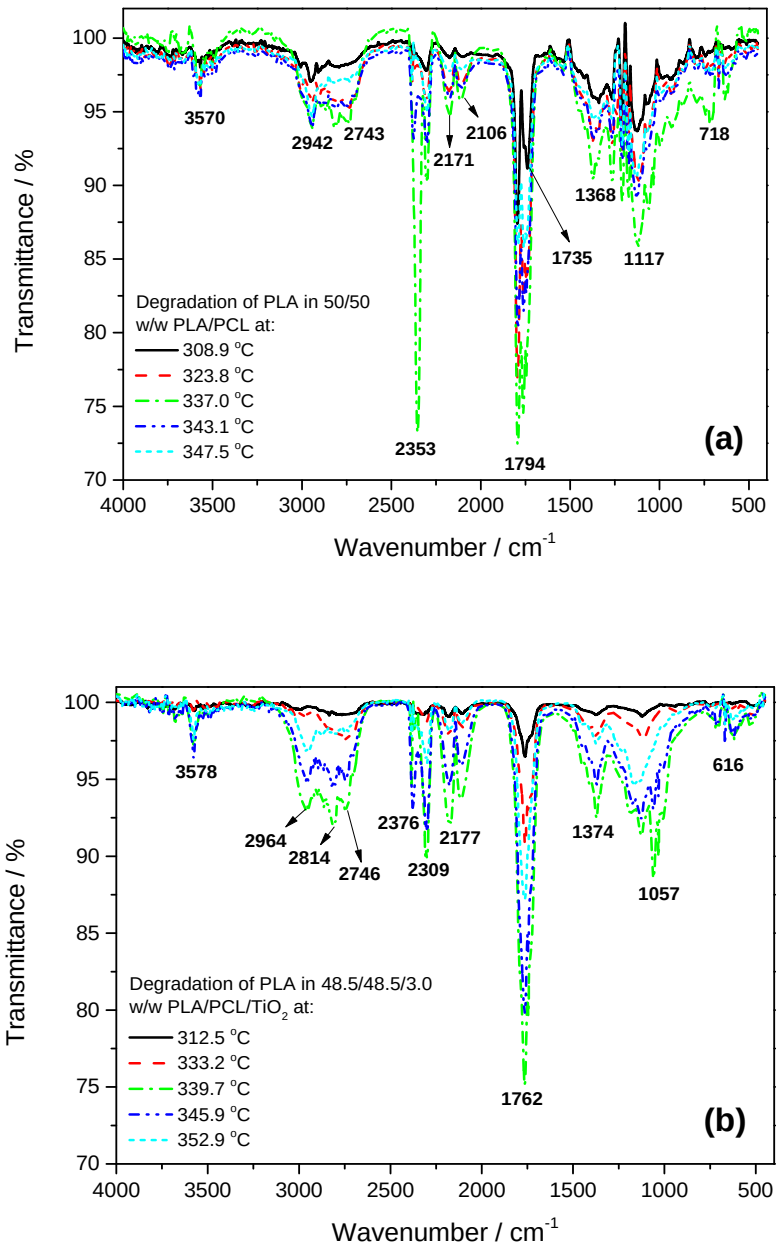

Figure A.5 TGA-FTIR spectra at different temperatures of (a) PLA degradation in 50/50 w/w PLA/PCL blend and (b) PLA degradation in a 48.5/48.5/3.0 w/w PLA/PCL/TiO_2 blend nanocomposite

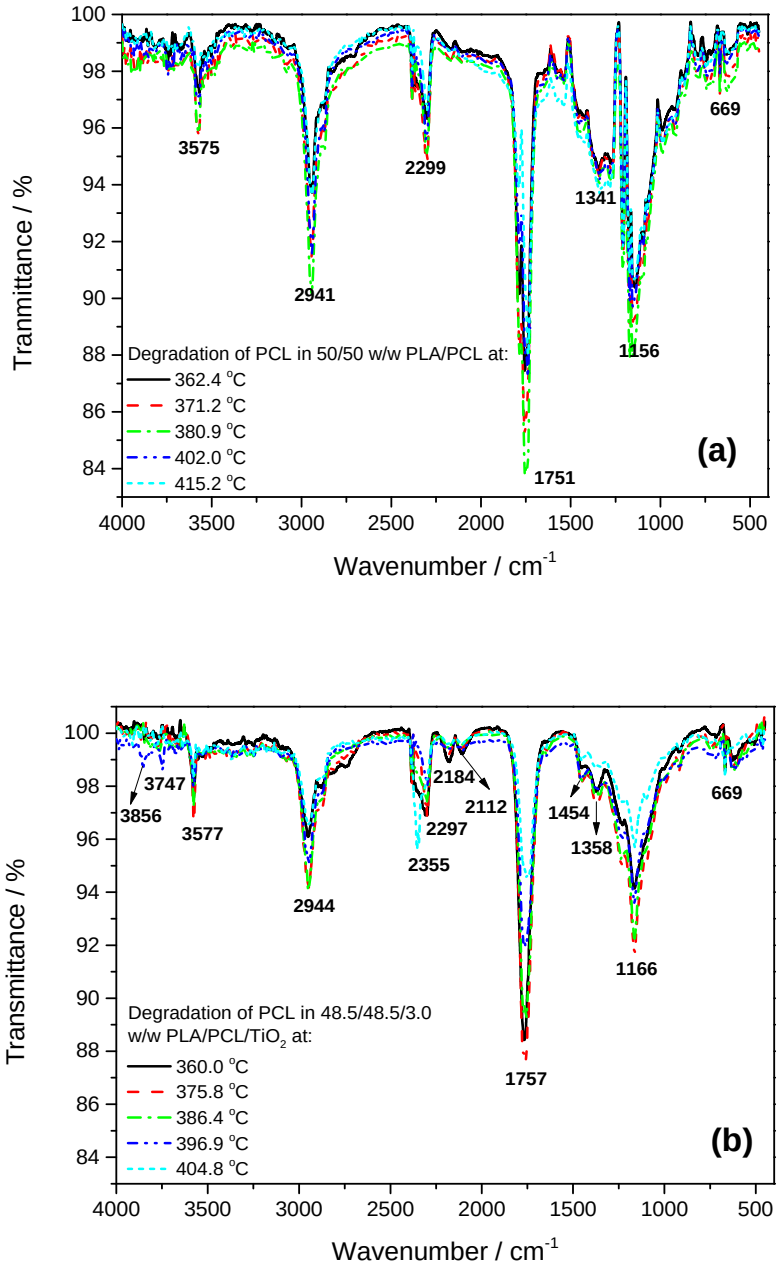

Figure A.6 TGA-FTIR spectra at different temperatures of (a) PCL degradation in 50/50 w/w PLA/PCL blend and (b) PCL degradation in a 48.5/48.5/3.0 w/w PLA/PCL/TiO_2 blend nanocomposite

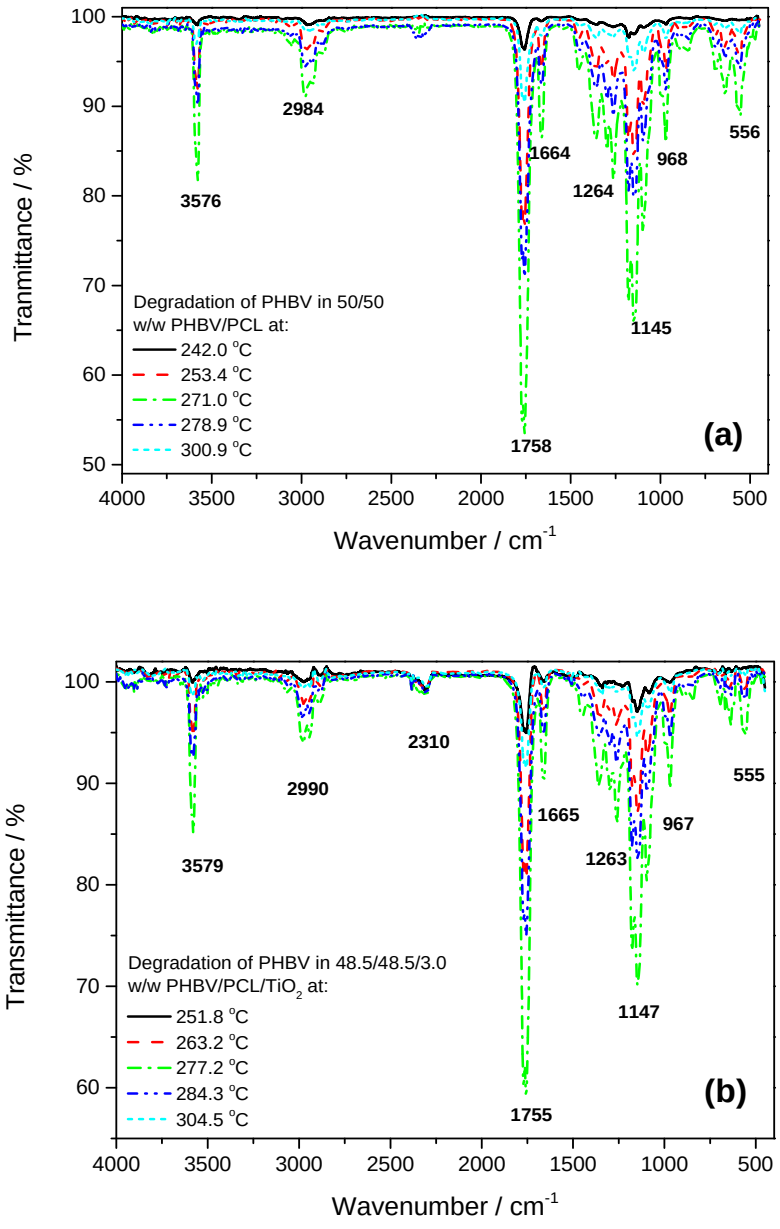

Figure A.7 TGA-FTIR spectra at different temperatures of (a) PHBV degradation in 50/50 w/w PHBV/PCL blend, and (b) PHBV degradation in a 48.5/48.5/3.0 w/w PHBV/PCL/TiO_2 blend nanocomposite

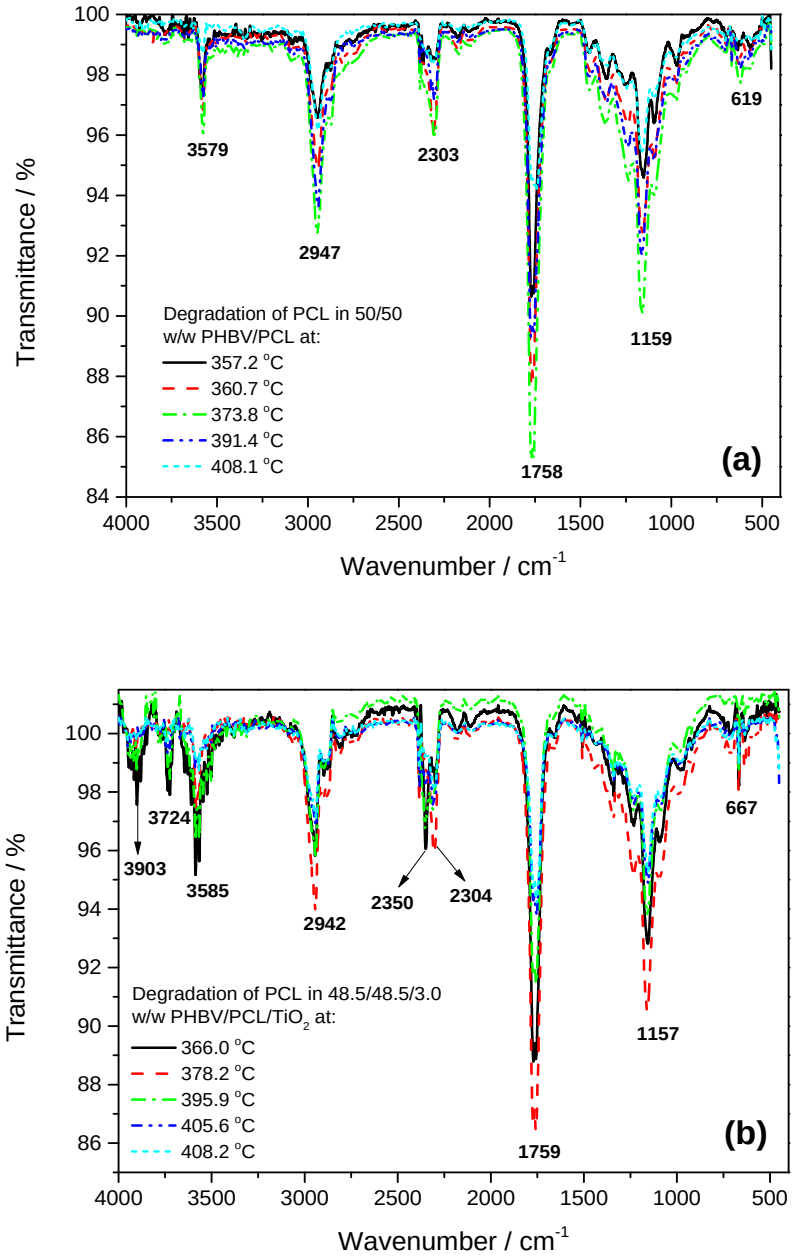

Figure A.8 TGA-FTIR spectra at different temperatures of (a) PCL degradation in 50/50 w/w PHBV/PCL blend, and (b) PCL degradation in a 48.5/48.5/3.0 w/w PHBV/PCL/TiO_2 blend nanocomposite